Flexible Evaluation of Auditory Evidence for Perceptual Decision Making

By

PREETHAM GANUPURU

DISSERTATION

Submitted in partial satisfaction of the requirements for the degree of

DOCTOR OF PHILOSOPHY

in

Neuroscience

in the

OFFICE OF GRADUATE STUDIES

of the

UNIVERSITY OF CALIFORNIA

DAVIS

Approved:

Timothy D. Hanks, Chair

Erie D Boorman

Gregg H. Recanzone

Simona Ghetti

Gene G Gurkoff

Committee in Charge

2022

Abstract

Perceptual decision making is a critical component of human cognition by which the brain processes raw sensory evidence from its environment to guide actions that best suit goals. However, the evidence that the environment provides is often ambiguous and requires the brain to evaluate it in an optimal way to maximize decision success. Although the extensive study has been conducted to understand how the brain evaluates noisy sensory evidence over time to guide perceptual decisions, it is unclear how different regions of the brain contribute to this evidence evaluation, and how these regions evaluate evidence differently demanding on the demands of a given situation.

One area of the brain, posterior parietal cortex (PPC), has long been a target of this study. PPC lies at the junction of brain regions canonically associated with sensory and motor processes, and neurons in PPC exhibit activity that scales with incoming sensory evidence during formation of perceptual decisions and reflects the time of decision commitment across multiple sensory modalities and species. Thus far, these studies have largely neglected the temporal component of evidence evaluation: In situations in which some epochs of evidence are more relevant than others, how do the dynamics of neural activity accommodate the different task demands to account for the animal's behavioral strategy? Also, do the distinct processing dynamics of PPC emerge locally or simply inherited from upstream sensory regions?

In this dissertation, I describe three studies involving human and rat subjects performing auditory perceptual decision making tasks involving varying timescales of evidence evaluation in which different epochs of evidence are relevant for the decision. In the first study, I show that humans are capable of employing multiple timescales of evidence

evaluation for different purposes during a multi-stage change detection task, and these timescales are selectively recruited depending on how circumstances progress regardless of the subject's expectations. In the second study, I use neuropixel probes to record single unit activity in the PPC of rats performing the same change detection task to examine a neural mechanism for how the brain can flexibly adapt timescales of decision making for different purposes. Finally, I describe a study in which the primary auditory cortex of rats is inactivated during an auditory discrimination task, with results suggesting that primary auditory cortex is not necessary for evaluation of evidence over time for auditory decisions and that this function emerges later in downstream brain regions.

Table of Contents

Chapter 1:

General introduction

What is perceptual decision making?

Perceptual decision making is the process by which raw sensory information in the environment is processed by the brain to guide an animal's actions (Gold and Shadlen, 2007). One of the most frequently applied functions in the human brain, perceptual decision making allows informed responses to events and interaction with objects to serve goals and motivations. Often, however, the environment makes this process difficult, providing only noisy, ambiguous information from which the brain must extract relevant variables to drive actions. To meet this challenge, the brain adapts its processing of this information to the demands of circumstances: What does the same evidence mean for a decision in one moment or context as opposed to another? Also, what parts of the brain are responsible for which components of decision making?

These questions have relevance to human health in addition to their academic worth. Decision making is often impaired in psychiatric disorders including schizophrenia, obsessive-compulsive disorder, Alzheimer's disorder, and attention-deficit hyperactivity disorder (Bechara et al., 2001; Cáceda et al., 2014; Murphy et al., 2001; Nestadt et al., 2016; van Wouwe et al., 2016). However, treatments for these disorders are generally limited to brain-wide pharmacological interventions, which can be fraught with off-target effects and other health complications (Geerts, 2009). Even more motivating to the questions posed here, impairments in *flexibility* in decision making and other cognitive behaviors is commonplace in these disorders (Bissonette et al., 2008; Cella et al., 2010; Mante et al., 2013; Monchi et al., 2001; Pasupathy and Miller, 2005). To develop more precisely targeted interventions to treat symptoms of these disorders, including decision making, it is critical to understand how the brain conducts these functions locally.

Perceptual decisions, in particular, allow a controlled, tractable substrate for studying decision making and behavioral flexibility.

Mechanistic models of perceptual decision making

Before tackling the primary topics of the present dissertation, it is worth briefly reviewing our understanding of perceptual decision making at large. Perceptual decision making research has a rich history rooted early in study of the relationship between simple stimulus and action, dating back to simple behavioral studies exploring operant functions in animals (Krebs, 1983). This line of study gives way to a more sophisticated view of decision making, both in terms of these simple stimulus-action relations and complex deliberative decisions. At its core, a decision involves inference of probabilities of competing hypotheses; this can be shifted by learned priors, but for our purposes, evidence is the key driver of this inference. Evidence, joined with other variables including priors, comprise the decision variable, which reflects the probability of a given hypothesis. This principle is central to most theory of perceptual decision making, including signal detection theory, which allows a simple conversion of a choice from decision variable that falls on one of two distributions, one representing noise and the other representing signal in addition to noise. Signal detection theory offers a simple means of understanding action of animals as a relation of the quality of evidence, a component relevant still to the tasks and models involved in this dissertation's studies.

This theoretical framework evolved to emphasize the general process of accumulating noisy information over time to a criterion threshold for decision commitment (Wald and Wolfowitz, 1950). Although signal detection theory offers a useful framework to study the class of decisions in which the brain pursues hypotheses based on comparing

evidence against a criterion, a critical additional component is collection of evidence *over time* and setting the time of decision development and events, particularly time of commitment.

A separate class of decision theory, sequential sampling framework, meets this need by including a stopping criterion with respect to time. Sequential probability ratio tests (SPRTs) are one such instantiation of this mechanism (McMillen and Holmes, 2006; Wald and Wolfowitz, 1948). Here, any number of independent pieces of evidence supporting different hypotheses combine over time into a decision variable. Once a particular decision variable value is reached, the decision maker can commit to a hypothesis, thus allowing a balance between not only accurate discrimination of signal from noise but minimizing decision time. Finally, expanding upon SPRTs, a class of sequential sampling "diffusion" models consolidates the aforementioned decision components (individual samples of evidence, sources of noise, stopping criteria) into a highly flexible and widely applicable framework based on a random walk instantiation of decision variables dictated by evidence-dependent drift (Ratcliff and McKoon, 2008; Ratcliff and Rouder, 1998; Smith and Ratcliff, 2004). These drift diffusion models allow tuning of paramterized decision components to explain various decision making processes, perceptual and otherwise, as a dynamic process that evolves over time. The studies conducted for this dissertation strongly source this model class, particularly Chapter 4 in which a standard drift diffusion model is employed to better understand the effects of cortical perturbation on decision making.

Experimental support for perceptual decision models

Pivoting toward empirical methods, experimental studies primarily conducted in non-human primates sought to explain how this theoretical framework could be instantiated in the brain's neural functioning. Seminal studies in this line of work involved monkeys performing visual discrimination tasks in which subjects identified coherent motion of noisy stimuli and reported a binary choice between left or right, usually through saccade to a choice target. During task performance, electrophysiological recordings of single units in area MT, which are selective for motion direction, were taken to reveal a disparity between sensory encoding and the eventual choices of the animal. In contrast, cells in posterior parietal cortex and prefrontal cortex faithfully encoded animal *choices* (Britten et al., 1993; Roitman and Shadlen, 2002; Shadlen and Newsome, 1996). Not only did these cells predict perceptual decisions, but their spiking activity also reflected a gradual dynamic in which sensory evidence is integrated over time to a terminal magnitude. As such, these studies suggested the brain indeed contains a neural correlate of the decision variable that accumulation-to-bound models posited decades earlier.

In the years since, these mechanistic principles have been observed across multiple species and sensory modalities, especially in the auditory and somatosensory domains (Hanks et al., 2015; Romo et al., 1996, 2002). Perceptual decision making study has expanded heavily into rodent subject use, allowing both higher throughput data collection and access to a greater toolbox of experimental methods while still offering complex behavioral possibilities (Brunton et al., 2013; Carandini and Churchland, 2013). However, though this expansion has rewarded our understanding of perceptual decision making, the question of how the brain *alters* its evaluation of evidence depending on

circumstantial demands is still relatively unexplored, especially with how a given population of evidence-selective cells facilitates these changes by altering its integration dynamics.

One such consideration for this problem is the timescale over which evidence is relevant for the choice at hand. An adaptable timescale of evidence evaluation is crucial for optimally navigating real world decisions. For example, while a school bus driver should combine evidence evaluated over a longer timescale, carefully judging the positions and movements of other cars before making a decision on the road, a Formula One racer should evaluate evidence over a shorter timescale, relying more on fast reactions to navigate a racecourse as quickly as possible. Everyday decision making requires us to choose how to evaluate evidence flexibly depending on the demands of the task, and in many circumstances, we must determine the optimal strategy for comparing recent to older evidence and the extent to which older evidence should be discounted, as when detecting changes in the environment (Boubenec et al., 2017; Glaze et al., 2015; Johnson et al., 2017).

Extensive investigation into the neural mechanisms of decision making and cognitive flexibility provides a strong foundation to study adaptability of evidence accumulation. In the domain of perceptual decisions, numerous studies have identified systems in the brain that track evidence for decisions over time, integrating new evidence with older evidence until a decision is reached (Ding and Gold, 2010; Gold and Shadlen, 2000; Hanks et al., 2015; Kim and Shadlen, 1999; Shadlen and Newsome, 1996). This work has provided insight into the neural basis of evidence evaluation in situations where evidence is treated similarly across time. However, those studies do not address how

these neural processes change across the wide range of decisions in which the influence of evidence depends on time. Studies targeting cognitive flexibility in decision making have addressed some related topics, such as adjustment of decision criteria (van den Berg et al., 2016; Purcell and Kiani, 2016), speed-accuracy tradeoff (Hanks et al., 2014; Thura and Cisek, 2017), and task switching in response to environmental state changes (Akam et al., 2015; Izquierdo et al., 2004). However, it is unknown how the neural mechanisms of decision making support changes to the timescale of evidence evaluation.

Previous studies have shown adaptability for timescales of evidence evaluation in a range of animal species. In humans, changes in the signal duration for a detection task lead to changes in timescales of evidence evaluation such that the influence of older information tapers off more quickly in situations with briefer signals (Ossmy et al., 2013). In rats, changes in "environmental volatility" (the probability the state of the environment changes) in tasks requiring discrimination of environmental state lead to changes in the timescale of evidence evaluation such that the influence of older information tapers off more quickly in more volatile environments (Piet et al., 2018). These studies suggest that adaptability for timescales of evidence evaluation is a core component of flexible decision making. This dissertation first explores how adaptations of the timescale of evidence evaluation assist in achieving optimal behavior and examines the neural mechanisms that support this. Second, it explores how different regions of the brain process sensory information differently to facilitate evaluation of evidence over time for perceptual decision making.

This introduction concludes with overviews of the two major brain regions studied in this dissertation: PPC and primary auditory cortex (A1). The dissertation itself

addresses the questions outlined above through studies involving these regions. Therefore, it is useful to first review some of the relevant knowledge on these topics from anatomical, neuropathological, and mechanistic perspectives.

Posterior parietal cortex

Posterior parietal cortex (PPC) is an associative area of the brain receiving direct sensory input from primary sensory cortices (e.g. primary visual cortex) and projecting to motor regions, other association areas, and back to primary sensory cortex (Berlucchi and Vallar, 2018; Chandler et al., 1992; Mishkin, 1972; Reep et al., 1994). This anatomical positioning makes it a strong candidate for the interface between sensory perception and action selection (Cohen, 2009). At the lowest level, signals related to motor coordination of eye and hand motion are found in primate PPC, specifically the lateral intraparietal area (LIP) (Andersen et al., 1998; Battaglia-Mayer et al., 2000; Gallese et al., 1994; Snyder et al., 1997). In both human and non-human primates, this part of PPC receives direct visual inputs from extrastriate cortex, lending to its role in motion-guided saccades (Asanuma et al., 1985; Blatt et al., 1990; Lynch et al., 1985) This connectivity made PPC's LIP a key target for studies in visual discrimination tasks that laid the foundation for future studies of evidence integration for perceptual decisions at large (Roitman and Shadlen, 2002; Shadlen and Newsome, 1996). On the auditory side, this same segment of PPC receives sound location information from auditory cortex, also in a way that guides saccades (Divac et al., 1977; Hyvärinen, 1982; Pandya et al., 1969) Regarding efferent connections, PPC projects directly to frontal orienting fields and super colliculus (Andersen et al., 1985) which directly control saccade direction. Together, this series of

connections provides a clear mechanism for association of stimuli of multiple sensory modalities to actions, both in terms of optical orientation and manual manipulation.

PPC's role in decision making extends far beyond that of simple stimulus-action associations, though. As mentioned, the neural activity of PPC embodies more complex, deliberative processing of evidence for perceptual decision making. Spiking activity of monkey LIP neurons ramps up gradually leading up to saccades during motion discrimination tasks; as motion evidence is presented, spiking activity increases according to the strength of evidence until reaching a common threshold of activity shortly before the saccade is executed (Roitman and Shadlen, 2002; Shadlen and Newsome, 1996). This principle extends to tasks with more than two choices (Churchland et al., 2008), tasks in which the environment limits the exposure to the sensory stimulus and control the timing of the choice (Kiani et al., 2008), and tasks involving other sensory modalities (Hanks et al., 2015; Licata et al., 2017; Romo et al., 1996).

In humans, studies of PPC's role in evidence evaluation has largely been limited to neuroimaging, EEG, and MEG measurements (Hanks and Summerfield, 2017; Kelly and O'Connell, 2015). These methods do not allow both spatially and temporally defined measurements of neural activity to establish parallels with monkey LIP physiology, but these studies have nonetheless identified signatures of evidence evaluation over time in humans. Using regression of EEG signals recorded during visual discrimination tasks, it was found that the coincidence of evidence with oscillatory activity in PPC dictated the influence of such evidence on decisions, suggesting a functional relationship between parietal neural dynamics and integration of evidence driving action selection (Bitzer et al., 2020; van Vugt et al., 2012; Wyart et al., 2012).

Most directly involved in this dissertation are the properties of rodent PPC, especially that of rats. Although the existence of PPC in rats is a point of controversy in itself (Whitlock et al., 2008), there is substantial anatomical evidence that indicates homologous parallels with PPC in primates (Chandler et al., 1992; Mcnaughton et al., 1989; McNaughton et al., 1994; Reep et al., 1994; Whitlock et al., 2008). In contrast with primate PPC, however, rat PPC seems to be somewhat more regionally consolidated, with only three primary subdivisions: medial PPC (mPPC), lateral PPC (lPPC), and caudolateral PPC (PtP) (Olsen and Witter, 2016; Olsen et al., 2019; Paxinos and Watson, 2013; but see Gilissen et al., 2021). These areas are strongly interconnected with somatosensory, visual, auditory, and motor cortices, as well as multiple thalamic nuclei (Chandler et al., 1992; Reep et al., 1994)

Of particular interest to perceptual decision making is mPPC, which we will use interchangeably with PPC for most of this discussion and in later chapters. Comparably to area LIP in primates, neurons in rat PPC exhibit ramping activity leading up to decisions in an auditory discrimination task, peaking immediately before decision execution. This ramping activity also scaled with strength of evidence, even exhibiting *negative* modulation with evidence for the opponent choice of the given cell (Hanks et al., 2015). This finding is significant for three major reasons. First, it demonstrates homology in PPC's evidence integration functionality between rodents and primates. Second, it generalizes PPC's function across multiple sensory modalities, i.e. visual and auditory integration. Third, it generalizes PPC's function across multiple motor modalities, i.e. saccades and whole-body orientations. Thus, PPC in rats offers a promising foundation

for studying how neural dynamics of evidence integration change between various forms of perceptual decision making, the primary aim of Chapter 2 of this dissertation.

Complications have arisen in PPC's role in perceptual decision making in both primates and rodents, though, complications that this dissertation's work seeks partly to address. Despite compelling electrophysiological results suggesting that PPC integrates sensory evidence for perceptual decisions, some pharmacological and optogenetic inactivation studies have called into question PPC's causal influence on these decisions (Erlich et al., 2015; Katz et al., 2016; Licata et al., 2017; Raposo et al., 2014). In contrast, other studies suggest that PPC may influence causal decisions conditionally, such as when the animal controls the time of the decisions (Hanks et al., 2006; Zhou and Freedman, 2019) and when compensation by other areas and recovery from pharmacological perturbation are less likely (Jeurissen et al., 2021). Nonetheless, it is unclear what role PPC occupies in these decisions, whether it be true integration of evidence over time or modulation of decision parameters related to the timing of decisions. Chapter 2 describes work conducted during this graduate work that attempts to address this gap in understanding

Primary auditory cortex

Primary auditory cortex (A1) is located bilaterally in the superior gyrus of the temporal lobe of primates, the first cortical recipient of auditory information originating in the cochlea (Purves et al., 2001). A1 inhabits a "core" of the superior gyrus along with two other subdivisions, all of which are surrounded by a "belt" comprising the secondary regions of auditory cortex (Doron et al., 2002; Kaas and Hackett, 2000; Purves et al., 2001). It receives direct inputs from medial geniculate nucleus of thalamus (Luethke et

al., 1989; Mesulam and Pandya, 1973) and projects to several other areas via the belt, including PPC (Reep et al., 1994), striatum (LeDoux et al., 1991) and several subregions of prefrontal cortex (Romanski, 2007). These projections make A1 a prominent subject of perceptual decision making involving auditory stimuli due to its direct influence on many decision centers in the brain.

Among the most well-studied features of A1's neuronal properties is its tonotopic organization, wherein preferred stimulus frequencies of cells change from low to high on a rostral to caudal axis (Clopton et al., 1974; Ehret and Romand, 1997; Kalatsky et al., 2005; Saenz and Langers, 2014). This property was established in non-human primates, and although it has been difficult to comparably establish it in humans due to the lack of spatial resolution in human imaging techniques, results preliminarily suggest functional homology through tonotopy and cytoarchitecture between human and non-human primate A1 (Humphries et al., 2010; Saenz and Langers, 2014). A1 also expresses an orthogonal dimension of periodicity, which may contribute to perceptual decisions in which the timing of a stimulus is informative (Barton et al., 2012; Langner et al., 2002).

Rats have also become a frequent subject of study in research of A1. Like most mammals, rats have a distinct tonotopic organization comparable to other species in organization and function (Malmierca, 2003). In general, however, rat auditory cortex is heavily consolidated compared to primates, with A1 being the primary aspect of a temporal area 1 and additional temporal areas located posteriorly and ventrally to this area more in line with the auditory belt of primates (Doron et al., 2002; Rutkowski et al., 2003) Functionally, a clear difference in rat A1 function from primate A1 pertinent to this

dissertation is the increase in hemispheric spatial selectivity, such that rat A1 neurons solely encode contralateral stimuli (Yao et al., 2013).

A1 possesses a few striking functions that are highly relevant to perceptual decision making. First, A1 has a role in perceptual working memory: A1 neurons encode stimulus identity following stimulus presentation when the stimulus identity informs later choices and is necessary for tracking stimulus identity over time (Runyan et al., 2017; Scott and Mishkin, 2016; Wigestrand et al., 2017; Yu et al., 2021). Second, A1 contains information for sound localization (Benson and Teas, 1976; Heffner, 1978; Kelly and Glazier, 1978; Malhotra and Lomber, 2007; Phillips and Irvine, 1981), which is critical in many of the lateralized decision tasks used to study the evaluation of evidence in perceptual decisions. Third, A1 is capable of driving auditory decisions through both stimulation and disruptive perturbation (Chen et al., 2019; Znamenskiy and Zador, 2013) as well as containing choice-dependent information that does not bear directly on stimulus identity (Francis et al., 2018; Guo et al., 2019; Tsunada et al., 2016). Interestingly, simple discrimination of tones does not seem to bear on auditory cortex (Gimenez et al., 2015; Kelly, 1970; Kelly and Glazier, 1978), so simple spectral information is likely routed in ways that bypass auditory cortex. Together, these results indicate potential for A1 to dictate perceptual decisions not merely in terms of simple auditory perception but in terms of more abstract transformations of that auditory information specific to decisions.

Aims of this dissertation

Using our knowledge of the neural basis of decision making outlined thus far, we seek here to expand knowledge of perceptual decision making by determining how the neural mechanisms of decisions adapt their dynamics according to task demands. First,

in Chapter 2, we study the extent to which the human brain adapts its dynamics of evidence evaluation flexibly for different purposes, specifically change point detection decisions and confidence judgments about those decisions. In Chapter 3, the neural basis of this flexibility in evidence evaluation will be explored by testing the specific hypothesis that neurons in PPC of rats performing the same change point detection task can adapt their dynamics of integration to serve a task-relevant timescale of evaluation, as well as the hypothesis that PPC has a causal role in setting this timescale. Finally, we seek to learn the extent to which the utilization of optimal evidence evaluation timescales depends on cortical regions that have traditionally been attributed a sensory role. To this end, the study in Chapter 4 involves perturbation of A1 and analysis of the resulting deficits in an auditory discrimination task in which rats evaluate evidence over time followed by identification of the mechanistic source of the deficit.

References

Akam, T., Costa, R., and Dayan, P. (2015). Simple Plans or Sophisticated Habits? State, Transition and Learning Interactions in the Two-Step Task. PLOS Computational Biology *11*, e1004648. https://doi.org/10.1371/journal.pcbi.1004648.

Andersen, R.A., Asanuma, C., and Cowan, W.M. (1985). Callosal and prefrontal associational projecting cell populations in area 7A of the macaque monkey: a study using retrogradely transported fluorescent dyes. J Comp Neurol *232*, 443–455. https://doi.org/10.1002/cne.902320403.

Andersen, R.A., Snyder, L.H., Batista, A.P., Buneo, C.A., and Cohen, Y.E. (1998). Posterior parietal areas specialized for eye movements (LIP) and reach (PRR) using a common coordinate frame. Novartis Found Symp *218*, 109–122; discussion 122-128, 171–175. https://doi.org/10.1002/9780470515563.ch7.

Asanuma, C., Andersen, R.A., and Cowan, W.M. (1985). The thalamic relations of the caudal inferior parietal lobule and the lateral prefrontal cortex in monkeys: divergent cortical projections from cell clusters in the medial pulvinar nucleus. J Comp Neurol *241*, 357–381. https://doi.org/10.1002/cne.902410309.

Barton, B., Venezia, J.H., Saberi, K., Hickok, G., and Brewer, A.A. (2012). Orthogonal acoustic dimensions define auditory field maps in human cortex. Proc Natl Acad Sci U S A *109*, 20738–20743. https://doi.org/10.1073/pnas.1213381109.

Battaglia-Mayer, A., Ferraina, S., Mitsuda, T., Marconi, B., Genovesio, A., Onorati, P., Lacquaniti, F., and Caminiti, R. (2000). Early Coding of Reaching in the Parietooccipital Cortex. Journal of Neurophysiology *83*, 2374–2391. https://doi.org/10.1152/jn.2000.83.4.2374.

Bechara, A., Dolan, S., Denburg, N., Hindes, A., Anderson, S.W., and Nathan, P.E. (2001). Decision-making deficits, linked to a dysfunctional ventromedial prefrontal cortex, revealed in alcohol and stimulant abusers. Neuropsychologia *39*, 376–389. https://doi.org/10.1016/S0028-3932(00)00136-6.

Benson, D.A., and Teas, D.C. (1976). Single unit study of binaural interaction in the auditory cortex of the chinchilla. Brain Research *103*, 313–338. https://doi.org/10.1016/0006-8993(76)90801-5.

van den Berg, R., Zylberberg, A., Kiani, R., Shadlen, M.N., and Wolpert, D.M. (2016). Confidence Is the Bridge between Multi-stage Decisions. Current Biology *26*, 3157–3168. https://doi.org/10.1016/j.cub.2016.10.021.

Berlucchi, G., and Vallar, G. (2018). Chapter 1 - The history of the neurophysiology and neurology of the parietal lobe. In Handbook of Clinical Neurology, G. Vallar, and H.B. Coslett, eds. (Elsevier), pp. 3–30.

Bissonette, G.B., Martins, G.J., Franz, T.M., Harper, E.S., Schoenbaum, G., and Powell, E.M. (2008). Double Dissociation of the Effects of Medial and Orbital Prefrontal Cortical Lesions on Attentional and Affective Shifts in Mice. J. Neurosci. *28*, 11124–11130. https://doi.org/10.1523/JNEUROSCI.2820-08.2008.

Bitzer, S., Park, H., Maess, B., von Kriegstein, K., and Kiebel, S.J. (2020). Representation of Perceptual Evidence in the Human Brain Assessed by Fast, Within-Trial Dynamic Stimuli. Frontiers in Human Neuroscience *14*. .

Blatt, G.J., Andersen, R.A., and Stoner, G.R. (1990). Visual receptive field organization and cortico-cortical connections of the lateral intraparietal area (area LIP) in the macaque. J Comp Neurol *299*, 421–445. https://doi.org/10.1002/cne.902990404.

Boubenec, Y., Lawlor, J., Górska, U., Shamma, S., and Englitz, B. (2017). Detecting changes in dynamic and complex acoustic environments. ELife *6*, e24910. https://doi.org/10.7554/eLife.24910.

Britten, K.H., Shadlen, M.N., Newsome, W.T., and Movshon, J.A. (1993). Responses of neurons in macaque MT to stochastic motion signals. Vis Neurosci *10*, 1157–1169. https://doi.org/10.1017/s0952523800010269.

Brunton, B.W., Botvinick, M.M., and Brody, C.D. (2013). Rats and Humans Can Optimally Accumulate Evidence for Decision-Making. Science *340*, 95–98. https://doi.org/10.1126/science.1233912.

Cáceda, R., Nemeroff, C.B., and Harvey, P.D. (2014). Toward an Understanding of Decision Making in Severe Mental Illness. JNP *26*, 196–213. https://doi.org/10.1176/appi.neuropsych.12110268.

Carandini, M., and Churchland, A.K. (2013). Probing perceptual decisions in rodents. Nat Neurosci *16*, 824–831. https://doi.org/10.1038/nn.3410.

Cella, M., Dymond, S., and Cooper, A. (2010). Impaired flexible decision-making in major depressive disorder. Journal of Affective Disorders *124*, 207–210. https://doi.org/10.1016/j.jad.2009.11.013.

Chandler, H.C., King, V., Corwin, J.V., and Reep, R.L. (1992). Thalamocortical connections of rat posterior parietal cortex. Neuroscience Letters *143*, 237–242. https://doi.org/10.1016/0304-3940(92)90273-A.

Chen, L., Wang, X., Ge, S., and Xiong, Q. (2019). Medial geniculate body and primary auditory cortex differentially contribute to striatal sound representations. Nat Commun *10*, 418. https://doi.org/10.1038/s41467-019-08350-7.

Churchland, A.K., Kiani, R., and Shadlen, M.N. (2008). Decision-making with multiple alternatives. Nat Neurosci *11*, 693–702. https://doi.org/10.1038/nn.2123.

Clopton, B.M., Winfield, J.A., and Flammino, F.J. (1974). Tonotopic organization: Review and analysis. Brain Research *76*, 1–20. https://doi.org/10.1016/0006-8993(74)90509-5.

Cohen, Y.E. (2009). Multimodal activity in the parietal cortex. Hear Res *258*, 100–105. https://doi.org/10.1016/j.heares.2009.01.011.

Ding, L., and Gold, J.I. (2010). Caudate Encodes Multiple Computations for Perceptual Decisions. Journal of Neuroscience *30*, 15747–15759. https://doi.org/10.1523/JNEUROSCI.2894-10.2010.

Divac, I., Lavail, J.H., Rakic, P., and Winston, K.R. (1977). Heterogeneous afferents to the inferior parietal lobule of the rhesus monkey revealed by the retrograde transport method. Brain Res *123*, 197–207. https://doi.org/10.1016/0006-8993(77)90474-7.

Doron, N.N., Ledoux, J.E., and Semple, M.N. (2002). Redefining the tonotopic core of rat auditory cortex: Physiological evidence for a posterior field. Journal of Comparative Neurology *453*, 345–360. https://doi.org/10.1002/cne.10412.

Ehret, A.V.N.G., and Romand, L. de N.R. (1997). The Central Auditory System (Oxford University Press).

Erlich, J.C., Brunton, B.W., Duan, C.A., Hanks, T.D., and Brody, C.D. (2015). Distinct effects of prefrontal and parietal cortex inactivations on an accumulation of evidence task in the rat. ELife Sciences *4*, e05457. https://doi.org/10.7554/eLife.05457.

Francis, N.A., Winkowski, D.E., Sheikhattar, A., Armengol, K., Babadi, B., and Kanold, P.O. (2018). Small Networks Encode Decision-Making in Primary Auditory Cortex. Neuron *97*, 885-897.e6. https://doi.org/10.1016/j.neuron.2018.01.019.

Gallese, V., Murata, A., Kaseda, M., Niki, N., and Sakata, H. (1994). Deficit of hand preshaping after muscimol injection in monkey parietal cortex. Neuroreport *5*, 1525–1529. https://doi.org/10.1097/00001756-199407000-00029.

Geerts, H. (2009). Of mice and men: bridging the translational disconnect in CNS drug discovery. CNS Drugs *23*, 915–926. https://doi.org/10.2165/11310890-000000000-00000.

Gilissen, S.R.J., Farrow, K., Bonin, V., and Arckens, L. (2021). Reconsidering the Border between the Visual and Posterior Parietal Cortex of Mice. Cerebral Cortex *31*, 1675–1692. https://doi.org/10.1093/cercor/bhaa318.

Gimenez, T.L., Lorenc, M., and Jaramillo, S. (2015). Adaptive categorization of sound frequency does not require the auditory cortex in rats. Journal of Neurophysiology *114*, 1137–1145. https://doi.org/10.1152/jn.00124.2015.

Glaze, C.M., Kable, J.W., and Gold, J.I. (2015). Normative evidence accumulation in unpredictable environments. ELife *4*, e08825. https://doi.org/10.7554/eLife.08825.

Gold, J.I., and Shadlen, M.N. (2000). Representation of a perceptual decision in developing oculomotor commands. Nature *404*, 390–394. https://doi.org/10.1038/35006062.

Gold, J.I., and Shadlen, M.N. (2007). The Neural Basis of Decision Making. Annual Review of Neuroscience *30*, 535–574. https://doi.org/10.1146/annurev.neuro.29.051605.113038.

Guo, L., Weems, J.T., Walker, W.I., Levichev, A., and Jaramillo, S. (2019). Choice-Selective Neurons in the Auditory Cortex and in Its Striatal Target Encode Reward Expectation. J. Neurosci. *39*, 3687–3697. https://doi.org/10.1523/JNEUROSCI.2585-18.2019.

Hanks, T.D., and Summerfield, C. (2017). Perceptual Decision Making in Rodents, Monkeys, and Humans. Neuron *93*, 15–31. https://doi.org/10.1016/j.neuron.2016.12.003.

Hanks, T., Kiani, R., and Shadlen, M.N. (2014). A neural mechanism of speed-accuracy tradeoff in macaque area LIP. ELife *3*, e02260. https://doi.org/10.7554/eLife.02260.

Hanks, T.D., Ditterich, J., and Shadlen, M.N. (2006). Microstimulation of macaque area LIP affects decision-making in a motion discrimination task. Nat. Neurosci. *9*, 682–689. https://doi.org/10.1038/nn1683.

Hanks, T.D., Kopec, C.D., Brunton, B.W., Duan, C.A., Erlich, J.C., and Brody, C.D. (2015). Distinct relationships of parietal and prefrontal cortices to evidence accumulation. Nature *520*, 220–223. https://doi.org/10.1038/nature14066.

Heffner, H. (1978). Effect of auditory cortex ablation on localization and discrimination of brief sounds. Journal of Neurophysiology *41*, 963–976. https://doi.org/10.1152/jn.1978.41.4.963.

Humphries, C., Liebenthal, E., and Binder, J.R. (2010). Tonotopic organization of human auditory cortex. Neuroimage *50*, 1202–1211. https://doi.org/10.1016/j.neuroimage.2010.01.046.

Hyvärinen, J. (1982). Posterior parietal lobe of the primate brain. Physiol Rev *62*, 1060–1129. https://doi.org/10.1152/physrev.1982.62.3.1060.

Izquierdo, A., Suda, R.K., and Murray, E.A. (2004). Bilateral Orbital Prefrontal Cortex Lesions in Rhesus Monkeys Disrupt Choices Guided by Both Reward Value and Reward Contingency. J. Neurosci. *24*, 7540–7548. https://doi.org/10.1523/JNEUROSCI.1921-04.2004.

Jeurissen, D., Shushruth, S., El-Shamayleh, Y., Horwitz, G.D., and Shadlen, M.N. (2021). Deficits in decision-making induced by parietal cortex inactivation are compensated at two time scales. 2021.09.10.459856. https://doi.org/10.1101/2021.09.10.459856.

Johnson, B., Verma, R., Sun, M., and Hanks, T.D. (2017). Characterization of decision commitment rule alterations during an auditory change detection task. Journal of Neurophysiology *118*, 2526–2536. https://doi.org/10.1152/jn.00071.2017.

Kaas, J.H., and Hackett, T.A. (2000). Subdivisions of auditory cortex and processing streams in primates. Proc Natl Acad Sci U S A *97*, 11793–11799. .

Kalatsky, V.A., Polley, D.B., Merzenich, M.M., Schreiner, C.E., and Stryker, M.P. (2005). Fine functional organization of auditory cortex revealed by Fourier optical imaging. PNAS *102*, 13325–13330. https://doi.org/10.1073/pnas.0505592102.

Katz, L.N., Yates, J.L., Pillow, J.W., and Huk, A.C. (2016). Dissociated functional significance of decision-related activity in the primate dorsal stream. Nature *535*, 285–288. https://doi.org/10.1038/nature18617.

Kelly, J.B. (1970). The effects of lateral lemniscal and neocortical lesions on auditory absolute thresholds and frequency difference thresholds of the rat. ProQuest Information & Learning.

Kelly, J.B., and Glazier, S.J. (1978). Auditory cortex lesions and discrimination of spatial location by the rat. Brain Res *145*, 315–321. https://doi.org/10.1016/0006-8993(78)90865-x.

Kelly, S.P., and O'Connell, R.G. (2015). The neural processes underlying perceptual decision making in humans: Recent progress and future directions. Journal of Physiology-Paris *109*, 27–37. https://doi.org/10.1016/j.jphysparis.2014.08.003.

Kiani, R., Hanks, T.D., and Shadlen, M.N. (2008). Bounded Integration in Parietal Cortex Underlies Decisions Even When Viewing Duration Is Dictated by the Environment. J Neurosci *28*, 3017–3029. https://doi.org/10.1523/JNEUROSCI.4761-07.2008.

Kim, J.-N., and Shadlen, M.N. (1999). Neural correlates of a decision in the dorsolateral prefrontal cortex of the macaque. Nature Neuroscience *2*, 176–185. https://doi.org/10.1038/5739.

Krebs, J.R. (1983). Animal behaviour: From Skinner box to the field. Nature *304*, 117. https://doi.org/10.1038/304117a0.

Langner, G., Albert, M., and Briede, T. (2002). Temporal and spatial coding of periodicity information in the inferior colliculus of awake chinchilla (Chinchilla laniger). Hear Res *168*, 110–130. https://doi.org/10.1016/s0378-5955(02)00367-2.

LeDoux, J.E., Farb, C.R., and Romanski, L.M. (1991). Overlapping projections to the amygdala and striatum from auditory processing areas of the thalamus and cortex. Neuroscience Letters *134*, 139–144. https://doi.org/10.1016/0304-3940(91)90526-Y.

Licata, A.M., Kaufman, M.T., Raposo, D., Ryan, M.B., Sheppard, J.P., and Churchland, A.K. (2017). Posterior Parietal Cortex Guides Visual Decisions in Rats. The Journal of Neuroscience *37*, 4954–4966. https://doi.org/10.1523/JNEUROSCI.0105-17.2017.

Luethke, L.E., Krubitzer, L.A., and Kaas, J.H. (1989). Connections of primary auditory cortex in the new world monkey, Saguinus. Journal of Comparative Neurology *285*, 487–513. https://doi.org/10.1002/cne.902850406.

Lynch, J.C., Graybiel, A.M., and Lobeck, L.J. (1985). The differential projection of two cytoarchitectonic subregions of the inferior parietal lobule of macaque upon the deep layers of the superior colliculus. J Comp Neurol *235*, 241–254. https://doi.org/10.1002/cne.902350207.

Malhotra, S., and Lomber, S.G. (2007). Sound Localization During Homotopic and Heterotopic Bilateral Cooling Deactivation of Primary and Nonprimary Auditory Cortical Areas in the Cat. Journal of Neurophysiology *97*, 26–43. https://doi.org/10.1152/jn.00720.2006.

Malmierca, M.S. (2003). The structure and physiology of the rat auditory system: an overview. Int Rev Neurobiol *56*, 147–211. https://doi.org/10.1016/s0074-7742(03)56005-6.

Mante, V., Sussillo, D., Shenoy, K.V., and Newsome, W.T. (2013). Context-dependent computation by recurrent dynamics in prefrontal cortex. Nature *503*, 78–84. https://doi.org/10.1038/nature12742.

McMillen, T., and Holmes, P. (2006). The dynamics of choice among multiple alternatives. Journal of Mathematical Psychology *50*, 30–57. https://doi.org/10.1016/j.jmp.2005.10.003.

Mcnaughton, B.L., Leonard, B., and Chen, L. (1989). Cortical-hippocampal interactions and cognitive mapping: A hypothesis based on reintegration of the parietal and inferotemporal pathways for visual processing. Psychobiology *17*, 230–235. https://doi.org/10.1007/BF03337774.

McNaughton, B.L., Mizumori, S.J.Y., Barnes, C.A., Leonard, B.J., Marquis, M., and Green, E.J. (1994). Cortical Representation of Motion during Unrestrained Spatial Navigation in the Rat. Cerebral Cortex *4*, 27–39. https://doi.org/10.1093/cercor/4.1.27.

Mesulam, M.M., and Pandya, D.N. (1973). The projections of the medial geniculate complex within the sylvian fissure of the rhesus monkey. Brain Res *60*, 315–333. https://doi.org/10.1016/0006-8993(73)90793-2.

Mishkin, M. (1972). Cortical Visual Areas and Their Interactions. In Brain and Human Behavior, A.G. Karczmar, and J.C. Eccles, eds. (Berlin, Heidelberg: Springer), pp. 187–208.

Monchi, O., Petrides, M., Petre, V., Worsley, K., and Dagher, A. (2001). Wisconsin Card Sorting Revisited: Distinct Neural Circuits Participating in Different Stages of the Task Identified by Event-Related Functional Magnetic Resonance Imaging. J. Neurosci. *21*, 7733–7741. https://doi.org/10.1523/JNEUROSCI.21-19-07733.2001.

Murphy, F.C., Rubinsztein, J.S., Michael, A., Rogers, R.D., Robbins, T.W., Paykel, E.S., and Sahakian, B.J. (2001). Decision-making cognition in mania and depression. Psychol Med *31*, 679–693. https://doi.org/10.1017/s0033291701003804.

Nestadt, G., Kamath, V., Maher, B.S., Krasnow, J., Nestadt, P., Wang, Y., Bakker, A., and Samuels, J. (2016). Doubt and the decision-making process in obsessive-compulsive disorder. Medical Hypotheses *96*, 1–4. https://doi.org/10.1016/j.mehy.2016.09.010.

Olsen, G.M., and Witter, M.P. (2016). Posterior parietal cortex of the rat: Architectural delineation and thalamic differentiation. J Comp Neurol *524*, 3774–3809. https://doi.org/10.1002/cne.24032.

Olsen, G.M., Hovde, K., Kondo, H., Sakshaug, T., Sømme, H.H., Whitlock, J.R., and Witter, M.P. (2019). Organization of Posterior Parietal–Frontal Connections in the Rat. Front. Syst. Neurosci. *13*. https://doi.org/10.3389/fnsys.2019.00038.

Ossmy, O., Moran, R., Pfeffer, T., Tsetsos, K., Usher, M., and Donner, T.H. (2013). The Timescale of Perceptual Evidence Integration Can Be Adapted to the Environment. Current Biology *23*, 981–986. https://doi.org/10.1016/j.cub.2013.04.039.

Pandya, D.N., Hallett, M., and Kmukherjee, S.K. (1969). Intra- and interhemispheric connections of the neocortical auditory system in the rhesus monkey. Brain Res *14*, 49–65. https://doi.org/10.1016/0006-8993(69)90030-4.

Pasupathy, A., and Miller, E.K. (2005). Different time courses of learning-related activity in the prefrontal cortex and striatum. Nature *433*, 873–876. https://doi.org/10.1038/nature03287.

Paxinos, G., and Watson, C. (2013). The Rat Brain in Stereotaxic Coordinates (Elsevier Science).

Phillips, D.P., and Irvine, D.R.F. (1981). Responses of single neurons in physiologically defined area AI of cat cerebral cortex: sensitivity to interaural intensity differences. Hearing Research *4*, 299–307. https://doi.org/10.1016/0378-5955(81)90014-9.

Piet, A.T., El Hady, A., and Brody, C.D. (2018). Rats adopt the optimal timescale for evidence integration in a dynamic environment. Nat Commun *9*, 4265. https://doi.org/10.1038/s41467-018-06561-y.

Purcell, B.A., and Kiani, R. (2016). Neural Mechanisms of Post-error Adjustments of Decision Policy in Parietal Cortex. Neuron *89*, 658–671. https://doi.org/10.1016/j.neuron.2015.12.027.

Purves, D., Augustine, G.J., Fitzpatrick, D., Katz, L.C., LaMantia, A.-S., McNamara, J.O., and Williams, S.M. (2001). The Auditory Cortex. Neuroscience. 2nd Edition.

Raposo, D., Kaufman, M.T., and Churchland, A.K. (2014). A category-free neural population supports evolving demands during decision-making. Nat Neurosci *17*, 1784–1792. https://doi.org/10.1038/nn.3865.

Ratcliff, R., and McKoon, G. (2008). The Diffusion Decision Model: Theory and Data for Two-Choice Decision Tasks. Neural Comput *20*, 873–922. https://doi.org/10.1162/neco.2008.12-06-420.

Ratcliff, R., and Rouder, J.N. (1998). Modeling Response Times for Two-Choice Decisions. Psychol Sci *9*, 347–356. https://doi.org/10.1111/1467-9280.00067.

Reep, R.L., Chandler, H.C., King, V., and Corwin, J.V. (1994). Rat posterior parietal cortex: topography of corticocortical and thalamic connections. Exp Brain Res *100*, 67–84. https://doi.org/10.1007/BF00227280.

Roitman, J.D., and Shadlen, M.N. (2002). Response of Neurons in the Lateral Intraparietal Area during a Combined Visual Discrimination Reaction Time Task. J. Neurosci. *22*, 9475–9489. .

Romanski, L.M. (2007). Representation and Integration of Auditory and Visual Stimuli in the Primate Ventral Lateral Prefrontal Cortex. Cerebral Cortex *17*, i61–i69. https://doi.org/10.1093/cercor/bhm099.

Romo, R., Merchant, H., Zainos, A., and Hernández, A. (1996). Categorization of somaesthetic stimuli: sensorimotor performance and neuronal activity in primary somatic sensory cortex of awake monkeys. Neuroreport *7*, 1273–1279. .

Romo, R., Hernández, A., Salinas, E., Brody, C.D., Zainos, A., Lemus, L., Lafuente, V. de, and Luna, R. (2002). From sensation to action. Behavioural Brain Research *135*, 105–118. https://doi.org/10.1016/S0166-4328(02)00161-4.

Runyan, C.A., Piasini, E., Panzeri, S., and Harvey, C.D. (2017). Distinct timescales of population coding across cortex. Nature *548*, 92–96. https://doi.org/10.1038/nature23020.

Rutkowski, R.G., Miasnikov, A.A., and Weinberger, N.M. (2003). Characterisation of multiple physiological fields within the anatomical core of rat auditory cortex. Hearing Research *181*, 116–130. https://doi.org/10.1016/S0378-5955(03)00182-5.

Saenz, M., and Langers, D.R.M. (2014). Tonotopic mapping of human auditory cortex. Hearing Research *307*, 42–52. https://doi.org/10.1016/j.heares.2013.07.016.

Scott, B.H., and Mishkin, M. (2016). Auditory short-term memory in the primate auditory cortex. Brain Research *1640*, 264–277. https://doi.org/10.1016/j.brainres.2015.10.048.

Shadlen, M.N., and Newsome, W.T. (1996). Motion perception: seeing and deciding. Proceedings of the National Academy of Sciences *93*, 628–633. https://doi.org/10.1073/pnas.93.2.628.

Smith, P.L., and Ratcliff, R. (2004). Psychology and neurobiology of simple decisions. Trends in Neurosciences *27*, 161–168. https://doi.org/10.1016/j.tins.2004.01.006.

Snyder, L.H., Batista, A.P., and Andersen, R.A. (1997). Coding of intention in the posterior parietal cortex. Nature *386*, 167–170. https://doi.org/10.1038/386167a0.

Thura, D., and Cisek, P. (2017). The Basal Ganglia Do Not Select Reach Targets but Control the Urgency of Commitment. Neuron *95*, 1160-1170.e5. https://doi.org/10.1016/j.neuron.2017.07.039.

Tsunada, J., Liu, A.S.K., Gold, J.I., and Cohen, Y.E. (2016). Causal contribution of primate auditory cortex to auditory perceptual decision-making. Nat Neurosci *19*, 135–142. https://doi.org/10.1038/nn.4195.

van Vugt, M., Simen, P., Nystrom, L., Holmes, P., and Cohen, J. (2012). EEG Oscillations Reveal Neural Correlates of Evidence Accumulation. Frontiers in Neuroscience *6*. .

Wald, A., and Wolfowitz, J. (1948). Optimum Character of the Sequential Probability Ratio Test. The Annals of Mathematical Statistics *19*, 326–339. https://doi.org/10.1214/aoms/1177730197.

Wald, A., and Wolfowitz, J. (1950). Bayes Solutions of Sequential Decision Problems. The Annals of Mathematical Statistics *21*, 82–99. https://doi.org/10.1214/aoms/1177729887.

Whitlock, J.R., Sutherland, R.J., Witter, M.P., Moser, M.-B., and Moser, E.I. (2008). Navigating from hippocampus to parietal cortex. Proceedings of the National

Academy of Sciences *105*, 14755–14762. https://doi.org/10.1073/pnas.0804216105.

Wigestrand, M.B., Schiff, H.C., Fyhn, M., LeDoux, J.E., and Sears, R.M. (2017). Primary auditory cortex regulates threat memory specificity. Learning & Memory *24*, 55–58. https://doi.org/10.1101/lm.044362.116.

van Wouwe, N.C., Kanoff, K.E., Claassen, D.O., Richard Ridderinkhof, K., Hedera, P., Harrison, M.B., and Wylie, S.A. (2016). The Allure of High-Risk Rewards in Huntington's disease. Journal of the International Neuropsychological Society *22*, 426–435. https://doi.org/10.1017/S1355617715001241.

Wyart, V., de Gardelle, V., Scholl, J., and Summerfield, C. (2012). Rhythmic Fluctuations in Evidence Accumulation during Decision Making in the Human Brain. Neuron *76*, 847–858. https://doi.org/10.1016/j.neuron.2012.09.015.

Yao, J.D., Bremen, P., and Middlebrooks, J.C. (2013). Rat primary auditory cortex is tuned exclusively to the contralateral hemifield. J Neurophysiol *110*, 2140–2151. https://doi.org/10.1152/jn.00219.2013.

Yu, L., Hu, J., Shi, C., Zhou, L., Tian, M., Zhang, J., and Xu, J. (2021). The causal role of auditory cortex in auditory working memory. ELife *10*, e64457. https://doi.org/10.7554/eLife.64457.

Zhou, Y., and Freedman, D.J. (2019). Posterior parietal cortex plays a causal role in perceptual and categorical decisions. Science *365*, 180–185. https://doi.org/10.1126/science.aaw8347.

Znamenskiy, P., and Zador, A.M. (2013). Corticostriatal neurons in auditory cortex drive decisions during auditory discrimination. Nature *497*, 482–485. https://doi.org/10.1038/nature12077.

Chapter 2:

Flexibility of timescales of evidence evaluation for decision making

Results and Discussion

The adaptive selection of behavior requires choosing appropriate actions based on available information. In many instances, adaptive behaviors are guided by detecting subtle signals in a dynamic environment. Previous studies have shown that humans, monkeys, and rodents are capable of quickly extracting information about the variability of changes in dynamic environments [2–5]; moreover, subjects can alter their timescale of evidence evaluation -- that is, the time period over which evidence has leverage over a decision -- based on the expected duration of signals in order to make judgments of when an actual signal occurs [1]. After individuals make a decision, the past evidence can be utilized for additional purposes, including the judgments of the degree of confidence that the selected option is correct [6–22]. To shed light on the flexibility of evidence evaluation, we examined if and how different timescales of evidence are utilized for change detection reports while subjects performed an auditory change detection task compared to confidence judgements in trials without detection reports.

Auditory change detection task

We trained subjects to perform an auditory change detection task in which they reported a change in the underlying rate in a sequence of auditory clicks generated by a stochastic Poisson process. Trials began when a subject placed their finger into a central port, which was followed by the onset of the auditory stimulus (**Figure 1**). The underlying rate was initially 50 Hz, and for 70% of trials, the rate increased at a random time and by a variable magnitude. The other 30% of trials ended without a change (catch trials). Subjects were required to remove their finger from the central port within 800 ms of change onset (hit) or withhold responding for catch trials (correct rejection;

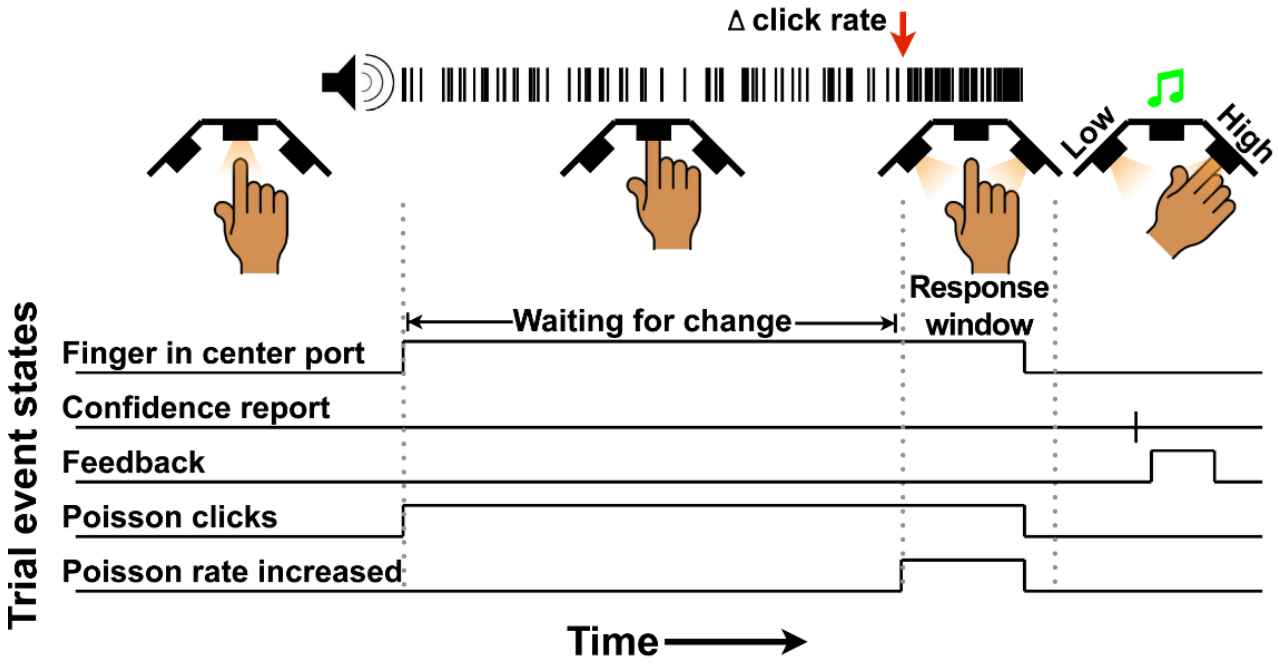

Figure 1. Auditory change detection task with confidence report showing the sequence of events for each trial: A trial began when the center port was illuminated, cuing subjects to insert their finger. Once the finger was inserted, a stream of auditory clicks began to play. The clicks were generated by a Poisson process with a generative baseline click rate of 50 Hz. 30% of trials were catch trials with no change in the generative click rate. In the other 70% of trials, the generative click rate increased by 10, 30, or 50 Hz at a random point (red arrow in example). Subjects had to withdraw their finger within 800 ms of the change for the trial to qualify as a hit on change trials, or withhold a response for the trial to qualify as a CR on catch trials. At the end of the trial (after response or stimulus end), the two peripheral ports illuminated, cuing subjects to indicate confidence in their decision: engaging the left port reported low confidence while engaging the right reported high confidence. Immediately following the confidence report, feedback was given via an auditory tone to indicate success or failure on that trial.

CR). There were two types of errors in this task: premature responses (false alarms; FA), which can occur in catch and non-catch trials, and failures to respond in time (misses). In all cases, subjects were then cued to report confidence using the two side ports. Confidence was assessed via a post-decision wager. Immediately following the

confidence report, feedback was given via an auditory tone to indicate success or failure on that trial.

Task performance and confidence ratings

All subjects were able to perform the task with high hit rates for the easiest trials and diminishing hit rates for medium and high difficulty trials (**Figure 2A**, left; see **Figure S1** for individual subject data), suggesting that they were attending to the stimuli. During catch trials, subjects displayed CR rates of ~85% or above, with a ~15% FA rate across both trial types (**Figure 2A**, right). For both hits and misses, confidence scaled with trial difficulty, with the largest changes in click rates evoking the highest level of confidence during hits and the lowest level of confidence during misses (**Figure 2B**, left). CR and FA trials by definition involved no change in the underlying generative click rate and evoked intermediate levels of confidence compared to hits and misses (**Figure 2B**, right).

Psychophysical reverse correlation

To examine the timescale of evidence evaluation, we first conducted psychophysical reverse correlation (RC) analyses [15,23–25]. RC traces were constructed by convolving click times with causal half-Gaussian filters (σ = 0.05s) and aligning the result to the end of the stimulus presentation. This allowed us to reconstruct the average stimulus that preceded a given trial outcome and confidence rating. We focused our initial analyses on FA trials and their associated confidence ratings. On these trials, responses were only affected by natural fluctuations in the stochastic stimulus and not tied to a generative change in click rate as occurs for hit trials. To

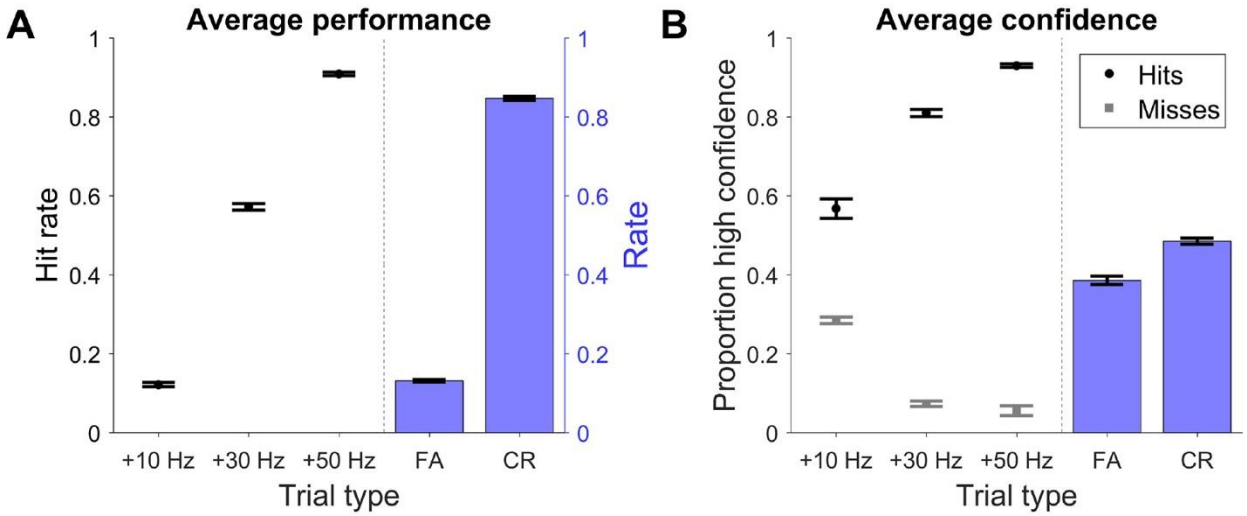

Figure 2. Task performance and confidence ratings: **A**, Combined data from 7 subjects showing performance as a function of the change in click rate (left) and proportion of FA and CR trials (right). Hit rate was calculated excluding FA trials. FA rate was calculated from all trial types. CR rate was calculated from trials in which no change in generative click rate occurred (30% of trials). **B**, Proportion of high confidence hits (black) and misses (gray) as a function of change in click rate (left) and proportion of high confidence FA and CRs (right). Error bars indicate +/- SEM. See Figure S1.

examine overall influence on choice independent of confidence, all FA RC traces were averaged together. Across subjects, FA choices were characterized by an average RC trace (hereafter referred to as the detection report kernel) showing a transient increase in click rate, which followed a time-course with a duration similar to the response window in which subjects were allowed to report an actual change in the generative click rate (**Figure 3A;** see **Figure S2** for individual subject data). There was a sharp increase starting ~800 ms before the detection report that collapsed to baseline just before the report, indicative of sensorimotor delays limiting the influence of the time period just before the response. Comparing RCs from high and low confidence FA trials (**Figure 3B;** see **Figure S2** for individual subject data), we found that evidence for confidence judgements was used during the period after which the detection report kernel returned

to baseline (**Figure S3**), consistent with previous work using a different task design that showed that confidence is based on continued accumulation of evidence after the decision but before the confidence response [26].

We next asked whether there is an influence of evidence on confidence that extends earlier in time than its influence on detection reports as this would be indicative of evidence being evaluated at multiple timescales. Surprisingly, we found that the point in time when RC kernels deviated from baseline differs depending on what is reported. In particular, kernels began to deviate from baseline for CR confidence reports earlier in time than for detection reports. To quantify this for detection reports, we fit the ascending phase of the detection report kernel with a 2-piece linear function (see methods). Across subjects, the parameter estimate of the detection report kernel start point was ~0.74 seconds (95% CI: 0.73 to 0.75 s) preceding the detection report (**Figure 3A**, arrow).

In contrast, the period of influence of evidence for CR confidence reports extended considerably earlier in time. High confidence CRs were characterized by a lower average click rate preceding the end of the stimulus compared with low confidence CRs (**Figure 3C;** see **Figure S2** for individual subject data). This difference gradually increased until the end of the trial. To estimate the point in time when the difference between high and low confidence CR reverse correlation deviated from baseline, we fit the difference (the "CR confidence difference kernel") with a 2-piece linear function (see methods). Across subjects, the pooled parameter estimate for when the CR confidence difference kernel diverged (i.e. differed from 0 Hz) was ~1.76 seconds before the end of the trial (95% CI: 1.68 to 1.84 s), more than twice as early as

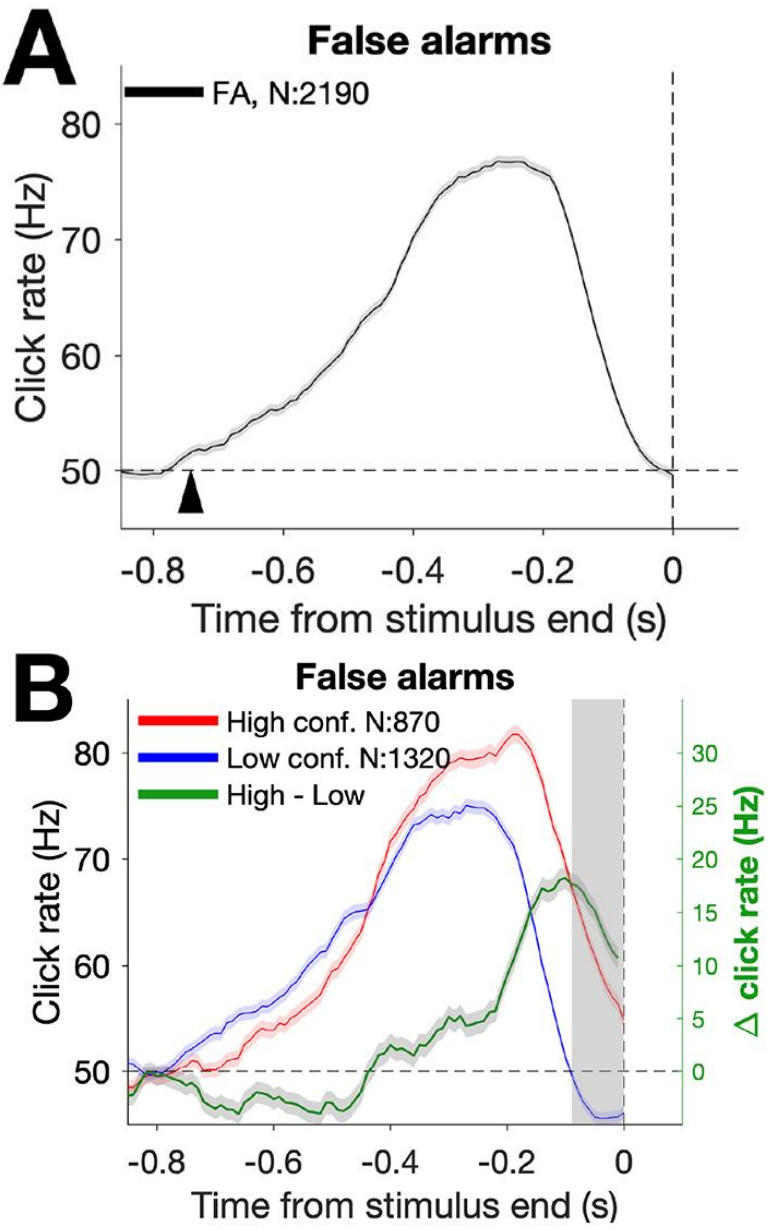
A
False alarms
FA, N:2190
Click rate (Hz)
80
70
60
50
-0.8
-0.6
-0.4
-0.2
0
Time from stimulus end (s)
B
False alarms
High conf. N:870
Low conf. N:1320
High - Low
Click rate (Hz)
80
70
60
50
30
25
20
15
10
5
0
Δ click rate (Hz)
-0.8
-0.6
-0.4
-0.2
0
Time from stimulus end (s)

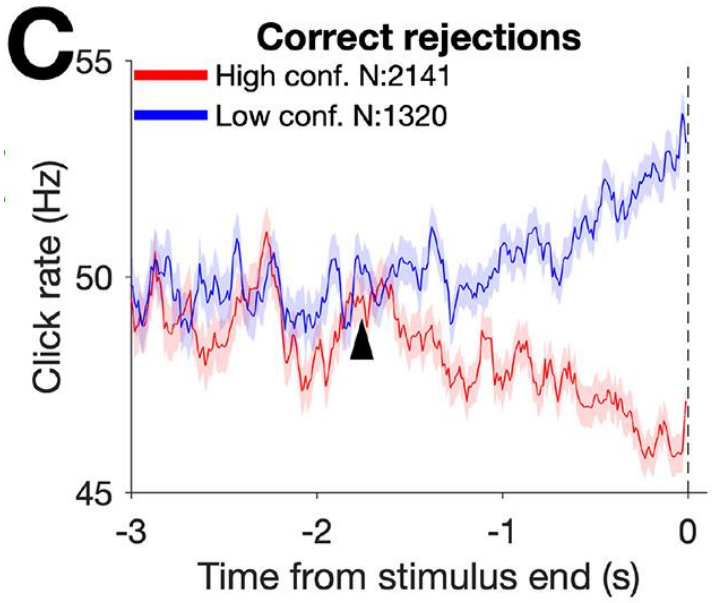

Figure 3. FA and CR reverse correlations: Combined data from 7 subjects was used to calculate average click rate over time for each outcome. RC traces were constructed by convolving click times preceding outcomes with causal half-Gaussian filters (σ = 0.05 s). **A**, Detection report kernel. RC trace (black line) is comprised of all FA trials, showing the average click rate preceding FAs. The start of the detection report kernel (arrow) was estimated by fitting the ascending phase of the kernel with a 2-piece linear function with 3 free parameters: the baseline click rate (left of arrow), the slope of the kernel's ascending phase (right of arrow), and the start of the ascending phase (arrow). Horizontal dotted line denotes the 50 Hz baseline generative click rate. **B**, Detection report confidence kernels. RC traces show the average click rate preceding high (red) and low (blue) confidence FAs, as well as the difference in click rate between the two confidence kernels (high - low; green). Same conventions as in **A**. The shaded portion of the graph near time 0 shows the temporal interval analyzed in Figure S3A. **C**, CR confidence kernels. As in **B**, but showing RC traces preceding CRs. The divergence point between the two confidence kernels (arrow) was estimated by fitting the difference between the two kernels (high - low; CR confidence difference kernel) with a 2-piece linear function with 2 free parameters (see Figure S2, column 4 for fits): the divergence point from a baseline difference of 0 Hz (arrow) and the slope from that point onward. For all kernels, shaded region shows +/- SEM. N = number of trials for each trace. See Figure S2 and S3.

the estimate of the start of the detection report kernels. This suggests that during the course of a trial, subjects have flexibility in the timescale of evidence evaluation, with different timescales more strongly linked to different types of reports.

Model-based analysis

While psychophysical RC analyses provide useful information for comparing the timescales of evidence evaluation, they are not a veridical representation of how evidence is temporally evaluated because they reflect the influence of a number of different components of evidence processing [27]. Therefore, we adopted a model-based approach to ask whether a single timescale of evidence evaluation can explain the differing start points revealed by the RC analyses. In the model, evidence in the form of the auditory clicks was convolved with a half-Gaussian filter with its width (σ) as a free parameter (**Figure 4A**). The filter width determined the timescale of evidence evaluation, with a wider filter corresponding to a longer timescale. The output of the filter governed the average dynamics of a decision variable. Variability was included in the process by adding Gaussian noise to the decision variable at each timestep with the standard deviation of the Gaussian as a second free parameter in the model. A third free parameter set a decision bound that caused triggering of a detection report when the decision variable reached that value. To account for sensorimotor delays inherent to decision processes, an additional period of "non-decision time" described by a Gaussian distribution with mean set by a fourth free parameter was added to the bound-crossing time to determine the final response time.

We first used this model to capture the choice behavior exhibited by our subjects. In particular, we found the values for the four free parameters of the model that best fit

the trial-by-trial choice responses made by our subjects (see methods). This yielded psychometric functions that closely approximated the behavioral data (**Figure 4B**). We then used model simulations with the best fit parameters to extract predictions for the detection report kernels and CR confidence difference kernels. These trials were classified as high or low confidence based on whether the final decision variable was higher or lower than a threshold set to 49 Hz. Comparing the predicted kernels to the actual data, we found that this single-timescale model predicted a start of the detection report kernel that was slightly earlier than the data (29.3 ± 6.4 ms earlier). Critically, this model predicted a start of the divergence of the CR confidence difference kernels that was substantially later than the experimental data (894.8 ± 12.6 ms later) (**Figure 4C**). We found similar results with a variety of filter shapes and non-decision time distributions (data not shown). We also tested whether trial-to-trial variability in decision bound could extend the divergence of CR confidence difference kernels closer to the experimental data, but we found no set of parameters capable of doing so (**Figure S4**). Finally, we extended the timescale of evidence evaluation in the model with a longer filter width to recapitulate the experimental divergence of the CR confidence difference kernels. In doing so, we found that the model predicted a start of the detection report kernel that was substantially earlier than the data (1082.6 ± 40.1 ms earlier). These analyses confirm our intuition that a neural mechanism with a single timescale of evidence evaluation cannot explain the result that the divergence of CR confidence difference kernels can extend more than twice as early relative to trial end than detection report kernels.

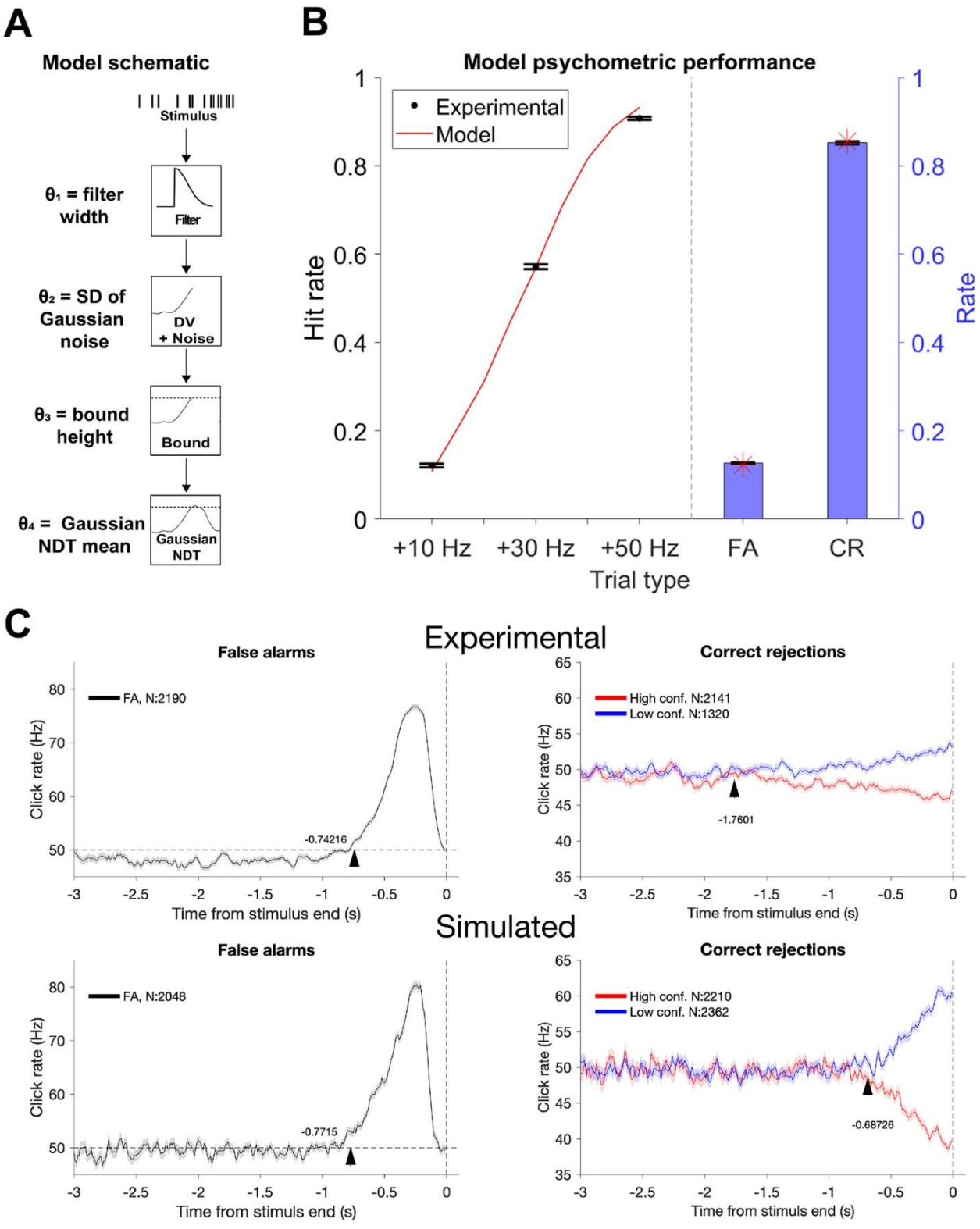
A
Model schematic
Stimulus
θ1 = filter width
Filter
θ2 = SD of Gaussian noise
DV + Noise
θ3 = bound height
Bound
θ4 = Gaussian NDT mean
Gaussian NDT
B
Model psychometric performance
Experimental
Model
Hit rate
Rate
+10 Hz
+30 Hz
+50 Hz
FA
CR
Trial type
C
Experimental
False alarms
FA, N:2190
Click rate (Hz)
-0.74216
Time from stimulus end (s)
Correct rejections
High conf. N:2141
Low conf. N:1320
-1.7601
Simulated
False alarms
FA, N:2048
-0.7715
Time from stimuls end (s)
Correct rejections
High conf. N:2210
Low conf. N:2362
-0.68726

Figure 4. Model simulation of behavioral data: **A**, Model schematic. The model included four free parameters: width of half-Gaussian filter (0.96 s), decision variable noise term standard deviation (13 Hz), decision bound (103 Hz), and mean Gaussian NDT (0.17 s). Best fit parameters are in parentheses. **B**, Model comparison with *psychometric data based on best fit parameters. Error bars indicate +/- SEM (as in Fig. 2). The red line indicates model hit rate as a function of change in click rate, with additional interpolated delta click rates (+15 Hz, +20 Hz, +25 Hz, +35 Hz, +40 Hz, +45 Hz). Red stars indicate FA and CR rates for the model.* ***C****, Experimental and simulated RCs. See Figure S4.*

Our study demonstrates that, in perceptual decisions, the timescale of evaluation of past evidence can be flexibly adjusted for use in detection and separately for confidence judgments when no detection is reported. This was revealed using a change detection task in which perfect integration of evidence is suboptimal. With perfect integration, evidence accumulated early retains its influence on the decision for the full duration of the deliberation period, which is the optimal strategy during perceptual discrimination tasks based on the full stimulus. In contrast, evidence has a more transient influence in our change detection task [24]. By including an additional confidence report, this paradigm allowed us to test whether the limited temporal influence of evidence on decision formation was similar for confidence judgments. We found that kernels for judgments of confidence could be influenced by evidence fluctuations earlier in time on trials without a detection report. Interestingly, information within different temporal epochs appears to be used for confidence judgments in a way that depends on how the trial ended. When the subject terminated the evidence stream by reporting a detection, as in the case of FAs, the confidence-influencing epoch began at approximately the same time as the detection report kernel. However, when the trial ended due to withholding a detection report, as in the case of CRs, the confidence-influencing epoch extended several hundred milliseconds earlier than the detection report kernel. While averaging

over many trials prevents us from quantifying which epochs of time had influence on a trial-to-trial basis, the magnitude of the mean psychophysical kernel nonetheless relates to the magnitude and frequency of evidence evaluation during a given epoch across trials.

Model-based analyses confirmed that our results cannot be explained by a neural mechanism involving a single, fixed timescale of evidence evaluation. The differences in the evidence evaluation period that we found between conditions, which reveal flexibility in the process, provide insights for the requirements of any specific mechanism responsible for this discrepancy. In particular, our results suggest that the mechanism, whatever it may be, has the capacity to either adjust the timescale of evidence weighting during individual deliberative decisions or access multiple distinct timescales for different purposes. We discuss possible representational architectures of the brain that would enable this below.

It is unclear why subjects adjusted their timescales of evidence evaluation depending on how the trial terminated. It is optimal to utilize evidence over the last 800ms for detection and associated confidence because if there was a change, it could have only happened in this period in this task. Thus, it is suboptimal for subjects to base their confidence on earlier evidence, as was observed in CR trials. However, we suggest it may be optimal in the more general class of change detection decisions individuals encounter in real life. Typically, confidence in a choice based on a perceived change should be judged based on recent evidence that evoked the perceived change. In contrast, confidence that no change has occurred in a real-world situation often involves judgment based on a longer interval of time during which a change would have been

possible. Our results are consistent with a strategy that would be appropriate for that more general type of situation.

Our results show that past evidence must be represented in a way that allows flexibility in the timescale of evidence evaluation. This extends the idea that adapting the timescale of evidence evaluation is necessary to optimize decision processes in changing environments [1,2,4,28]. In those studies, the dynamics of the environment dictate the optimal timescale, but only one timescale needs to be accessible for any given context or trial. In contrast, we find that multiple timescales of evidence are used within the same context. Thus, mechanisms are necessary to adjust the timescale of evaluation even as the evidence is being presented and used. Mid-deliberation adjustments of decision processes have been described extensively with regard to decision bounds. Collapsing decision bounds can furnish urgency onto the decision process [29–31], and changes of mind about decisions and confidence are best explained with altered post-commitment decision bounds [26]. In most of those cases, decisions were made in situations that involved near perfect integration of sensory evidence, so there was no opportunity to look for changes in the timescale of evidence evaluation at earlier periods of deliberation. Here we show this timescale to be an important factor that can be adjusted online during deliberations based on a single stream of evidence.

Previous studies with yes-no detection tasks have suggested separate neural representations for stimulus present and stimulus absent choices [32,33]. While those tasks involved a delay between the stimulus epoch and the choice report (unlike our task), the separate neural representations they found could provide a substrate for distinct timescales of evidence evaluation. Thus, one possible neural architecture that could

explain our results is having one population of neurons evaluating evidence over a shorter timescale for the detection decision and another population of neurons evaluating evidence in parallel over a longer timescale for confidence judgments on trials without a detection report. We suggest that neural mechanisms that allow flexibility in the timescale of evidence evaluation may be used in the service of multiple components of decision making behavior, rather than flexibility being a unique feature of decisions that are combined with confidence judgments.

It is tempting to speculate that recurrent network models of integration that require a fine level of tuning to avoid leaky dynamics [34], which is usually viewed as a shortcoming [35], may instead be a virtue by providing flexibility in the timescale of evidence evaluation. Under this idea, changes in the timescales of evidence evaluation could be introduced through small adjustments of tuning that would result in altered leakiness of integration. Alternatively, flexibility in the timescale of evidence evaluation could be implemented at an earlier stage of sensory processing, such as through gating of deliberation by stimulus salience [36,37]. In this alternative schema, sensory responses must exceed a salience threshold to be considered for the decision process, and alterations of the salience threshold would influence the evidence evaluation process. Neither of these mechanisms alone allows use of multiple timescales of evidence evaluation for the same stream of evidence. Memory traces that allow recall and re-processing of past evidence would be one mechanism to use multiple timescales of evidence evaluation for the same stream of evidence. Another related mechanism that would allow parallel access to multiple timescales for the same stream of evidence derives from theoretical work showing that memory traces may be encoded through

neurons with heterogeneous dynamics that form a temporal basis set for previous events [38]. Selective readout of sets of neurons with differing timescales would allow flexible access that depends on task demands [39,40]. This would be readily achievable in networks that encode accumulated evidence with a diversity of timescales [41]. This mechanism could also allow adjustments of the timescale of evidence evaluation even after the evidence has been presented, which would enable meta-cognitive operations [11,42,43]. We therefore suggest that our paradigm provides a powerful approach to understand the neural mechanisms and representational architectures in the brain that could support meta-cognitive operations for decision making.

Acknowledgements

We thank Mark Goldman for helpful discussions and Shuqi Wang for helping to improve the efficiency of model-based analyses. This research was supported by a National Alliance for Research on Schizophrenia and Depression Young Investigator Award to T.D.H. and a Whitehall Foundation Grant.

Author Contributions

Conceptualization, T.D.H., P.G., R.H., A.B.G.; Methodology, T.D.H., P.G., R.H., A.B.G.; Software, T.D.H., P.G., R.H., A.B.G.; Validation, R.H.; Formal Analysis, T.D.H., P.G., R.H.; Investigation, T.D.H., P.G., R.H., A.B.G.; Resources, T.D.H.; Data Curation, T.D.H., P.G., R.H., A.B.G.; Writing -- Original Draft, T.D.H., P.G., R.H., A.B.G.; Writing -- Review and Editing, T.D.H., P.G., R.H., A.B.G.; Visualization, T.D.H., P.G., R.H., A.B.G.; Supervision, T.D.H., P.G., R.H., A.B.G.; Funding Acquisition, T.D.H.

Declaration of Interests

The authors declare no competing interests.

STAR Methods

CONTACT FOR REAGENT AND RESOURCE SHARING

Further information and requests for resources and reagents should be directed to and will be fulfilled by the Lead Contact, Timothy Hanks (thanks@ucdavis.edu).

EXPERIMENTAL MODEL AND SUBJECT DETAILS

There were 7 subjects (2 female, 5 male) included in this study, all aged 18-34 and members of UC Davis. For the 7 subjects included for analysis, 3 subjects (S1, S2, S3) were knowledgeable about the task design and research motivations prior to data collection, while the remaining subjects were naive. Study procedures were approved by the UC Davis Institutional Review Board, and all subjects provided informed consent. Subjects were compensated with a $10 Amazon gift card for each 1-hour experimental session completed, for a total of 6-11 sessions. Each subject received full payment, irrespective of task performance.

METHOD DETAILS

Apparatus

Control of the task was programmed in MATLAB (Mathworks, RRID: SCR_001622) and facilitated by Bpod (Sanworks, RRID: SCR_015943), which measures output of behavioral tasks in real time. Task stimuli were generated by the open source device Pulse Pal [44]. The stimulus-response apparatus consisted of 3 cone-shaped ports, each containing an infrared LED beam that can detect the insertion of a finger when

the beam is obstructed. Each port can also be illuminated by an LED light, which signals to the subject that the port can be used during that stage of the trial. Sounds were played through headphones worn by the subject.

Change detection task

Subjects began each trial by inserting their index finger into the illuminated center port of the apparatus, which initiated a train of auditory clicks randomly generated by a Poisson process. The initial baseline frequency of this click train was 50 Hz, and the stimulus persisted at this frequency for a variable time period, during which the subject was to keep their finger in the port. In 70% of trials, the frequency of the stimulus increased with a magnitude of 10, 30, or 50 Hz at a random time sampled from a truncated exponential distribution (minimum 0.5 s, maximum 10 s, mean 4 s). This sampling produced an approximately flat hazard rate, such that the instantaneous probability of a change at the given moment did not increase or decrease as the trial progressed. When a change occurred, the subject was to respond by removing their finger from the port within 0.8 s of the change. The stimulus ended immediately upon finger removal. In the remaining 30% of trials (“catch” trials), no frequency increase occurred; in these trials, the subject was to maintain finger insertion for the full duration of the stimulus, which ended at a random time from 0.5 to 10.8 s. The same exponential distribution was used as for the change times in the non-catch trials plus the 0.8 s response window in order to match the distribution of catch trial durations to that of non-catch trials. Thus, the timing of trial termination provided no information about catch versus non-catch trial.

Finger removal occurring within the 0.8 s following a change was recorded as a “hit”. Failure to correctly respond in time to a change was recorded as a “miss”. Correctly

responding to catch trials required the subject to maintain finger insertion until the stimulus ended, which was recorded as a “correct rejection” (CR). Whereas, if a subject removed their finger from the port while there was no change in the generative rate of clicks, either on a catch or non-catch trial, the response was recorded as a “false alarm” (FA).

After the auditory stimulus concluded, the peripheral ports of the apparatus illuminated, cuing the subject to report confidence in the decision. Subjects were given a choice between “low” or “high” confidence, which was reported by inserting a finger into either the left or right peripheral port, respectively. Subjects were instructed to report low confidence if the subject was “probably not successful” and high confidence if the subject was “probably successful” in the trial. Performance was tracked by a points system: Reporting high confidence on a correct decision awarded the subject with 2 points, while low confidence on a correct decision yielded only 1 point. Reporting high confidence on an incorrect decision cost the subject 3 points, while reporting low confidence on these trials cost the subject only 1 point. A running total of accumulated points in the experimental block was displayed on a monitor in front of the subject as a blue bar that changed size with the points total, which could not fall below 0 points. This points scheme encouraged subjects to report high confidence for trials in which the evidence especially favored their choices, because they were asymmetrically punished for erroneous high confidence reports. Subjects then received auditory feedback on their initial decisions, regardless of confidence report, indicating whether the response was correct. The center port then illuminated once again, allowing the subject to start a new trial.

If the subject removed their finger in response to a perceived change, a brief noise was played through the headphones to indicate the response preceded the end of the stimulus. This “haptic feedback” sound allowed subjects to determine whether they reacted to perceived changes in time so that they were registered as detection reports. Thus, subjects knew that trials with haptic feedback were either hits or FAs, because a detection report was registered, while trials without haptic feedback were either misses or CRs, because a detection report was not registered. This feedback allowed subjects to report confidence with full knowledge of the decision that had been registered. The feedback did not indicate the correctness of the decision.

Supplemental instruction and post-training criteria

Before subject data was used for analysis, subjects completed training sessions until reaching performance criteria. Subjects advanced past this training stage after completing a session in which they attained hits in 45% of non-catch trials, avoided FAs on at least 75% of all trials, and had fewer than 1 mean “haptic errors” (high confidence misses with confidence reports occurring within 0.5 s of stimulus end) per block. We established this criterion for identifying haptic errors because if subjects reported confidence this quickly, they would likely have failed to incorporate the haptic feedback sound, or lack thereof. Their high confidence reports would thus be informed only by recognition of the change and not success in responding to it. Any haptic errors that occurred during data collection were not excluded from our analyses, though post-training haptic errors were rare. During training, we occasionally provided subjects with supplemental instruction to allow them to better understand the haptic feedback if they accumulated excess haptic errors. Additionally, to better furnish analyses that required a

large sample size of both confidence reports, we suggested to subjects who had low rates of high confidence judgments during training that they choose the “high confidence” option more often when certain of their decisions so that they may earn more points; subjects still established their own criteria for which trials to assign high confidence, given those supplemental instructions.

Model-based analyses

To further test whether our experimental results could be explained with a mechanism involving a single timescale of evidence evaluation, we used a model-based approach. With maximum likelihood estimation methods, we fit the behavioral choice data with a model that had four free parameters (**Figure 4A**). The first stage of the model was to convolve the auditory clicks (sensory evidence) with a filter having a half-Gaussian functional form with a free parameter for its standard deviation and the filter defined out to 3 standard deviations. We note that we also used other functional forms including exponential filters, square wave filters, and trapezoid filters with similar conclusions (data not shown). In all cases, the result of the convolution stage delineated the evolution of a decision variable over time. At the second stage of the model, noise was added to the decision variable at each time step with the noise taken from a Gaussian distribution with a free parameter for its standard deviation. Thus, for any given stream of clicks, there was a distribution of possible decision variable values at each point in time. The model prescribes detection reports for any part of this distribution that reaches or exceeds a threshold level set by a decision bound, the third free parameter of the model. To account for attrition due to detection reports, the remaining probability distribution of the decision variable decreased by the probability of bound crossing at each time step. Finally, to

account for non-decision sensory and motor processing that adds delays, an additional non-decision time (NDT) was added to the bound crossing time to yield the full reaction time. The non-decision time was taken from a Gaussian distribution with a free parameter for its mean and its standard deviation constrained to be one-fifth of the mean. It has been shown in other tasks that the shape of the non-decision time distribution can be quite variable across tasks/subjects and is not necessarily Gaussian [45]. Our model-based analysis results were robust to departures from the Gaussian non-decision time distribution that altered its skew (data not shown).

For any given set of parameters and sensory input, the model yields a probability distribution for the reaction times. Using this distribution of reaction times and the trial specifications, we calculated the probability of each trial outcome (hit, miss, FA, CR) for every trial performed by our subjects based on the stimulus that was presented. We used brute force grid search to find the values of the four free parameters that maximized the likelihood of the actual trial outcomes for every trial from the combined experimental data of all subjects. Thus, the exact timing of the auditory clicks for every trial was used for the parameter estimations.

To show the best fit behavior from the model, we applied the model with best fit parameters to both experimental stimuli and new stimuli generated in a fashion similar to the experimental stimuli to interpolate at intermediate stimulus strengths (**Figure 4B**). In particular, additional interpolated stimulus strengths were included at +15 Hz, +20 Hz, +25 Hz, +35 Hz, +40 Hz, +45 Hz to create a smooth psychometric curve. 8000 trials were generated for each of these new stimulus strengths, roughly the same number of trials of each experimental delta click rate. These interpolated values had no bearing on the fitting

procedure itself. Psychometric behavioral rates for the model were computed by taking the mean likelihood for a given trial type: for CR trials, the sum of CR likelihoods for all catch trials divided by the number of all catch trials; for FA trials, the sum of FA likelihoods for all trials divided by the number of all trials; for hits and misses, the sum of each trial type's likelihoods normalized by the number of non-FA trials (i.e. hits and misses) and divided by the number of non-catch trials.

Next, we used model simulations to generate predicted RCs (**Figure 4C**). This was done by simulating 17,383 trials (matching the total number of experimental trials) with the same stimulus parameters as used for the experiments and with 30% catch trial probability, also matched to the experiments. In these simulations, the model was applied to the trials as before, but with the trial type being classified depending on if and when the model predicted a response. Similar to the model fitting described above, the stimulus was convolved with the filter whose shape was defined by the fitted parameters to compute the mean decision variable. Instantaneous noise in the decision variable was drawn at each time interval from a Gaussian distribution with standard deviation specified by the fitted parameters, with NDT also drawn from a distribution with the fitted parameters in the event of bound crossing. FA RCs were generated similarly as the experimental RCs. FA trials were aligned to the time of response, and stimuli were convolved with a causal half-Gaussian filter. In the case of CR confidence RCs, trials were classified as high or low confidence by thresholding the final decision variable at 49 Hz, with high confidence CRs having a final decision variable lower than 49 Hz. Kernel start points were calculated as they were in analysis of the experimental data. In summary, the simulations used parameters fit to the behavioral choice data to make

predictions for the RC analyses. In addition to generating predicted RCs with model fit parameters, we performed simulations using a wider half-Gaussian filter (σ =0.8 s) such that the predicted CR confidence difference kernell approximated the experimental start of CR confidence difference kernel (1760.1 ± 73.6 ms vs. 1773.9 ± 43.5 ms). For this analysis, we decreased the bound from 103 Hz to 95.2 Hz in order to maintain FA rates at experimental levels.

We also sought to test the possibility of whether a result similar to the experimental RCs could be recovered by adjustments to the model that still involved a single timescale of evidence evaluation (**Figure S4**). This model recovery approach involved manipulating the trial-to-trial variability in bound height from 0-144 Hz^2 and adjusting the bound for each bound variability value to yield the same FA rate as observed experimentally (12.6%). Simulations with each of the 25 model variants produced their own RC kernel start points for FA choice reports and CR confidence reports, and the values of these kernel start points were compared to the experimental kernel start points to determine whether the experimental start points could be recapitulated.

QUANTIFICATION AND STATISTICAL ANALYSIS

Exclusion Criteria

Beyond the 7 subjects analyzed in this study, we excluded 2 subjects from post-training data collection for the inability to adequately detect changes in task stimuli at our criterion rate of 45% in any trial session and 2 subjects for failing to report high confidence for at least 10% of CRs of all trials, making the session data unviable for analysis.

Data analysis

Individual trials were classified as hits, misses, CRs, and FAs. Hit rates were calculated as proportion of hit trials out of trials in which a change occurred (non-catch, non-FA trials). FA rates were calculated as proportion of FA trials out of all trials, and CR rates were calculated as proportion of CR trials out of all catch trials (**Figure 2A**). Because there were two confidence ratings available (high and low), average confidence for each response type and stimulus condition (Δ click rate) was calculated as proportion of high confidence reports for each response/stimulus combination (**Figure 2B**). Rates were calculated for both the combined data, which included every trial from each individual (**Figure 2**), and for each individual subject (**Figure S1**).

FA and CR RCs (**Figure 3**) were generated by smoothing click times with a causal half-Gaussian filter having a standard deviation of 0.05 s and sampling every 0.01 s. Note that trials differed in duration. Rather than discard trials with shorter durations, each time bin represents a mean over a different number of trials with shorter duration trials not contributing to earlier time points. For the confidence-based kernels (**Figure 3B-C**), data were first separated into sets of low and high confidence trials, and these individual data sets were each convolved with the half-Gaussian filter. The detection report kernel (**Figure 3A**) was created by convolving the click times of all FA trials, regardless of confidence. We calculated difference plots for FA RCs (**Figure 3B**, green line) by subtracting the mean low confidence kernel from the mean high confidence kernel at each time point. RCs included all trials of the associated trial type (e.g., FA RCs included every FA trial recorded).

The start point and slope of the detection report kernel's ascending phase were then quantified (**Figure S2**). For each subject's FA kernels, as well as FA kernels for the

combined data, we fit the early phase of the FA kernel, from 3 s before stimulus end to the peak value of the kernel, with a 2-piece linear function with three free parameters using MATLAB's *fit* function. These parameters provided estimates for the average baseline click rate leading up to the FA, the average start time of the kernel, and the slope of the function from the start time to the peak of the kernel. The start time was the time point at which the function first diverged from the baseline.

Start point and slope of CR confidence difference kernels were estimated similarly (**Figure S2**), by fitting the last 5 s of the CR confidence difference kernel to a 2-piece linear function with two free parameters for start point and slope. The start point was the first time point that diverged from a 0 Hz differential click rate, and the slope was the slope of the line connecting this start point to the stimulus end.

To estimate kernel endpoint for FAs (**Figure S3**), we convolved the click times with a square-wave function encompassing the descending phase of the FA kernel. This allowed for a more precise estimate of the detection kernel endpoint that minimized the influence of clicks on later times in the kernel compared to using a causal half-Gaussian filter. Starting from 75% of the peak FA choice kernel, a 5 ms bin was moved by 1 ms toward the end of the stimulus, providing a 5 ms wide average click rate for each ms time point. This kernel was then fit to a 2-piece linear function as before, this time with two free parameters: slope and kernel endpoint. Because the subject's choice of whether to respond would no longer be influenced by the stimulus after the kernel endpoint, the mean click rate should return to the generative click rate of 50 Hz. Therefore, the rate after the endpoint was set to a fixed constant of 50 Hz. The average excess click rate for high and

low confidence trials was calculated by subtracting the mean click rate for high and low confidence trials, respectively, from 50 Hz.

DATA AND SOFTWARE AVAILABILITY

The data that support the findings of this study and the analysis code are available from the Lead Contact upon request.

SUPPLEMENTAL FIGURES

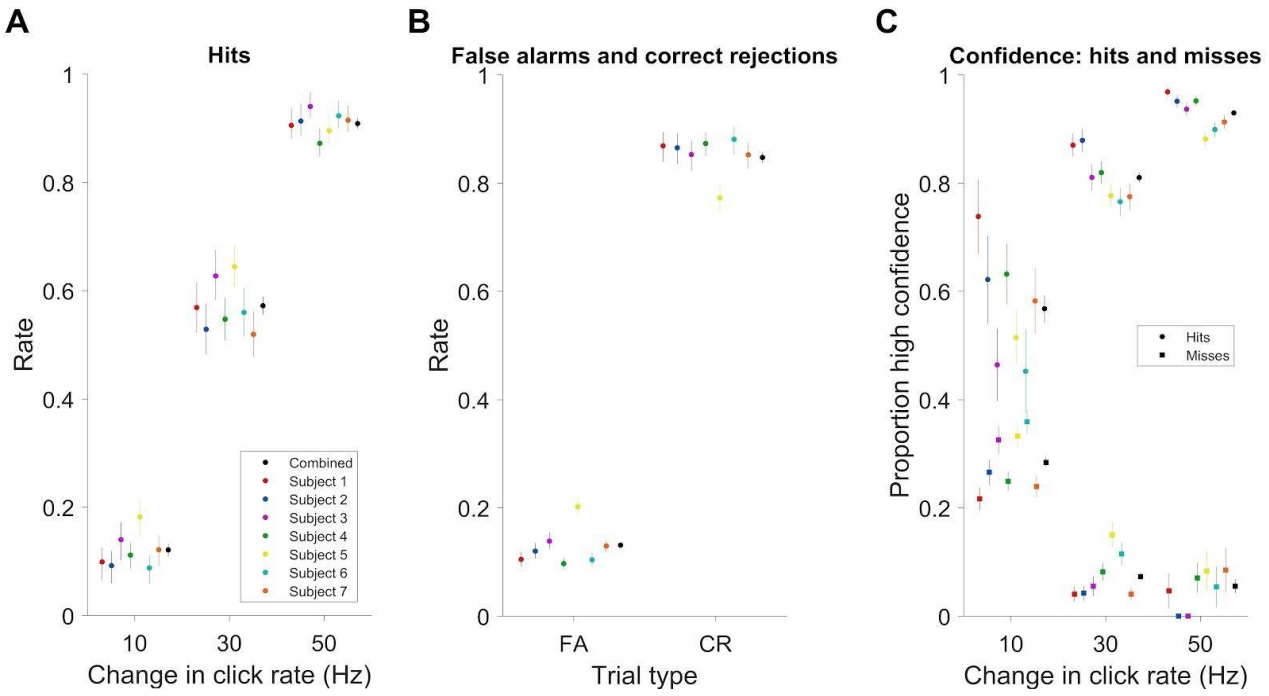

Figure S1. Task performance and confidence ratings: individual and pooled subject data, Related to Figure 2: (**A**) Hit rate as a function of change in click rate for each subject (colored) and combined data (black), calculated as a proportion of trials in which a generative change in click rate occurred (same conventions as Figure 2). (**B**) FA and CR rates across individual and combined subjects. FA rates calculated as a proportion of all trials. CR rates calculated as a proportion of catch trials. (**C**) Proportion of high confidence trials for hits (circles) and misses (squares) across individuals and combined subject as a function of change in click rate. Error bars are +/- SEM.

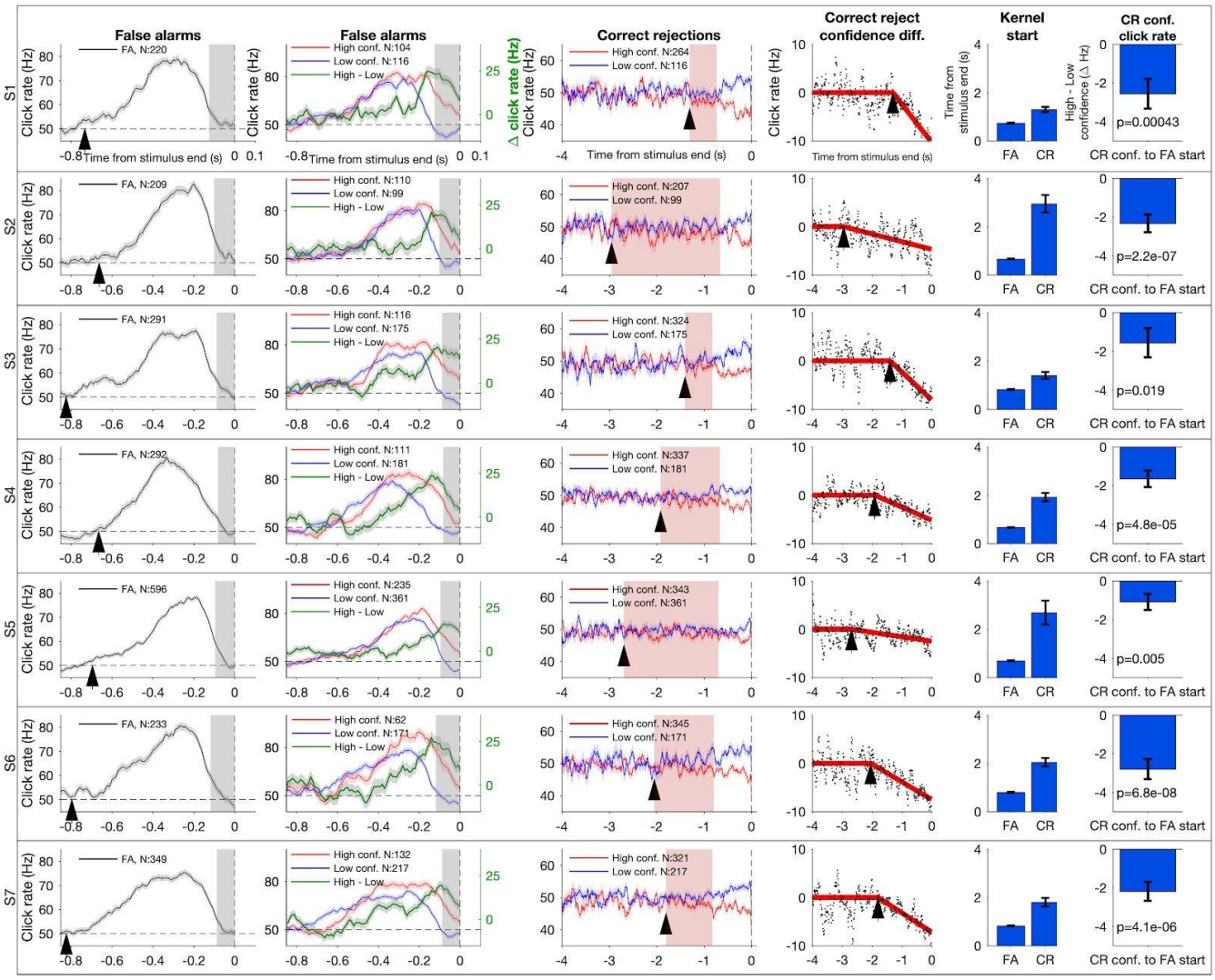

Figure S2. FA and CR reverse correlations: individual subject data, Related to Figure 3: Detection report kernels (*1st column*), detection report confidence kernels (*2nd column*), CR confidence kernels (*3rd column*) for each of the 7 subjects. The red shaded region represents the interval between the start of the CR confidence and FA kernels. The start of CR confidence kernels were estimated from a fit of the CR confidence kernels expressed as a difference of high and low confidence (*4th column*). The start of FA and CR confidence kernels are shown in the *5th column*, where error bars represent 95% CI. The final column depicts the difference in mean click rate between high and low confidence CR trials for each subject within the intervals highlighted in red in column 3. Here, error bars represent the pooled standard error of the mean and significance calculations were determined from t tests. Conventions for columns 1-3 are the same as Figure 3. The 7 subjects completed 2100, 1962, 2101, 3096, 3091, 2286, and 2747 trials, respectively.

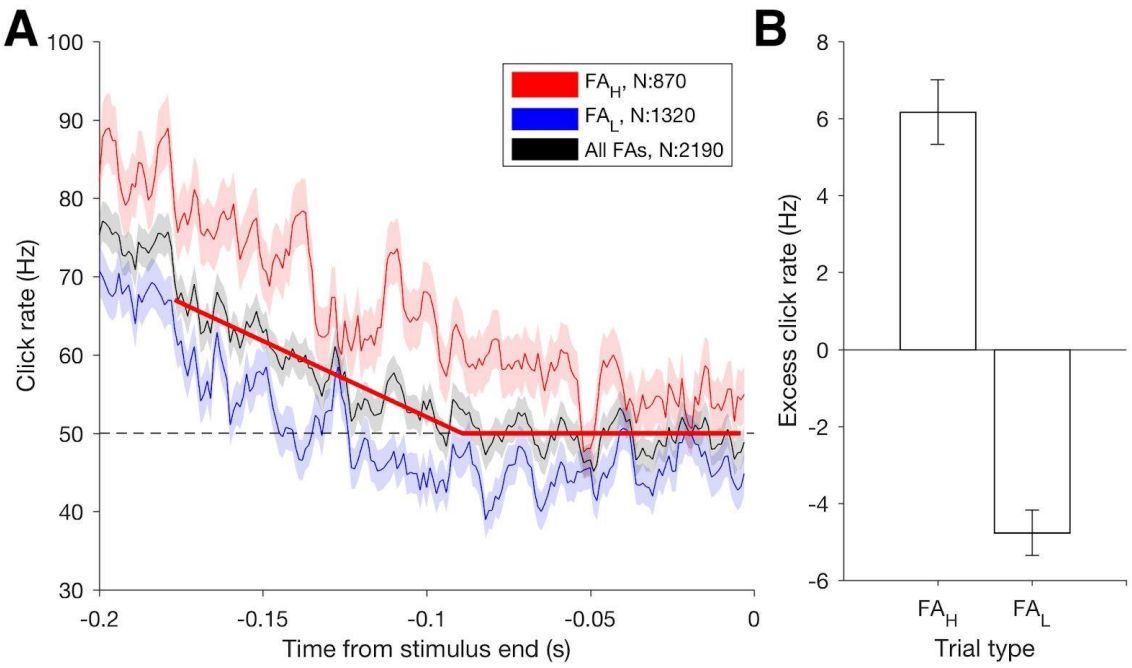

Figure S3. Pooled estimate of detection kernel endpoint, Related to Figure 3: (**A**) Kernel endpoint was estimated by convolving clicks with a square-wave filter (5 ms width) so that clicks would have minimal influence on the kernel after they occurred (black trace). The descending phase of the kernel was fit with a 2-piece linear function (red lines). The two free parameters were the point at which the kernel returned to the 50 Hz baseline (inflection point of red lines) and the descending slope from 75% of the peak detection report kernel height. The same convolution was applied to the high (red) and low (blue) confidence FA trials to visualize the difference between them. (**B**) mean excess click rate above or below the 50 Hz baseline for high (left bar) and low (middle bar) FA confidence trials from kernel endpoint until stimulus end. Shaded region on traces and error bars are +/- SEM.

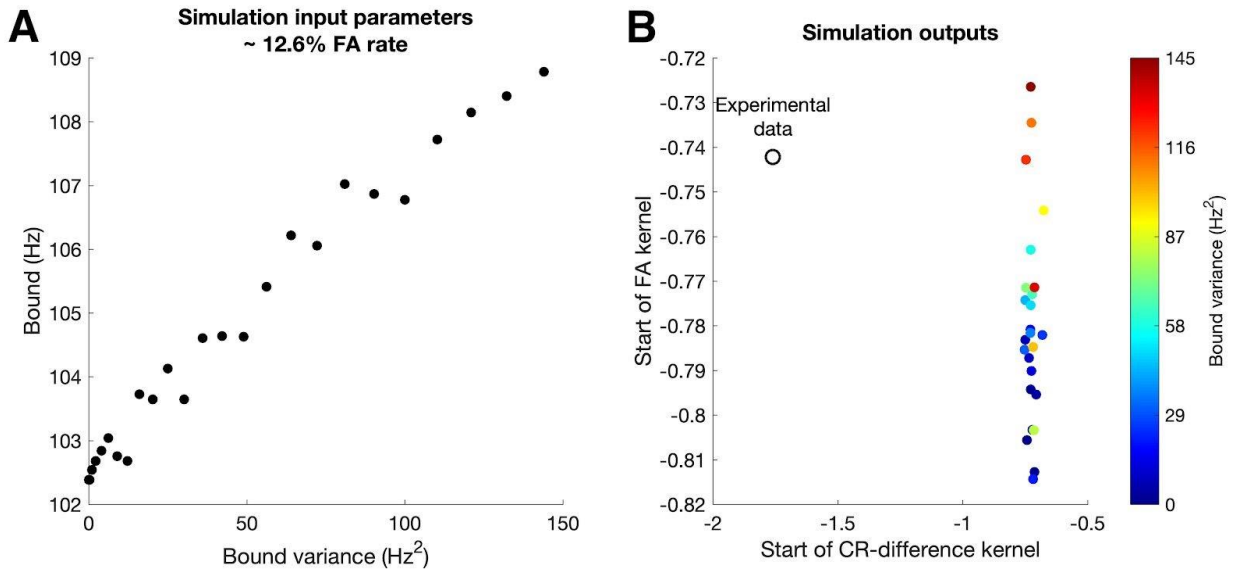

Figure S4. Simulated effects of bound variability on RC kernels and hit rates, Related to Figure 4: (**A**) The bound variability parameters were chosen from a range of 0-144 Hz and corresponding bounds that resulted in approximately 12.6% FA rates were used for simulations. This resulted in 25 sets of bound and bound variability simulation conditions. All other simulation parameters were set to the maximum likelihood estimations of the combined experimental data. (**B**) Increasing bound variability tended to shorten the estimated detection kernel but did not have an appreciable effect on the CR-confidence kernel. Thus, bound variability could not recapitulate the earlier start of CR confidence difference kernel in the experimental data (black circle).

References

1. Ossmy, O., Moran, R., Pfeffer, T., Tsetsos, K., Usher, M., and Donner, T.H. (2013). The timescale of perceptual evidence integration can be adapted to the environment. Curr. Biol. *23*, 981–986.

2. Glaze, C.M., Kable, J.W., and Gold, J.I. (2015). Normative evidence accumulation in unpredictable environments. Elife *4*. Available at: http://dx.doi.org/10.7554/eLife.08825.

3. Sugrue, L.P., Corrado, G.S., and Newsome, W.T. (2004). Matching behavior and the representation of value in the parietal cortex. Science *304*, 1782–1787.

4. Piet, A.T., El Hady, A., and Brody, C.D. (2018). Rats adopt the optimal timescale for evidence integration in a dynamic environment. Nat. Commun. *9*, 4265.

5. Gold, J.I., and Stocker, A.A. (2017). Visual Decision-Making in an Uncertain and Dynamic World. Annu Rev Vis Sci *3*, 227–250.

6. Fetsch, C.R., Kiani, R., and Shadlen, M.N. (2014). Predicting the Accuracy of a Decision: A Neural Mechanism of Confidence. Cold Spring Harb. Symp. Quant. Biol. *79*, 185–197.

7. Hangya, B., Sanders, J.I., and Kepecs, A. (2016). A Mathematical Framework for Statistical Decision Confidence. Neural Comput. *28*, 1840–1858.

8. Sanders, J.I., Hangya, B., and Kepecs, A. (2016). Signatures of a Statistical Computation in the Human Sense of Confidence. Neuron *90*, 499–506.

9. Pouget, A., Drugowitsch, J., and Kepecs, A. (2016). Confidence and certainty: distinct probabilistic quantities for different goals. Nat. Neurosci. *19*, 366–374.

10. Hanks, T.D., and Summerfield, C. (2017). Perceptual Decision Making in Rodents, Monkeys, and Humans. Neuron *93*, 15–31.

11. Yeung, N., and Summerfield, C. (2012). Metacognition in human decision-making: confidence and error monitoring. Philos. Trans. R. Soc. Lond. B Biol. Sci. *367*, 1310–1321.

12. De Martino, B., Fleming, S.M., Garrett, N., and Dolan, R.J. (2012). Confidence in value-based choice. Nat. Neurosci. *16*, 105.

13. Insabato, A., Pannunzi, M., Rolls, E.T., and Deco, G. (2010). Confidence-related decision making. J. Neurophysiol. *104*, 539–547.

14. Drugowitsch, J., Moreno-Bote, R., Churchland, A.K., Shadlen, M.N., and Pouget, A. (2012). The cost of accumulating evidence in perceptual decision making. J.

Neurosci. *32*, 3612–3628.

15. Zylberberg, A., Barttfeld, P., and Sigman, M. (2012). The construction of confidence in a perceptual decision. Front. Integr. Neurosci. *6*, 79.

16. Fetsch, C.R., Kiani, R., Newsome, W.T., and Shadlen, M.N. (2014). Effects of cortical microstimulation on confidence in a perceptual decision. Neuron *83*, 797–804.

17. Kiani, R., Corthell, L., and Shadlen, M.N. (2014). Choice certainty is informed by both evidence and decision time. Neuron *84*, 1329–1342.

18. Gherman, S., and Philiastides, M.G. (2015). Neural representations of confidence emerge from the process of decision formation during perceptual choices. Neuroimage *106*, 134–143.

19. Moran, R., Teodorescu, A.R., and Usher, M. (2015). Post choice information integration as a causal determinant of confidence: Novel data and a computational account. Cogn. Psychol. *78*, 99–147.

20. Pleskac, T.J., and Busemeyer, J.R. (2010). Two-stage dynamic signal detection: a theory of choice, decision time, and confidence. Psychol. Rev. *117*, 864–901.

21. Fleming, S.M., and Daw, N.D. (2017). Self-evaluation of decision-making: A general Bayesian framework for metacognitive computation. Psychological Review *124*, 91–114. Available at: http://dx.doi.org/10.1037/rev0000045.

22. Peters, M.A.K., Thesen, T., Ko, Y.D., Maniscalco, B., Carlson, C., Davidson, M., Doyle, W., Kuzniecky, R., Devinsky, O., Halgren, E., *et al.* (2017). Perceptual confidence neglects decision-incongruent evidence in the brain. Nat Hum Behav *1*. Available at: http://dx.doi.org/10.1038/s41562-017-0139.

23. Churchland, A.K., and Kiani, R. (2016). Three challenges for connecting model to mechanism in decision-making. Curr Opin Behav Sci *11*, 74–80.

24. Johnson, B., Verma, R., Sun, M., and Hanks, T.D. (2017). Characterization of decision commitment rule alterations during an auditory change detection task. J. Neurophysiol. *118*, 2526–2536.

25. Kiani, R., Hanks, T.D., and Shadlen, M.N. (2008). Bounded integration in parietal cortex underlies decisions even when viewing duration is dictated by the environment. J. Neurosci. *28*, 3017–3029.

26. van den Berg, R., Anandalingam, K., Zylberberg, A., Kiani, R., Shadlen, M.N., and Wolpert, D.M. (2016). A common mechanism underlies changes of mind about decisions and confidence. Elife *5*, e12192.

27. Okazawa, G., Sha, L., Purcell, B.A., and Kiani, R. (2018). Psychophysical reverse

correlation reflects both sensory and decision-making processes. Nat. Commun. *9*, 3479.

28. Radillo, A.E., Veliz-Cuba, A., Josić, K., and Kilpatrick, Z.P. (2017). Evidence Accumulation and Change Rate Inference in Dynamic Environments. Neural Comput. *29*, 1561–1610.

29. Hanks, T., Kiani, R., and Shadlen, M.N. (2014). A neural mechanism of speed-accuracy tradeoff in macaque area LIP. Elife *3*, 1–17.

30. Purcell, B.A., and Kiani, R. (2016). Neural Mechanisms of Post-error Adjustments of Decision Policy in Parietal Cortex. Neuron *89*, 658–671.

31. Churchland, A.K., Kiani, R., and Shadlen, M.N. (2008). Decision-making with multiple alternatives. Nat. Neurosci. *11*, 693–702.

32. Merten, K., and Nieder, A. (2012). Active encoding of decisions about stimulus absence in primate prefrontal cortex neurons. Proc. Natl. Acad. Sci. U. S. A. *109*, 6289–6294.

33. Deco, G., Pérez-Sanagustín, M., de Lafuente, V., and Romo, R. (2007). Perceptual detection as a dynamical bistability phenomenon: a neurocomputational correlate of sensation. Proc. Natl. Acad. Sci. U. S. A. *104*, 20073–20077.

34. Seung, H.S., Lee, D.D., Reis, B.Y., and Tank, D.W. (2000). Stability of the memory of eye position in a recurrent network of conductance-based model neurons. Neuron *26*, 259–271.

35. Goldman, M.S., Compte, A., and Wang, X.J. (2009). Neural integrator models. Encyclopedia of neuroscience *6*, 165–178.

36. Purcell, B.A., Schall, J.D., Logan, G.D., and Palmeri, T.J. (2012). From salience to saccades: multiple-alternative gated stochastic accumulator model of visual search. J. Neurosci. *32*, 3433–3446.

37. Teichert, T., Grinband, J., and Ferrera, V. (2016). The importance of decision onset. J. Neurophysiol. *115*, 643–661.

38. Goldman, M.S. (2009). Memory without feedback in a neural network. Neuron *61*, 621–634.

39. Murray, J.D., Bernacchia, A., Freedman, D.J., Romo, R., Wallis, J.D., Cai, X., Padoa-Schioppa, C., Pasternak, T., Seo, H., Lee, D., *et al.* (2014). A hierarchy of intrinsic timescales across primate cortex. Nat. Neurosci. *17*, 1661–1663.

40. Bernacchia, A., Seo, H., Lee, D., and Wang, X.-J. (2011). A reservoir of time constants for memory traces in cortical neurons. Nat. Neurosci. *14*, 366–372.

41. Scott, B.B., Constantinople, C.M., Akrami, A., Hanks, T.D., Brody, C.D., and Tank, D.W. (2017). Fronto-parietal Cortical Circuits Encode Accumulated Evidence with a Diversity of Timescales. Neuron *95*, 385–398.e5.

42. Boldt, A., and Yeung, N. (2015). Shared Neural Markers of Decision Confidence and Error Detection. Journal of Neuroscience *35*, 3478–3484.

43. Kepecs, A., and Mainen, Z.F. (2012). A computational framework for the study of confidence in humans and animals. Philos. Trans. R. Soc. Lond. B Biol. Sci. *367*, 1322–1337.

44. Sanders, J.I., and Kepecs, A. (2014). A low-cost programmable pulse generator for physiology and behavior. Front. Neuroeng. *7*, 43.

45. Verdonck, S., and Tuerlinckx, F. (2016). Factoring out nondecision time in choice reaction time data: Theory and implications. Psychological Review *123*, 208–218. Available at: http://dx.doi.org/10.1037/rev0000019.

Chapter 3:

Flexible integration of evidence and causal role of posterior parietal cortex for perceptual decisions

Introduction

In navigating and engaging environments, animals must evaluate incoming sensory evidence to make informed decisions according to their goals. Often, these decisions require collection of evidence over time until a criterion level of evidence is met, at which point the animal commits to a decision (Gold and Shadlen, 2007; Ratcliff and McKoon, 2008; Shadlen and Newsome, 1996; Wald and Wolfowitz, 1950). Environmental variables can create obstacles for this process. Incoming sensory noise can be noisy, requiring the brain to extract relevant signal to inform decisions (Green and Swets, 1966). Also, it is crucial for the animal to establish rules for evidence evaluation that maximize decision accuracy. For example, some environments may impose urgency upon decisions, demanding different evidence criteria and, critically, different timescales of evaluating a sequence of evidence.

Abundant research has been devoted to delineating how the brain executes perceptual decision making mediated by a network of connected brain regions. Posterior parietal cortex (PPC), prefrontal cortex (PFC), and dorsomedial striatum have been key foci in these investigations (Brody and Hanks, 2016; Gold and Shadlen, 2007; Hanks and Summerfield, 2017; Yartsev et al., 2018). In the case of PPC, numerous studies in primate LIP have suggested a role for the region in accumulating sensory evidence for decisions; these studies have been augmented by research in humans and rodents expanding potential for PPC's involvement in decision making across varying forms of evidence, both sensory and abstract, and associated motor actions (Hanks et al., 2015; Licata et al., 2017; Roitman and Shadlen, 2002; Shadlen and Newsome, 1996; van Vugt et al., 2012; Wyart et al., 2012). However, while PFC and striatum have

gained empirical support for their causal role in specific components of decision execution (Erlich et al., 2015; Piet et al., 2017; Yartsev et al., 2018), PPC's necessity in perceptual decision making has been challenged. Studies in both primates and rodents involving perturbation of PPC function resulted in minimal impairments to performance when the timing of the decision is controlled by the experimenter, despite PPC still exhibiting the striking neural characteristics described above (Erlich et al., 2015; Katz et al., 2016; Licata et al., 2017; Raposo et al., 2014).

Despite this challenge, among the several functional centers for decision making in the brain, PPC is still prominently positioned to facilitate adaptive *changes* in evidence evaluation, particularly setting a timescale of evidence evaluation for perceptual decisions. In this context, we define "timescale of evidence evaluation" refers to the period of time over which past evidence bears on a decision from the time of the decision, which can be influenced by several factors including the threshold for decision commitment, the time constant of integration of a given quantity of evidence, and sensorimotor lag (i.e. non-decision time) (Berg et al., 2016; Okazawa et al., 2018; Ossmy et al., 2013). Many studies of PPC have featured an experimental design in which evidence evaluated linearly over an extended period of time and with a task structure prohibiting subjects from choosing when to commit to a decision. PPC may instead contribute an unexplored function in decisions involving an adjustment of evaluation timescale when it is necessary to assess how long a given period of evidence should be considered for a decision and when it is appropriate to commit to a decision.

Three key properties of PPC make it a well-suited candidate region for serving these functions. First, it is anatomically centered as an interface of sensory and motor networks, receiving direct input from primary sensory cortices and outputting to motor-related structures such as the basal ganglia and motor cortex (Chandler et al., 1992; Cheatwood et al., 2003; McGeorge and Faull, 1989; Reep et al., 1994; Selemon and Goldman-Rakic, 1988). Second, neurons in PPC appear to encode the relative strength of evidence for perceptual decisions such that their firing rates scale with the magnitude of accumulated evidence before peaking at decision time, a property found in primate and rodent brains (Hanks et al., 2015; Roitman and Shadlen, 2002; Shadlen and Newsome, 1996). Third, neurons in PPC have been shown to encode time in decisions, both in terms of absolute elapsed time and estimation of hazard rates, and electrical microstimulation of monkey PPC can alter reaction times for decisions in free-response decisions (Hanks et al., 2006; Janssen and Shadlen, 2005; Leon and Shadlen, 2003; Scott et al., 2017). This combination of properties suggest PPC may track evidence for decisions flexibly depending on the optimal timescale of evaluation, especially when that timescale is shorter as in the case of change detection.

To test PPC's role in establishing the timescale of evidence evaluation for decision making, we trained rats to perform an auditory change detection task in which subjects evaluated sequences of auditory pulses for increases and responded to increases in frequency of pulses, a task previously employed in human subjects (Ganupuru et al., 2019; Harun et al., 2020; Johnson et al., 2017). During task performance, single unit electrophysiological recordings were taken from PPC with

Neuropixel probes (Jun et al., 2017) to determine neural dynamics of PPC cells with respect to incoming sensory evidence and the subject's choice. PPC neurons adapted their dynamics to the task by way of contracted integration time constants as well as reflecting corresponding and competing modalities of choice (i.e. go vs no-go). In addition, we tested the necessity of PPC in auditory change detection through pharmacological reversible inactivation. We identified a causal role of PPC in determining the subject's timescales of evidence evaluation, namely that PPC is necessary in setting a shorter timescale of evaluation suitable for the demands of change detection. Together, these results support a mechanistic role of PPC in modulating timescales of evidence evaluation for perceptual decision making.

Results

Behavioral performance

We trained rats to perform a free-response auditory change detection task adapted from previous studies involving human subjects (Johnson et al., 2017). Rats insert their noses into the central port of an operant apparatus, which initiates a stream of auditory pulses ("clicks") generated via a Poisson process. Starting at a baseline rate of 20 Hz, the clicks may increase in rate at a random time by a variable magnitude, to which subjects must respond within 0.8 s by withdrawing from the central port. A timely withdrawal in response to a change is a "hit," which leads to a water reward delivered from a separate port on the side of the apparatus. Failure to withdraw in time results in a "miss," with no reward. Withdrawal in the absence of a change is a "false alarm," also denying a reward. Finally, on a subset of trials, no change in stimulus rate occurs;

during these “catch” trials, the rat must maintain central port fixation until the stimulus ends, resulting in a “correct rejection” accompanied by water reward (**Figure 1A**).

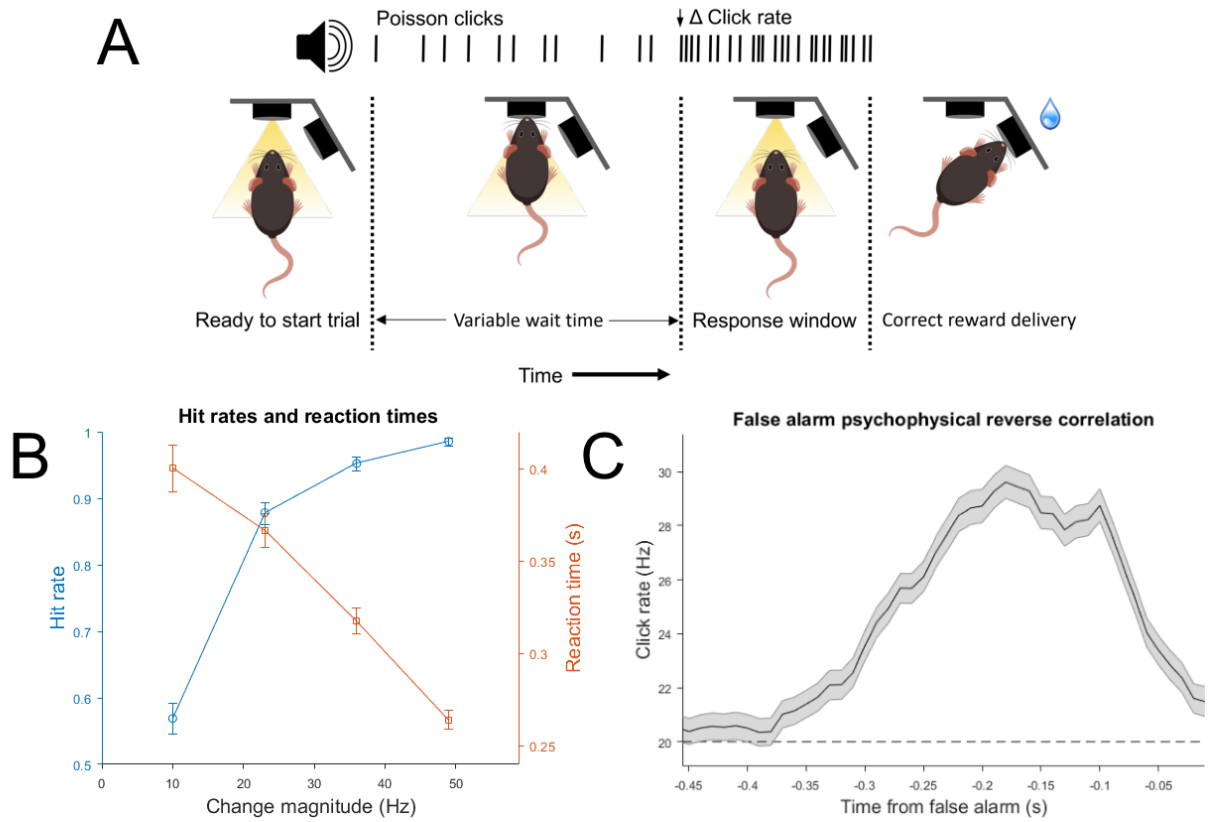

Figure 1: Task design and subject performance. A) A trial begins when a rat subject engages an illuminated center port in the apparatus with their nose. Port engagement triggers initiation of a stream of Poisson-generated auditory pulses (“clicks”) at a baseline generative rate of 20 Hz. At a random point (marked by black arrow) in 70% of trials, the generative rate increases by a variable magnitude of 10 Hz, 23 Hz, 36 Hz, 49 Hz. After the rate change, rats have 0.8 s to withdraw their nose from the center port in order to receive a water reward from either the left or right side port according to subject. In the remaining 30% of trials, no change occurs, and rats must maintain port fixation for the full random duration of the stimulus to receive the water reward. **B)** Combined hit rates and reaction times for 2 subjects as a function of change magnitude. Hit rate was calculated excluding false alarm trials (i.e. only including trials in which the rat was presented with a change). Reaction times were calculated as the time of center port withdrawal following a change. Error bars show 95% confidence intervals. **C)** Psychophysical reverse correlation (PRC), combined between subjects. All false alarms were included, which shorter latency false alarms contributing to less of the PRC earlier in time (i.e. from right to left). Horizontal line demarcates the 20 Hz baseline rate.

Like humans, rats consistently detected changes, achieving higher hit rates with higher change magnitudes (μ=0.54, all change trials excluding false alarms). Higher change magnitudes also yielded lower reaction times (μ=0.33 s, all hit trials) (**Figure 1B**). These metrics suggest rats perform the task by evaluating the strength of the presented sensory evidence, and greater quantities of evidence lead to faster, more accurate choices. Conversely, rats often withheld responses when appropriate, achieving a correct rejection rate of 0.43. The average false alarm rate was 0.41.

To better gauge the strategy rats employ on this task, we conducted psychophysical reverse correlation (PRC) using false alarm trials to assess how rats evaluated evidence over time leading to choices. Briefly, baseline stimuli preceding false alarm responses were aligned to the time of the false alarm, averaged together, and plotted. This analysis allows us to determine the epoch of evidence that has bearing on change detection reports. Because the Poisson stimulus may vary about a generative mean from trial to trial, it is possible that false alarms are triggered by stochastic transient fluctuations in click rate. Therefore, the PRC illustrates not only the pattern of evidence evaluation for detection reports but the timescale over which evidence is evaluated on average (Ganupuru et al., 2019; Okazawa et al., 2018).

As expected, the false alarm PRC exhibits an upward fluctuation in click rate leading to false alarms, indicating false alarms were generally triggered by brief increases in click rate (**Figure 1C**). The period of this upward fluctuation extended 0.38 s prior to the rat's choice, consistent with a short timescale of evidence evaluation. The PRC thus illustrates a behavioral strategy on the part of the rats of evaluating evidence

over brief intervals and down-weighting older evidence to detect increases in stimulus rate, consistent with task demands.

Evidence-modulated neural responses in PPC

After characterizing the rats' dynamics of evidence evaluation at the behavioral level, we sought to examine their neural underpinnings. The spiking responses of 552 neurons in PPC were recorded while rats performed the change detection task, and those neurons were then assessed for task-related activity. We found 57 neurons that were positively modulated by the stimulus, such that firing rates peaked immediately before and through the rat's response on hit trials (**Figure 2A**). These neurons were, on average, also modulated by the strength of sensory evidence; greater stimulus magnitudes elicited greater firing rate increases preceding detection reports up to 0.26 s prior to the detection report (Linear regression, $b=0.028 \pm 0.003$, $p<0.05$) and between 0.35 s and 0.83 s prior to the detection report (Linear regression, $b=0.095 \pm 0.008$, $p<0.05$). Although the positive modulation by click rate exhibited a gap between those two periods, the lack of modulation shortly before hits corroborated previous findings in PPC in which firing rates converge to a common peak near the decision point regardless of evidence strength (Hanks et al., 2014; Kiani et al., 2008). Interestingly, the ramp in firing rate began only within several hundred milliseconds before the choice as opposed to steadily progressing over a longer period of time from stimulus onset, possibly reflecting evidence integration with a short time constant.

We also aligned firing rates on hit trials to the time of click rate increase. Further indicating modulation by evidence strength, firing rates increased to a peak level more steeply with greater change magnitude (**Figure 2B**). Following a change, the click rate

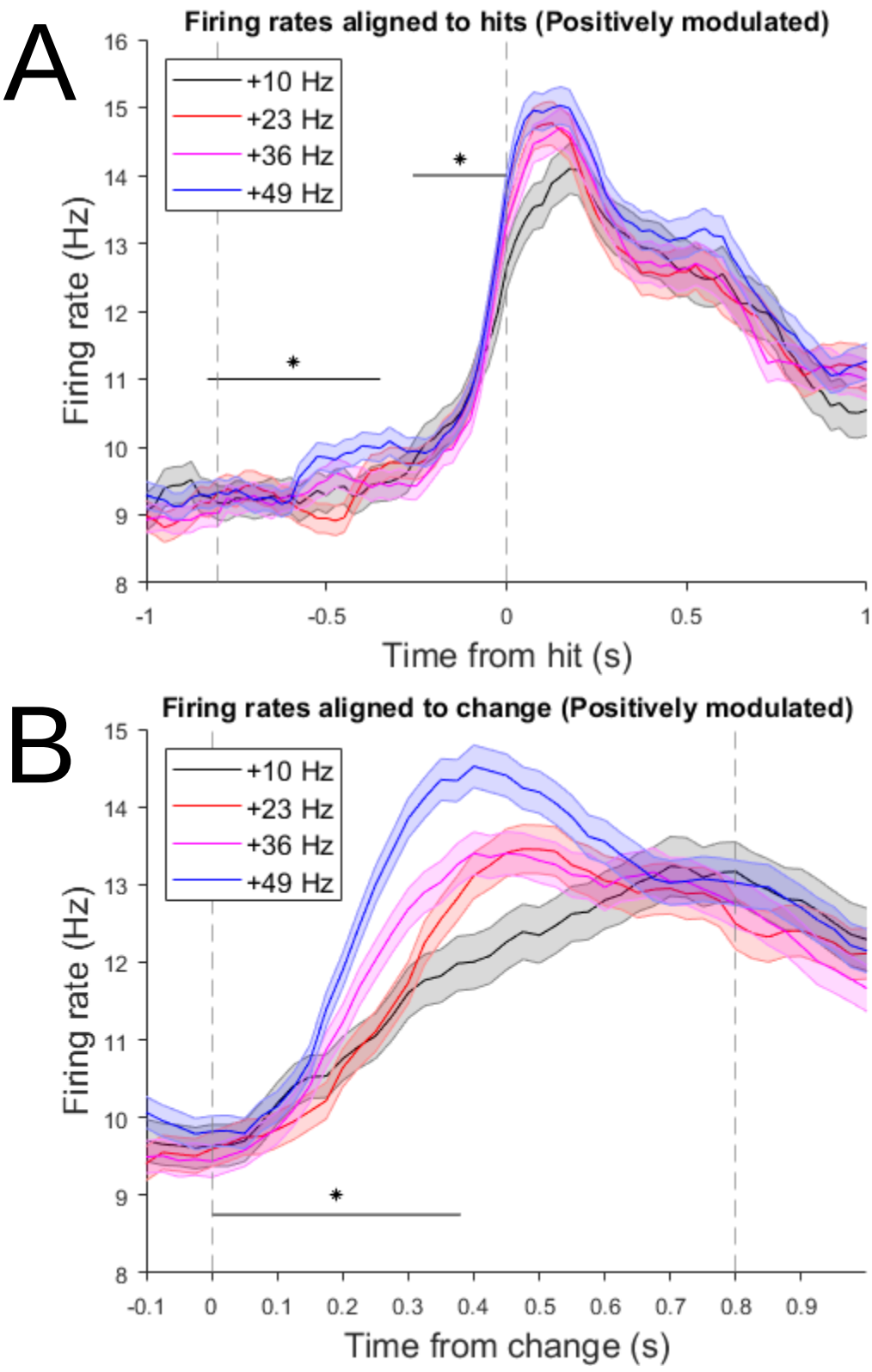
A
Firing rates aligned to hits (Positively modulated)
+10 Hz
+23 Hz
+36 Hz
+49 Hz
Firing rate (Hz)
Time from hit (s)
B
Firing rates aligned to change (Positively modulated)
+10 Hz
+23 Hz
+36 Hz
+49 Hz
Firing rate (Hz)
Time from change (s)

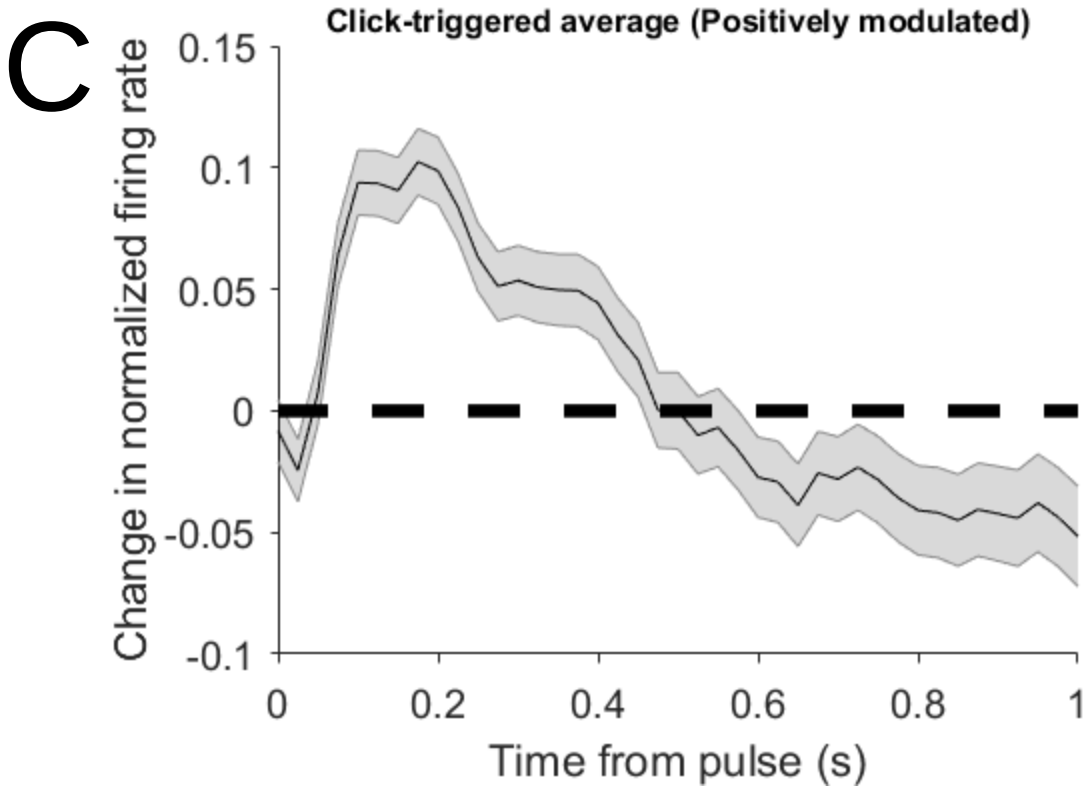

Figure 2: Responses of PPC neurons positively modulated by evidence. A) Population responses of 57 units showing significant positive modulation by evidence strength for same rats in Figure 1 aligned to time of hit. Firing rate traces sorted by change magnitude with error shading showing S.E.M. Left dotted line shows maximum time of change at 0.8 s, though contributing trials and resulting traces represent hits occurring within less than 0.8 s of change. Right dotted line shows the time of the hit. Starred line shows period of significant positive relationship between stimulus strength and neural response prior to response (Linear regression, b=X +/- X, $p<0.05$). **B)** Population responses of same units in panel A aligned to the time of change. Left dotted line shows the time of change, and right dotted line shows maximum response window. Starred line shows period of significant positive relationship between stimulus strength and neural response prior to response (Linear regression, b=0.0407 +/- 0.0034, $p<0.05$). **C)** Population click-triggered average for same units in panel A-B. Responses are averaged from each unit's response to each pulse during the baseline period of each trial. Dotted line shows the average firing rate during the baseline of each trial contributing to the average, with plotted values representing changes from this baseline following a pulse.

had a positive modulation on neural response out to 0.38 s (Linear regression, b=0.041 +/- 0.003, $p<0.05$), roughly corresponding to the evidence evaluation timescale observed through reverse correlation. Together, these neural responses could explain

both higher hit rates and faster reaction times with greater stimulus changes as observed in decision behavior.

To more directly test the hypothesis that PPC neural dynamics adjust to task demands with shorter timescales of evidence integration, we computed a click-triggered average representing the average neural responses of positively modulated neurons to single units of evidence. The resulting average showed a transient increase in firing rate following clicks that waned over time. Notably, the time course of this transient increase roughly followed the time course of the false alarm PRC in Figure 1, extending to 0.48 s. This pattern of response also differs from that seen in similar analysis conducted on PPC neurons in an auditory Poisson discrimination task, a pattern of linear increase that does not attenuate toward baseline over time (Hanks et al., 2015). Notably, the average also fell below baseline after the initial transient increase, which may be explained by the fact that evidence's influence wanes over time according to behavioral metrics (**Figure 1C**) and may actively suppress a decision trigger if sufficient time elapses from incidence of a stimulus. Plotting click-triggered averages for individual units in the population, we also observed heterogeneity in response time courses; response peaks ranged from 0.1 s following a stimulus pulse to over 0.8 s following stimulus pulses (**Figure 3**). Thus, PPC neurons exhibit multiple timescales of integration that are respectively suited for different behavioral strategies.

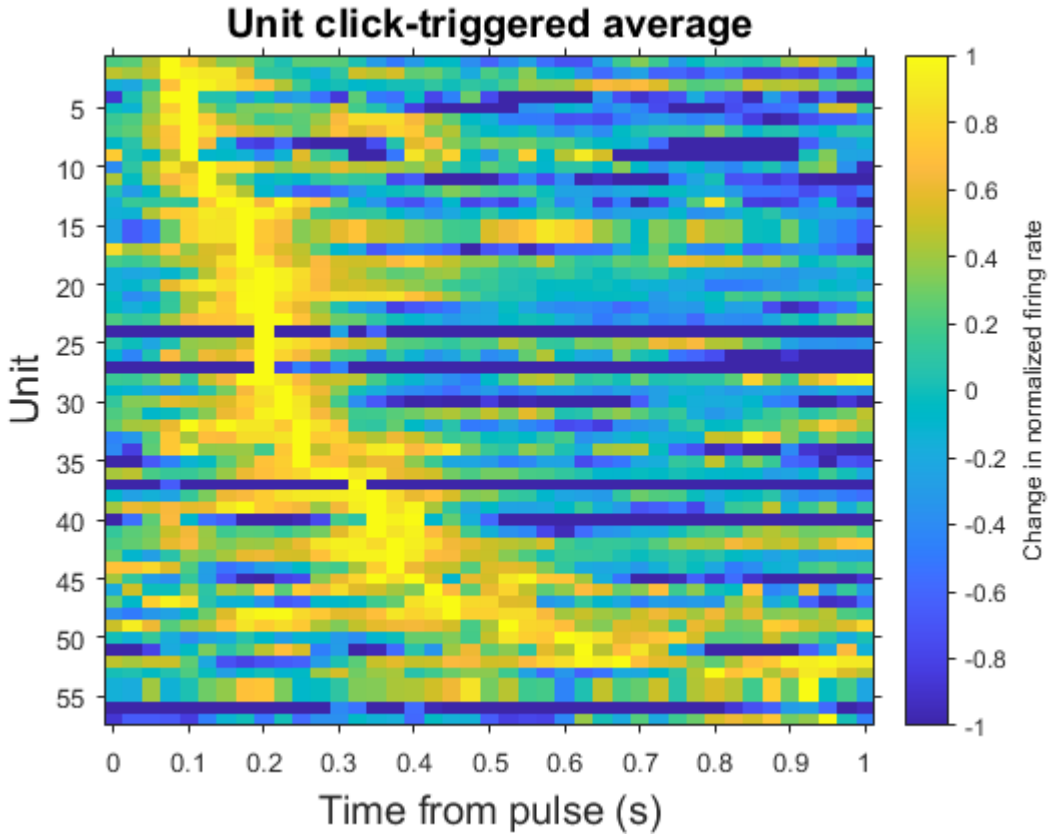

Figure 3: Individual unit click-triggered averages. Click triggered average over time for each unit in Figure A as a function of time from pulse. Each row represents one of 57 positively modulated units, with color indicating normalized change in response at each 25 ms time bin. Plotted values are normalized to the maximum value of the average for each unit, such that the bin with the highest average firing rate has a change in normalized firing rate of 1. Units are ordered ascendingly in time of maximum response (i.e. highest normalized value in click-triggered average).

Flexibility in neural dynamics was not limited to integration timescales, however. Besides positively evidence-modulated neurons, we found a larger subset of neurons (n=156) that were *negatively* modulated by evidence strength (**Figure 4A**). These neurons exhibited a downshift in firing rate leading up to the change, and greater change magnitudes elicited a greater decrease in firing rate up to 0.70 s (Linear regression, b=-0.050 +/- 0.002, $p<0.05$). When aligned to the time of change, we

observed a pattern of evidence modulation that was inverted compared to the positively modulated neurons; stronger change magnitudes elicited earlier downshifts in firing rate up to and showing significant negative modulation by click rate up to 0.14 s (Linear regression, b=-0.021 +/- 0.001, $p<0.05$) (**Figure 4B**). This finding suggests the propensity for PPC neurons to adapt to task demands not only through integration timescales but choice modality: respond vs withhold to suit change detection as opposed to left vs right to suit discrimination. PPC's neural responses have distinctly differentiating on a lateral dichotomy in past decision making studies because those studies employed tasks requiring subjects to make a lateralized choice involving some form of leftward or rightward movement (Churchland and Ditterich, 2012; Churchland et al., 2008). Because our task requires a choice between response or no response, the response dichotomy in PPC neurons seems to manifest along that dimension.

We also calculated click-triggered averages for this population of negatively modulated neurons. Accordingly, neurons modulated negatively by sensory evidence exhibited a transient decrease in firing rate following clicks (**Figure 4C**) rather than the increase observed in the positively modulated subpopulation. Similarly to the click-triggered average of positively modulated neurons, this average adhered to a 0.42 s timescale of modulation, which in turn adhered to behavioral timescales of evidence evaluation.

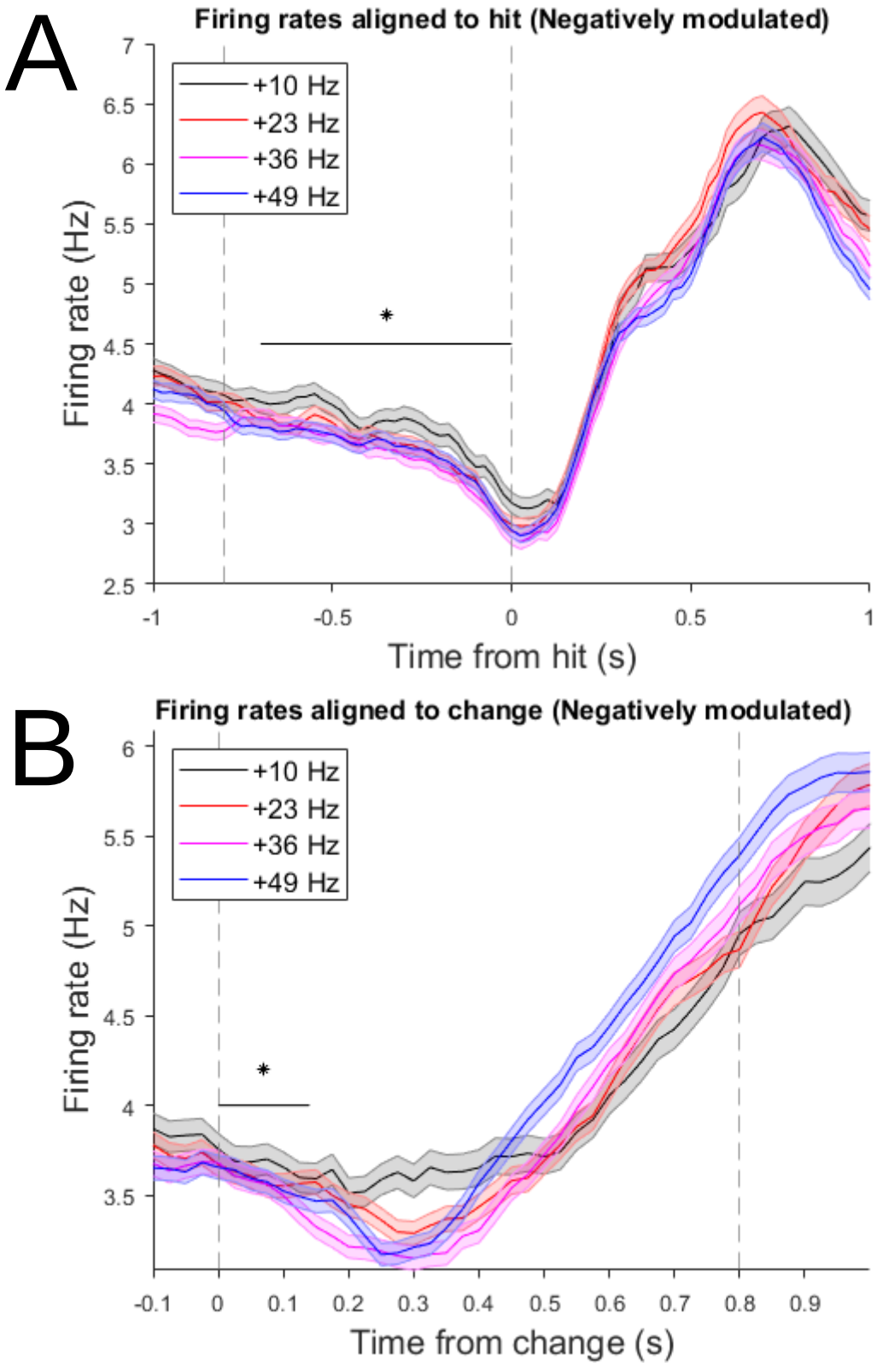
A
Firing rates aligned to hit (Negatively modulated)
+10 Hz
+23 Hz
+36 Hz
+49 Hz
Firing rate (Hz)
Time from hit (s)
B
Firing rates aligned to change (Negatively modulated)
+10 Hz
+23 Hz
+36 Hz
+49 Hz
Firing rate (Hz)
Time from change (s)

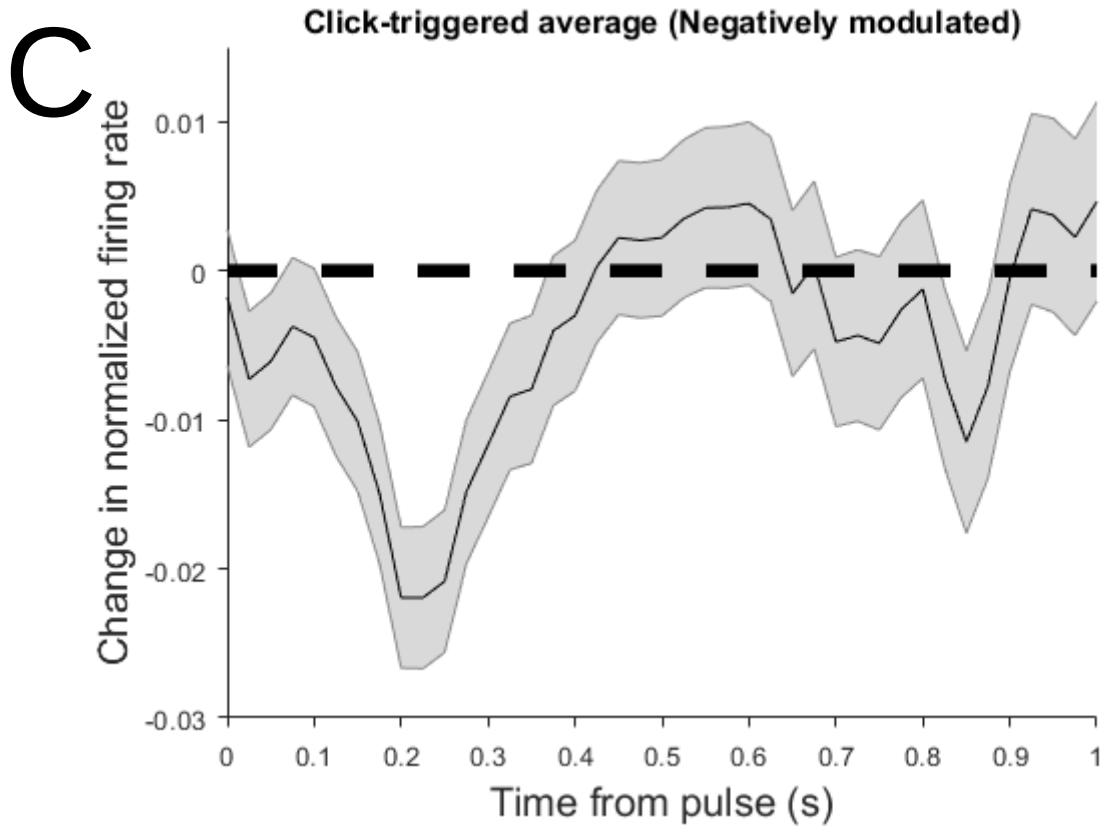

Figure 4: Responses of PPC neurons negatively modulated by evidence. A) Population response of 156 units showing significant negative modulation by evidence strength for same rats in Figure 1 aligned to time of hit. All plotting conventions identical to those in Figure 2A. Starred line shows period of significant negative relationship between stimulus strength and neural response prior to response (Linear regression, b=-0.021 +/- 0.0008, p<0.05). **B)** Population responses of same units in Panel A aligned to the time of change. All plotting conventions identical to those in Figure 2B. **C)** Population click-triggered average for same units in Panel A-B. Same calculation and plotting conventions as in Figure 2C.

Adaptation of PPC neural responses across decision times

Although these results suggest flexibility of neural dynamics between task regimes with varying demands, they do not alone reveal the propensity of individual parietal cells to adapt dynamics *within* a task regime with a consistent modality of evidence and requisite motor response. We therefore wanted to test whether changes

in neural integration properties aligned with changes in behavior within the change detection task. To develop a proxy for testing changes in behavioral strategy for this purpose, we took advantage of the fact that rats' evaluation timescales tended to contract over the course of the trial: PRCs for false alarms occurring earlier than 2 s into a trial) possessed a wider kernel at 0.46 s than for false alarms occurring later than 2 s into a trial) at 0.36 s (**Figure 5A**). Furthermore, the PRC for early false alarms reached a peak amplitude of 30.60 Hz +/- 1.49 Hz, exceeding the peak amplitude of late false alarm PRC (27.9 Hz +/- 1.01 Hz, 95% CI, $p<0.05$). At the psychophysical level, this disparity may represent a shorter timescale of evidence evaluation owing to a smaller amount of evidence required to reach a decision threshold. Therefore, it seemed plausible that if recorded PPC units causally influence detection choices, those cells would accordingly exhibit differing integration dynamics over the course of each decision to engender a quicker or slower decision.

Figure 5B shows click-triggered averages for early and late periods of trials averaged across positively modulated cells. Although the click triggered averages exhibit similar timescales, they notably exhibit different amplitudes, with cells responding more strongly to units of evidence in later trial periods (0.08 +/- 0.02 change from baseline for early and 0.15 +/- 0.02 for late, 95% CI, $p<0.05$). This disparity is consistent with a mechanism in which PPC cells increase the gain of integration as decision time elapses to expedite a response, which would, in turn, shrink the overall timescale of evidence evaluation later in a trial.

A

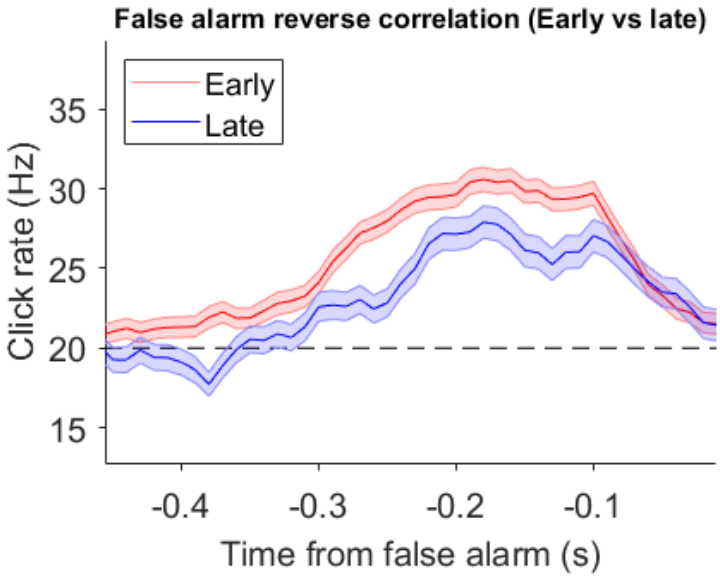
False alarm reverse correlation (Early vs late)
Early
Late
Click rate (Hz)
35
30
25
20
15
-0.4
-0.3
-0.2
-0.1
Time from false alarm (s)

B

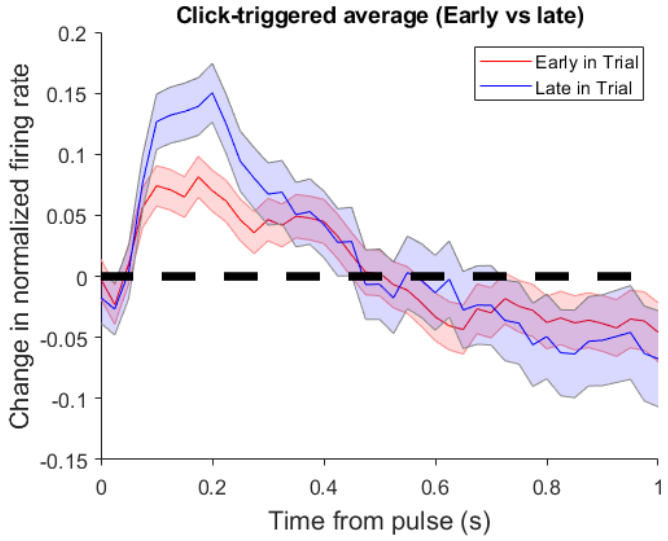
Click-triggered average (Early vs late)
Early in Trial
Late in Trial
Change in normalized firing rate
0.2
0.15
0.1
0.05
0
-0.05
-0.1
-0.15
0
0.2
0.4
0.6
0.8
1
Time from pulse (s)

C

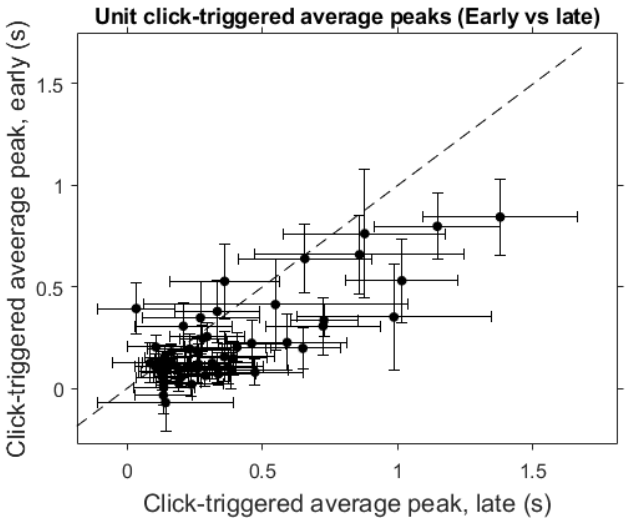
Unit click-triggered average peaks (Early vs late)
Click-triggered averege peak, early (s)
1.5
1
0.5
0
0
0.5
1
1.5
Click-triggered average peak, late (s)

Figure 5: Behavioral and PPC neural responses for early and late stimulus periods. A) False alarm psychophysical reverse correlation for same rats in Figure 1 separated by time of false alarm. Red trace represents trials in which a false alarm occurred within 2 s of stimulus start and blue trace represents trials in which a false alarm occurred later than 2 s after stimulus start. Otherwise, plotting conventions are identical to those in Figure 1C. **B)** Population click-triggered averages for 57 positively modulated units from Figure 2 separated by time of pulse. Red trace represents the average response to baseline pulses occurring earlier than 2 s in all trials. Blue trace represents the average response to baseline pulses occurring later than 2 s in all trials. **C)** Click-triggered average peak amplitudes for 57 positively modulated units from Figure 2. Each marker represents the maximum click-triggered average value for one of 57 units, plotted for responses to early (<2 s) pulses against late (>2 s) pulses. Dotted reference line marks values of equivalence between peak responses to early and late pulses. Error bars show S.E.M.

responding more strongly to units of evidence in later trial periods (0.08 +/- 0.02 change from baseline for early and 0.15 +/- 0.02 for late, 95% CI, $p<0.05$). This disparity is consistent with a mechanism in which PPC cells increase the gain of integration as decision time elapses to expedite a response, which would, in turn, shrink the overall timescale of evidence evaluation later in a trial.

We also sought to determine whether this change in integration properties was driven by alterations of individual cell dynamics or simply by a shift in activeness between subpopulations of units with different integration properties. Therefore, we calculated peak click-triggered average amplitudes for individual units during early and late periods trial periods and compared the two. Corroborating the hypothesis that individual cells adjust dynamics according to adjustments in behavioral dynamics, most units independently exhibited a higher amplitude response later in trials compared to the first 2 s of trials (**Figure 5C**). In summary, adjustments in timescale of evidence evaluation at the behavioral level directly align with adjustments in response properties of PPC cells during evidence processing.

Causal role of PPC in evidence evaluation in change detection

Finally, we sought to determine whether PPC was necessary for establishing timescales of evidence evaluation. Though examinations of PPC neural dynamics have prominently posited a role for evidence integration for decision making, various studies involving perturbation of PPC during decision making have instead suggested a lack of causal contribution of PPC to decision making (Erlich et al., 2015; Katz et al., 2016; Licata et al., 2017). However, these studies commonly featured a decision time controlled by the environment rather than by the subject. Indeed, PPC seems to maintain a causal role when the animal and not the environment controls the time of decision (Hanks et al., 2006; Zhou and Freedman, 2019), as in the case of our task. Therefore, it is plausible that, even though PPC may not be necessary in the accumulation of sensory evidence for perceptual decisions over long timescales, it may be necessary in setting short timescales of evidence evaluation for situations in which the animal decides how and when to respond to incoming stimuli.

We tested the necessity of PPC functionality in setting a particular timescale of evidence evaluation when the environment does not control decision time by infusing PPC of rat subjects with the GABA agonist muscimol. Then, we compared performance on the change detection task between muscimol sessions and sessions in which subjects were infused with vehicle saline solution. With muscimol inactivation of PPC, rat subjects achieved lower hit rates on average (Veh: 0.61 +/- 0.02, Mus: 0.55 +/- 0.02, 95% CI, $p<0.05$) (**Figure 6A**), but they also accumulated fewer false alarms (Veh: 0.44 +/- 0.02, Mus: 0.29 +/- 0.02, 95% CI, $p<0.05$) (**Figure 6C**). Reaction times on hit trials also increased with PPC inactivation (Veh: 0.31 s +/- 0.007 s, Mus: 0.33 s +/- 0.006 s,

95% CI, p<0.05) (**Figure 6B**), which together with the other changes in metrics illustrates a reduction in propensity to commit to a report.

These patterns in metrics suggested a change in patterns of evidence evaluation in that rats seem to evaluate evidence more conservatively with PPC inactivation. Longer timescales of evidence evaluation lend themselves to lessened influence of brief changes in evidence strength, which would in turn reduce incidence of both accurate and erroneous detection reports. We tested this hypothesis by calculating and comparing false alarm PRCs for vehicle control and inactivation sessions. As predicted by psychometric results, false alarm PRCs for PPC inactivation sessions showed a greater width than that of vehicle sessions (0.43 s +/- 0.03 s for vehicle and 0.52 s +/- 0.05 s for muscimol, 95% CI, p<0.05) (**Figure 6D**). This difference in PRC width demonstrates a longer average timescale of evaluation when PPC is inactive, thus supporting a role of PPC in establishing the timescale of evidence evaluation for decision making.

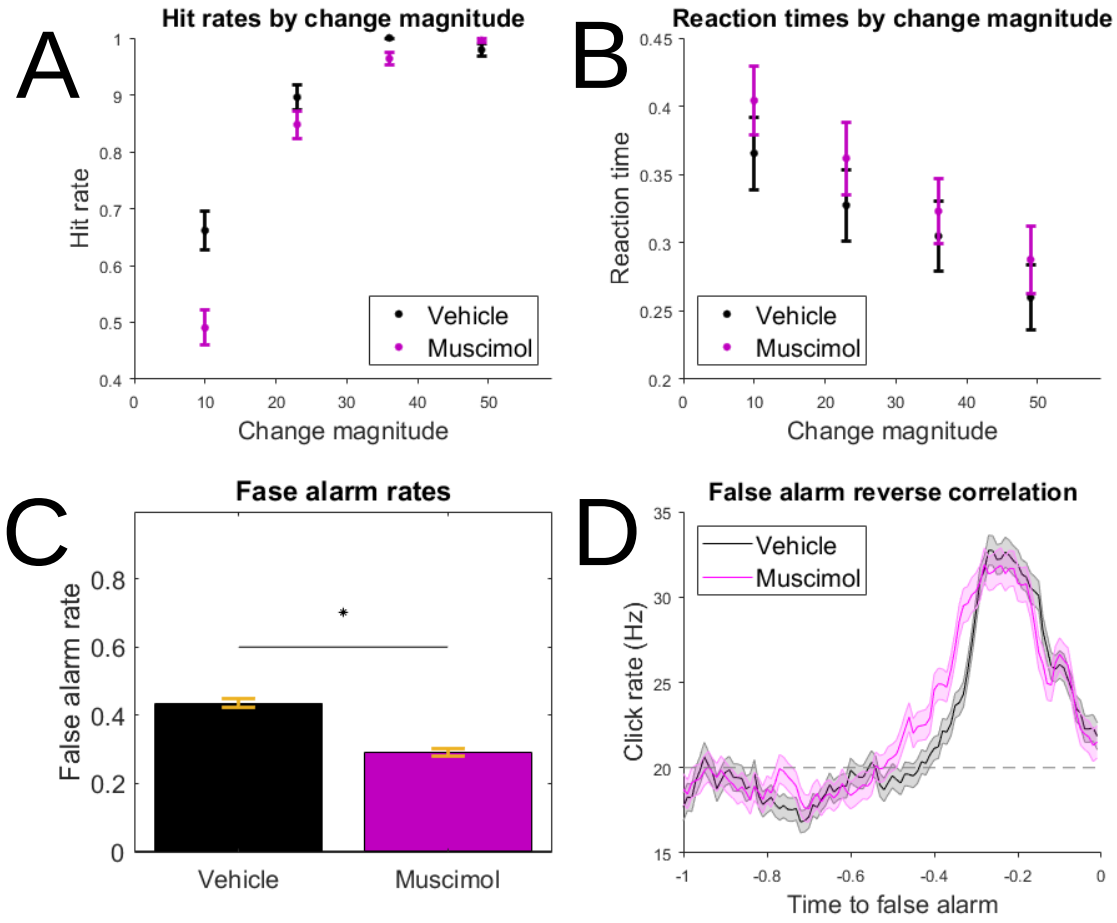

Figure 6: Rat behavioral performance following muscimol inactivation of PPC. A) Hit rates across change magnitudes for 2 rats during task performance following PPC infusion of vehicle (black) or muscimol (purple). Error bars show 95% confidence intervals. **B)** Reaction times across change magnitudes for 2 rats during task performance following PPC infusion of vehicle (black) or muscimol (purple). Error bars show 95% confidence intervals. **C)** False alarm rates for 2 rats during task performance following PPC infusion of vehicle (black) or muscimol (purple). Error bars show 95% confidence intervals. **D)** False alarm psychophysical reverse correlations for 2 rats durin task performance following PPC infusion of vehicle (black) or muscimol (purple). Error bars show S.E.M.

Discussion

PPC has long been a subject of controversy in decision making neuroscience, and its role in evaluation of evidence has been repeatedly called into question (Brody

and Hanks, 2016; Hanks and Summerfield, 2017). Past studies of PPC in the context of decision making have largely focused on its potential role as an evidence accumulator. Our results posit an alternative putative function of PPC in setting the timescale of evidence evaluation for decision making by demonstrating both electrophysiological neural dynamics suitable for short timescale evidence evaluation, in contrast with previous results demonstrating suitability for long timescale evidence evaluation, and a causal role in short timescale evidence evaluation. We collected these results using a novel auditory change point detection task for rat subjects, also able to be performed by humans, that allows us to study how the brain evaluates evidence over short timescales.

Our findings imply PPC neuronal activity can be tuned to task demands, which more clearly defines PPC's role in a larger decision making network. These timescales are not observed in decisions involving linear accumulation of evidence, and the timescales could not emerge solely in downstream populations because they would not be observed in our observed units. Therefore, the short timescales we see must be instantiated either within the PPC population or in their afferents. The former possibility may be implemented, for example, through PPC's robust interneuron population, which has been shown to selectively suppress sensory responses in PPC (Song et al., 2017, 2020). This circuit property, combined with negative feedback in the form of recurrence, could potentially lead to short integration timescales. The latter possibility is more readily explained by previously observed properties of PPC's sensory afferents, which showcase diverse timescales of modulation following sensory stimulation (Bernacchia et al., 2011; Murray et al., 2014; Scott et al., 2017). These timescales could therefore

simply be inherited by PPC from primary sensory regions. In either case, other nodes in the perceptual decision making network, such as anterior dorsal striatum, may also inherit these timescales, which would further position PPC as a crucial mediator of evidence evaluation timescales.

The dichotomy in PPC dynamics between positively and negatively modulated cells demonstrates an additional dimension of flexibility beyond timescale. While most studies of PPC's role in evidence evaluation involve lateralized tasks in which subjects choose between left and right, our task instead requires choice between responding and withholding a response from moment to moment. This task, a member of a larger category of go vs no-go tasks (Donders, 1969; Gomez et al., 2007), accordingly introduces different motor demands and more greatly emphasizes inhibition of response. The subpopulation of negatively modulated PPC neurons may contribute to successful change detection by suppressing aberrant responses at baseline and releasing inhibition on appropriate responses in change periods, in line with downstream motor systems of perceptual decision making as in primate saccade circuits (Fuchs et al., 1985; Sparks, 2002) or the indirect pathway in the basal ganglia (Albin et al., 1989; DeLong, 1990). As such, the behavior evoked by the demands of our change detection task evoke multiple forms of unique neural dynamics in PPC that can plausibly serve that behavior.

We also discovered flexibility of neural responses in PPC within a single task modality, wherein both the neural population and individual units seem to tune their response properties from decision to decision and also within decisions with respect to an observed change in evidence integration gain over time. PPC cells altered the gain

of processing to individual pulses of evidence, responding more strongly to incoming evidence as trials progressed. Strikingly, this change in neural response property corresponded with changes at the behavioral level. False alarms occurring late in trials were associated with a shorter timescale of evidence evaluation as demonstrated by psychophysical reverse correlation compared to false alarms occurring earlier in trials. Along the orthogonal dimension of the magnitude of the evidence integration and the associated evidence criterion, we also see a decrease in the required amount of evidence required to trigger a decision in the case of these late false alarms. Adjustments in PPC neural dynamics therefore provide a putative explanation for the observed behavioral changes because stronger responses to evidence could instantiate a shorter evaluation timescale by allowing attainment of an evidence criterion over a shorter period. Previous studies have suggested neural mechanisms in PPC and elsewhere for expediting decision time due to sources of urgency or changes in environmental statistics (Hanks et al., 2014; Janssen and Shadlen, 2005; Thura and Cisek, 2016, 2017). Here, though, we have identified an instance of altered evaluation timescales that can serve a similar function in controlling decision time at the level of integration of incoming evidence and adjustments in the dynamics of such integration.

Although these electrophysiological responses present a strong case for PPC's involvement in the perceptual decision making process, past perturbation studies of PPC challenged a causal role in that process (Erlich et al., 2015; Katz et al., 2016). In contrast, inactivation of PPC produced marked changes in auditory change detection: Subjects responded less impulsively, accruing both fewer hits and false alarms, and evaluated evidence over longer timescales. We surmise that, without PPC functionality,

rats may be unable to employ the evaluation timescale they developed in training and default to a longer timescale. This deficit would be less likely to affect performance in a task where all evidence is evaluated over a long timescale with equal weighting, in turn. In this way, we hypothesize PPC plays a modulatory role in evidence evaluation; even if it does not serve as the brain's causal accumulator of evidence, it may mediate the timescale of evidence integration in downstream brain regions that do serve in that capacity.

Methods

Subjects

A total of 4 male Long-Evans rats from 1-2 years were used for this study. 2 rats were used for neural recordings and 2 rats were used for the inactivation experiment. Rats were water restricted outside of behavioral sessions but given free access to water thirty minutes following completion of a session for one hour.

Apparatus

Tasks were programmed and run in MATLAB (Mathworks) and facilitated by Bpod (Sanworks) to measure real-time behavioral output. Operant chambers used to facilitate behavioral data collection consisted of three ports made of stainless steel (training and inactivation data collection) or Delrin polymer (electrophysiological data collection). Each port contains an infrared LED beam that detects rat nose insertion upon obstruction of the beam, as well as an LED light that signals to rats when the port is active.

Behavior

We trained rats to perform an auditory change detection task previously employed in studies involving human subjects (Ganupuru et al., 2019; Johnson et al., 2017). In this study's implementation, rats insert their nose into the central port of a behavioral apparatus cued by an LED light. Upon nose insertion, a stream of auditory pulses ("clicks") is generated at a baseline rate of 20 Hz according to a Poisson process. At a random point in time, with a mean of 2 s and a maximum time of 4 s, the generative click rate increases by a variable magnitude of 10 Hz, 23 Hz, 36 Hz, or 49 Hz. The hazard rate for change times was flat. After a change occurs, the rat has 0.8 s to respond by withdrawing from the port. Successful withdrawal within the allotted time window is recorded as a "hit," which is rewarded with a drop of water from a port on either the left or right of the central port. Failure to withdraw within the allotted time is recorded as a "miss," with reward withheld. Premature response in the absence of a change is recorded as a "false alarm," with reward withheld. Finally, on 30% of trials, no change occurs, in which case the rat must maintain fixation in the central port until the stimulus ends to achieve a "correct rejection." Sessions lasted 80 minutes.

Before implantation of electrodes, rats were acclimated to a separate, electrically inert chamber for behavioral training. For behavioral criteria, we chose rats with at least a 0.4 correct rejection rate and 0.5 hit rate on >300 trials per session.

Electrophysiological recordings

Single unit recordings were taken with Neuropixel 1.0 probes (Jun et al., 2017; Steinmetz et al., 2018). Probe implants were assembled according to previous methods

(Juavinett et al., 2020). A silver wire is soldered to the grounding contacts on the probe, and the probe is glued to a 3D-printed internal mount that is affixed to a stereotax adapter for implantation. The internal mount is then bound to an external mount by epoxy that holds a headstage circuit board for data transmission.

Probes were stereotactically implanted at -3.95 mm AP relative to Bregma, +/-2.2 mm ML relative to bregma (probe implanted contralateral to the side of the reward port assigned to the subject), and 1.5 mm ventral to brain surface. Probes were lowered slowly, roughly 20 seconds per 0.1 mm, while simultaneously recording to ensure probe function and verify implantation depth. Ground wires were inserted into the cerebellum approximately 2 mm posterior to IA0. After implantation of probe and ground wire, both craniotomies were filled with sterile optical lubricant. Dental acrylic was applied to the external mount of the probe and the ground wire to bind the implant to the skull, and absolute dentin was applied over the skull to seal the wound. The headstage was taped to the external mount with Kapton tape and the implant was covered with self-adhesive wrapping. Rats were left with free access to food and water to recover for one week following surgery before resumption of training and recordings.

During recording sessions, self-adhesive wrapping was removed and an interface cable was plugged into the headstage. The interface cable was wrapped around a gel toe sleeve to relieve strain from the rat moving. The cable was fed through a simple pully system to prevent the rat from grasping the cable while rearing, connecting to a PXIe acquisition module. This module interfaced with the Bpod and recording computer. Recordings were operated through Open Ephys 3.

Drug Infusions

Rats were implanted bilaterally with guide cannulas with a length of 4mm at +/- 2.2 mm lateral and at either 3.80 or 3.95 mm posterior to bregma. Guide cannulas were lowered to the brain surface then cemented in place as describe above. Dummy cannulas extending 0.5 mm past the tip of the guide cannula were inserted into the guide cannulas at the end of surgery. Following recovery from surgery and 3-4 days before the first infusion and data collection session, rats underwent a sham infusion in which rats were lightly anesthetized with 2% isoflurane and internal cannulas extending 1.5 mm past the tip of the guide cannula were inserted into the brain for four minutes. Rats were allowed to recover for 30 minutes before the behavioral session began.

Rats were infused twice a week before behavioral sessions with 0.3 µL of either saline solution (vehicle condition) or 1 mg/mL muscimol and saline solution (muscimol condition), alternatively. Volumes and concentrations were based on those of previous inactivation studies of this region, which were, in turn, based on autoradiographic and electrophysiological validation of muscimol spread dynamics (Krupa et al., 1999; Martin, 1991). After being anesthetized with 2% isoflurane, rats were injected with either muscimol or vehicle through an internal cannula fitting inside the guide cannula and extending 1.5 mm past the tip of the guide. The internal cannula was attached to a tube filled with mineral oil, which was attached on the opposite end to a Hamilton syringe used to control the injection. After slowly injecting the fluid over a period of two minutes, the internal cannula was left in the brain for four minutes to allow full diffusion of fluid and relief of any backflow through the cannula's shaft. This process was repeated for

each of the two cannulas. Like in the sham infusion, rats were left to recover for 30 minutes before the behavioral session began.

Behavioral data analysis

Hit rates were calculated as the proportion of trials in which rats withdrew their nose within 0.8 s of change point, excluding false alarm and catch trials. False alarm trials included all trials in which rats withdrew their nose during stimulus baseline, including change and catch trials. Reaction times were calculated as the time of nose withdrawal after change point.

Psychophysical reverse correlations were generated by aligning the click times of each false alarm trial to the time of the rat's report. False alarm trials were used to avoid the confound of generative rate change associated with hit trials, which allowed us to study the relationship between stimulus and response by taking advantage solely of the stimulus's Poisson property. For visualization, each false alarm click time vector was convolved with a causal half-Gaussian filter with a standard deviation of 0.03 s and sampling every 0.01 s. Regardless of false alarm time and thus duration of stimulus preceding the detection report, all false alarms were included in the PRC, with false alarms with shorter stimulus durations simply contributing to a smaller epoch of the PRC. After this smoothing, false alarm reverse correlations were averaged together. For calculation of early and late false alarms, false alarm trials were categorized as early if the false alarm occurred within 2 s of stimulus start and late if the false alarm occurred later than 2 s after stimulus start.

Electrophysiological data processing and analysis

We used the Kilosort 3 spike sorting algorithm (Pachitariu et al., 2016) to identify single units clusters of spiking activity in our data to include for data processing. Following initial sorting, the Phy 2.0 cluster viewing software (Rossant, 2022) was used to manually curate clusters to remove units with drop-out due to drift via visualization of amplitude plots over the course of a session. Phy also allowed us to merge clusters that clearly originated from the same unit by assessing correlation of spike times between clusters and correlations in drift. Units that drifted out of the probe's recording radius during a session were excluded from analysis to avoid distortion of trial-by-trial response observations.

We further filtered single units for inclusion in analysis by identifying units with at least a 1 Hz firing rate during active task engagement (i.e. during stimulus presentation and reward collection). The remaining units were again filtered for task modulation by comparing firing rates during the post-change period of increased stimulus rate to the pre-change period of baseline stimulus rate (Wilcoxon ranked sum test, $p<0.05$). Units were sorted into two groups: those with a higher firing rate during baseline, comprising negatively modulated units, and those with a higher firing rate following stimulus change, comprising positively modulated units.

Peri-stimulus time histograms (PSTHs) were calculated by aligning spikes to one of two stimulus events, time of response or time of change. Spikes were convolved with a causal half-Gaussian filter (0.01 s bin size, using MATLAB's *maskraster* function for visualization). To test periods of significant correlation between stimulus strength and neural responses leading up to detection reports, a sliding average of spikes over 100

ms increments was calculated from the time of report to 1 s prior to the detection report. For each increment, a linear regression model was calculated using MATLAB's *fitlm* function, and the slope, standard error of the slope, and p-value (calculated from the fit's t-statistic) were ascertained. We demarcated the period of significant modulation as the end of the final increment during which $p<0.05$ for the model fit, moving from report time to earlier time points, also noting the sign of the slope (positive for positively modulated units, negative for negatively modulated units).

Click-triggered averages were calculated by aligning neural responses to the time of each pulse during baseline for each trial during the recording. For pooled unit click-triggered averages, we combined responses of all units into a single "meta unit" using all baseline pulse responses from all trials. Crucially, we subtracted each trial's baseline firing rate from the pulse responses for all units recorded during a given trial. This allowed us to neutralize time-dependent modulation and response contamination from other pulses in the calculated the averages. Unit-specific click-triggered averages (Figure 3) were calculated in the same way, but plotted values are normalized to the peak click-triggered response for each unit, such that all responses are divided by the value of the click-triggered average's peak and bins with values below -1 being rounded up to -1. For comparing click-triggered averages occurring early or late in trials, we included responses to pulses occurring before 2 s during stimulus presentation in the early category and responses occurring later than 2 s in the late category.

References

Albin, R.L., Young, A.B., and Penney, J.B. (1989). The functional anatomy of basal ganglia disorders. Trends Neurosci *12*, 366–375. https://doi.org/10.1016/0166-2236(89)90074-x.

Berg, R. van den, Anandalingam, K., Zylberberg, A., Kiani, R., Shadlen, M.N., and Wolpert, D.M. (2016). A common mechanism underlies changes of mind about decisions and confidence. ELife Sciences *5*, e12192. https://doi.org/10.7554/eLife.12192.

Bernacchia, A., Seo, H., Lee, D., and Wang, X.-J. (2011). A reservoir of time constants for memory traces in cortical neurons. Nat Neurosci *14*, 366–372. https://doi.org/10.1038/nn.2752.

Brody, C.D., and Hanks, T.D. (2016). Neural underpinnings of the evidence accumulator. Curr. Opin. Neurobiol. *37*, 149–157. https://doi.org/10.1016/j.conb.2016.01.003.

Chandler, H.C., King, V., Corwin, J.V., and Reep, R.L. (1992). Thalamocortical connections of rat posterior parietal cortex. Neuroscience Letters *143*, 237–242. https://doi.org/10.1016/0304-3940(92)90273-A.

Cheatwood, J.L., Reep, R.L., and Corwin, J.V. (2003). The associative striatum: cortical and thalamic projections to the dorsocentral striatum in rats. Brain Research *968*, 1–14. https://doi.org/10.1016/S0006-8993(02)04212-9.

Churchland, A.K., and Ditterich, J. (2012). New advances in understanding decisions among multiple alternatives. Current Opinion in Neurobiology *22*, 920–926. https://doi.org/10.1016/j.conb.2012.04.009.

Churchland, A.K., Kiani, R., and Shadlen, M.N. (2008). Decision-making with multiple alternatives. Nat Neurosci *11*, 693–702. https://doi.org/10.1038/nn.2123.

DeLong, M.R. (1990). Primate models of movement disorders of basal ganglia origin. Trends Neurosci *13*, 281–285. https://doi.org/10.1016/0166-2236(90)90110-v.

Donders, F.C. (1969). On the speed of mental processes. Acta Psychol (Amst) *30*, 412–431. https://doi.org/10.1016/0001-6918(69)90065-1.

Erlich, J.C., Brunton, B.W., Duan, C.A., Hanks, T.D., and Brody, C.D. (2015). Distinct effects of prefrontal and parietal cortex inactivations on an accumulation of evidence task in the rat. ELife Sciences *4*, e05457. https://doi.org/10.7554/eLife.05457.

Fuchs, A.F., Kaneko, C.R., and Scudder, C.A. (1985). Brainstem control of saccadic eye movements. Annu Rev Neurosci *8*, 307–337. https://doi.org/10.1146/annurev.ne.08.030185.001515.

Ganupuru, P., Goldring, A.B., Harun, R., and Hanks, T.D. (2019). Flexibility of Timescales of Evidence Evaluation for Decision Making. Current Biology *29*, 2091-2097.e4. https://doi.org/10.1016/j.cub.2019.05.037.

Gold, J.I., and Shadlen, M.N. (2007). The Neural Basis of Decision Making. Annual Review of Neuroscience *30*, 535–574. https://doi.org/10.1146/annurev.neuro.29.051605.113038.

Gomez, P., Ratcliff, R., and Perea, M. (2007). A Model of the Go/No-Go Task. J Exp Psychol Gen *136*, 389–413. https://doi.org/10.1037/0096-3445.136.3.389.

Green, D.M., and Swets, J.A. (1966). Signal detection theory and psychophysics (Oxford, England: John Wiley).

Hanks, T.D., and Summerfield, C. (2017). Perceptual Decision Making in Rodents, Monkeys, and Humans. Neuron *93*, 15–31. https://doi.org/10.1016/j.neuron.2016.12.003.

Hanks, T., Kiani, R., and Shadlen, M.N. (2014). A neural mechanism of speed-accuracy tradeoff in macaque area LIP. ELife *3*, e02260. https://doi.org/10.7554/eLife.02260.

Hanks, T.D., Ditterich, J., and Shadlen, M.N. (2006). Microstimulation of macaque area LIP affects decision-making in a motion discrimination task. Nat. Neurosci. *9*, 682–689. https://doi.org/10.1038/nn1683.

Hanks, T.D., Kopec, C.D., Brunton, B.W., Duan, C.A., Erlich, J.C., and Brody, C.D. (2015). Distinct relationships of parietal and prefrontal cortices to evidence accumulation. Nature *520*, 220–223. https://doi.org/10.1038/nature14066.

Harun, R., Jun, E., Park, H.H., Ganupuru, P., Goldring, A.B., and Hanks, T.D. (2020). Timescales of Evidence Evaluation for Decision Making and Associated Confidence Judgments Are Adapted to Task Demands. Front. Neurosci. *14*. https://doi.org/10.3389/fnins.2020.00826.

Janssen, P., and Shadlen, M.N. (2005). A representation of the hazard rate of elapsed time in macaque area LIP. Nature Neuroscience *8*, 234–241. https://doi.org/10.1038/nn1386.

Johnson, B., Verma, R., Sun, M., and Hanks, T.D. (2017). Characterization of decision commitment rule alterations during an auditory change detection task. Journal of Neurophysiology *118*, 2526–2536. https://doi.org/10.1152/jn.00071.2017.

Juavinett, A.L., Bekheet, G., and Churchland, A.K. (2020). Implanting and Recycling Neuropixels Probes for Recordings in Freely Moving Mice. Bio Protoc *10*, e3503. https://doi.org/10.21769/BioProtoc.3503.

Juavinett, A.L., Bekheet, G., and Churchland, A.K. Chronically implanted Neuropixels probes enable high-yield recordings in freely moving mice. ELife *8*, e47188. https://doi.org/10.7554/eLife.47188.

Jun, J.J., Steinmetz, N.A., Siegle, J.H., Denman, D.J., Bauza, M., Barbarits, B., Lee, A.K., Anastassiou, C.A., Andrei, A., Aydın, Ç., et al. (2017). Fully Integrated Silicon Probes for High-Density Recording of Neural Activity. Nature *551*, 232–236. https://doi.org/10.1038/nature24636.

Katz, L.N., Yates, J.L., Pillow, J.W., and Huk, A.C. (2016). Dissociated functional significance of decision-related activity in the primate dorsal stream. Nature *535*, 285–288. https://doi.org/10.1038/nature18617.

Kiani, R., Hanks, T.D., and Shadlen, M.N. (2008). Bounded Integration in Parietal Cortex Underlies Decisions Even When Viewing Duration Is Dictated by the Environment. J Neurosci *28*, 3017–3029. https://doi.org/10.1523/JNEUROSCI.4761-07.2008.

Krupa, D.J., Ghazanfar, A.A., and Nicolelis, M.A.L. (1999). Immediate thalamic sensory plasticity depends on corticothalamic feedback. Proc Natl Acad Sci U S A *96*, 8200–8205. .

Leon, M.I., and Shadlen, M.N. (2003). Representation of Time by Neurons in the Posterior Parietal Cortex of the Macaque. Neuron *38*, 317–327. https://doi.org/10.1016/S0896-6273(03)00185-5.

Licata, A.M., Kaufman, M.T., Raposo, D., Ryan, M.B., Sheppard, J.P., and Churchland, A.K. (2017). Posterior Parietal Cortex Guides Visual Decisions in Rats. The Journal of Neuroscience *37*, 4954–4966. https://doi.org/10.1523/JNEUROSCI.0105-17.2017.

Martin, J.H. (1991). Autoradiographic estimation of the extent of reversible inactivation produced by microinjection of lidocaine and muscimol in the rat. Neurosci Lett *127*, 160–164. https://doi.org/10.1016/0304-3940(91)90784-q.

McGeorge, A.J., and Faull, R.L.M. (1989). The organization of the projection from the cerebral cortex to the striatum in the rat. Neuroscience *29*, 503–537. https://doi.org/10.1016/0306-4522(89)90128-0.

Murray, J.D., Bernacchia, A., Freedman, D.J., Romo, R., Wallis, J.D., Cai, X., Padoa-Schioppa, C., Pasternak, T., Seo, H., Lee, D., et al. (2014). A hierarchy of intrinsic timescales across primate cortex. Nat Neurosci *17*, 1661–1663. https://doi.org/10.1038/nn.3862.

Okazawa, G., Sha, L., Purcell, B.A., and Kiani, R. (2018). Psychophysical reverse correlation reflects both sensory and decision-making processes. https://doi.org/10.1101/273680.

Ossmy, O., Moran, R., Pfeffer, T., Tsetsos, K., Usher, M., and Donner, T.H. (2013). The Timescale of Perceptual Evidence Integration Can Be Adapted to the Environment. Current Biology *23*, 981–986. https://doi.org/10.1016/j.cub.2013.04.039.

Pachitariu, M., Steinmetz, N., Kadir, S., Carandini, M., and Kenneth D., H. (2016). Kilosort: realtime spike-sorting for extracellular electrophysiology with hundreds of channels (Neuroscience).

Piet, A.T., Erlich, J.C., Kopec, C.D., and Brody, C.D. (2017). Rat Prefrontal Cortex Inactivations during Decision Making Are Explained by Bistable Attractor Dynamics. Neural Computation *29*, 2861–2886. https://doi.org/10.1162/neco_a_01005.

Raposo, D., Kaufman, M.T., and Churchland, A.K. (2014). A category-free neural population supports evolving demands during decision-making. Nat Neurosci *17*, 1784–1792. https://doi.org/10.1038/nn.3865.

Ratcliff, R., and McKoon, G. (2008). The Diffusion Decision Model: Theory and Data for Two-Choice Decision Tasks. Neural Comput *20*, 873–922. https://doi.org/10.1162/neco.2008.12-06-420.

Reep, R.L., Chandler, H.C., King, V., and Corwin, J.V. (1994). Rat posterior parietal cortex: topography of corticocortical and thalamic connections. Exp Brain Res *100*, 67–84. https://doi.org/10.1007/BF00227280.

Roitman, J.D., and Shadlen, M.N. (2002). Response of Neurons in the Lateral Intraparietal Area during a Combined Visual Discrimination Reaction Time Task. J. Neurosci. *22*, 9475–9489. .

Rossant, C. (2022). phy: interactive visualization and manual spike sorting of large-scale ephys data (The Cortical Processing Laboratory at UCL).

Scott, B.B., Constantinople, C.M., Akrami, A., Hanks, T.D., Brody, C.D., and Tank, D.W. (2017). Fronto-parietal Cortical Circuits Encode Accumulated Evidence with a Diversity of Timescales. Neuron *95*, 385-398.e5. https://doi.org/10.1016/j.neuron.2017.06.013.

Selemon, L.D., and Goldman-Rakic, P.S. (1988). Common cortical and subcortical targets of the dorsolateral prefrontal and posterior parietal cortices in the rhesus monkey: evidence for a distributed neural network subserving spatially guided behavior. J. Neurosci. *8*, 4049–4068. .

Shadlen, M.N., and Newsome, W.T. (1996). Motion perception: seeing and deciding. Proceedings of the National Academy of Sciences *93*, 628–633. https://doi.org/10.1073/pnas.93.2.628.

Song, Y.-H., Kim, J.-H., Jeong, H.-W., Choi, I., Jeong, D., Kim, K., and Lee, S.-H. (2017). A Neural Circuit for Auditory Dominance over Visual Perception. Neuron *93*, 940-954.e6. https://doi.org/10.1016/j.neuron.2017.01.006.

Song, Y.-H., Hwang, Y.-S., Kim, K., Lee, H.-R., Kim, J.-H., Maclachlan, C., Dubois, A., Jung, M.W., Petersen, C.C.H., Knott, G., et al. (2020). Somatostatin enhances visual processing and perception by suppressing excitatory inputs to parvalbumin-positive interneurons in V1. Sci Adv *6*, eaaz0517. https://doi.org/10.1126/sciadv.aaz0517.

Sparks, D.L. (2002). The brainstem control of saccadic eye movements. Nat Rev Neurosci *3*, 952–964. https://doi.org/10.1038/nrn986.

Steinmetz, N.A., Koch, C., Harris, K.D., and Carandini, M. (2018). Challenges and opportunities for large-scale electrophysiology with Neuropixels probes. Curr Opin Neurobiol *50*, 92–100. https://doi.org/10.1016/j.conb.2018.01.009.

Thura, D., and Cisek, P. (2016). Modulation of Premotor and Primary Motor Cortical Activity during Volitional Adjustments of Speed-Accuracy Trade-Offs. J. Neurosci. *36*, 938–956. https://doi.org/10.1523/JNEUROSCI.2230-15.2016.

Thura, D., and Cisek, P. (2017). The Basal Ganglia Do Not Select Reach Targets but Control the Urgency of Commitment. Neuron *95*, 1160-1170.e5. https://doi.org/10.1016/j.neuron.2017.07.039.

van Vugt, M., Simen, P., Nystrom, L., Holmes, P., and Cohen, J. (2012). EEG Oscillations Reveal Neural Correlates of Evidence Accumulation. Frontiers in Neuroscience *6*. .

Wald, A., and Wolfowitz, J. (1950). Bayes Solutions of Sequential Decision Problems. The Annals of Mathematical Statistics *21*, 82–99. https://doi.org/10.1214/aoms/1177729887.

Wyart, V., de Gardelle, V., Scholl, J., and Summerfield, C. (2012). Rhythmic Fluctuations in Evidence Accumulation during Decision Making in the Human Brain. Neuron *76*, 847–858. https://doi.org/10.1016/j.neuron.2012.09.015.

Yartsev, M.M., Hanks, T.D., Yoon, A.M., and Brody, C.D. (2018). Causal contribution and dynamical encoding in the striatum during evidence accumulation. ELife *7*, e34929. https://doi.org/10.7554/eLife.34929.

Zhou, Y., and Freedman, D.J. (2019). Posterior parietal cortex plays a causal role in perceptual and categorical decisions. Science *365*, 180–185. https://doi.org/10.1126/science.aaw8347.

Chapter 4: The role of primary auditory cortex in accumulation of evidence for auditory decisions

Introduction

Perceptual decision making requires processing of raw sensory information into task-related decision variables to inform action selection. Often, this information must be integrated over long periods, such that newer decision evidence is combined with older evidence to most accurately evaluate environmental events to make successful decisions (Gold and Shadlen, 2007; Hanks and Summerfield, 2017). This function has been modeled as a complex “accumulation” process by which each incoming unit of evidence is combined with a fluctuating abstract decision variable, the value of which is evaluated at a variable point dependent on either the decision maker’s own criteria or the point at which evidence is no longer available (Ratcliff and McKoon, 2008; Ratcliff and Rouder, 1998). Several brain regions have been implicated in this accumulation process, including posterior parietal cortex (PPC) (Roitman and Shadlen, 2002; Shadlen and Newsome, 1996), anterior dorsal striatum (Yartsev et al., 2018), and prefrontal cortex (PFC) (Hanks et al., 2015; Noppeney et al., 2010). However, it is unclear the extent to which these regions accumulate evidence via their own intrinsic neural response properties as opposed to inheriting these patterns of responses from upstream brain regions.

Primary sensory regions of the brain represent the first cortical regions receiving sensory inputs, making them key targets of study for understanding the dynamics of information flow in the brain for perceptual decisions. These regions project directly to association areas exhibiting accumulation-like neural responses during decision deliberation (Chandler et al., 1992; Cheatwood et al., 2003; McGeorge and Faull, 1989; Selemon and Goldman-Rakic, 1985; Siegel et al., 2015). The connectivity between

primary auditory cortex (A1) and these regions is especially interesting because of its causal nature, wherein perturbation of its connections with PPC (Zhong et al., 2019) and striatum (Xiong et al., 2015; Znamenskiy and Zador, 2013) directly influences choices on various perceptual decision making tasks. A1 also possesses functions critical to evidence accumulation for auditory decisions, including detection of temporal patterns in evidence (Jaramillo and Zador, 2011; Rybalko et al., 2010), activity reflecting choice selectivity leading up to auditory decisions (Guo et al., 2019), and maintenance of stimulus representation after the end of a stimulus, in line with a short term memory function (Scott and Mishkin, 2016; Yu et al., 2021). Together, these properties could support accumulation of evidence over time in the brain for auditory decisions. Despite these properties, A1 is not necessary for auditory discriminations bearing on simple spectral features of stimuli (Gimenez et al., 2015; Heffner, 1978), suggesting that A1 may be more involved in complex processing of sounds than purely representing spectral qualities of stimuli.

To test the hypothesis that A1 is necessary for evidence accumulation in auditory decision making, we reversibly inactivated A1 of rats performing an auditory discrimination task using the GABA agonist muscimol. We found that A1 is necessary for performance in the task, as A1 inactivation led to decreased accuracy in discrimination. We also inactivated A1 on an auditory change detection task in which evidence is evaluated over a shorter timescale than in the discrimination task, thus not requiring linear accumulation of evidence, resulting in minimal effect on performance. Using model-free analysis, we determined that A1 is necessary for computing the

sensory identity of incoming sensory information for auditory decisions but not necessarily accumulating that information over time.

Results

We trained rats to perform an auditory discrimination task in which subjects poked their nose into the central port of an operant apparatus to trigger two trains of auditory pulses ("clicks"), each emitting from a speaker to either the left or the right (**Figure 1**). The stimulus endured for 1 s, during which the rats maintained port fixation. The stimulus played at a mean total rate of 40 Hz, generated through a Poisson process, but differed in the proportion of left and right clicks from trial to trial. At the end of the stimulus period, the rats poked either a left or right port to indicate the side that emitted more clicks. A correct response yielded a water reward. 30 minutes before each session, rats were infused with either the GABA agonist muscimol or a saline vehicle solution. Muscimol infusions were performed either bilaterally or unilaterally, with vehicle infused to the contralateral side in the latter case.

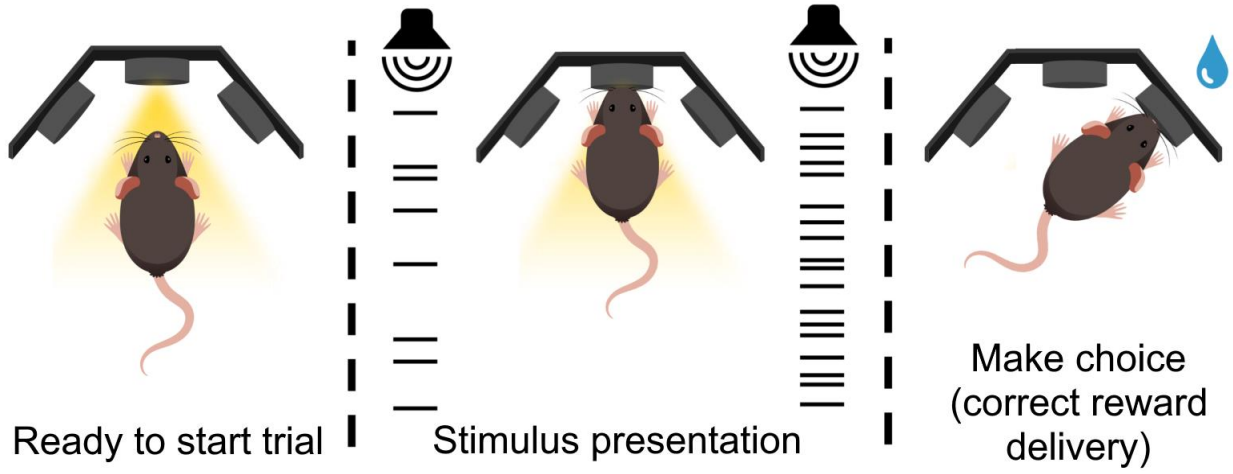

Figure 1: Auditory discrimination task. A trial begins when a rat engages an illuminated central port, triggering two trains of auditory "clicks," one on each side of the rat. After 1 s of stimulus presentation, the rat must engage the left or right port to report

its choice of which train contained more clicks. A correct choice results in a water reward.

Rats performed the task successfully, achieving higher hit rates with greater lateralized click differences (**Figure 2A**). Bilateral muscimol inactivation reduced performance across most stimulus difficulties significantly, with more rightward choices for left trials and more leftward choices for right trials (Two-proportion z-test, $p<0.05$). Performance on all trial types trended this way. With unilateral inactivation, only right muscimol infusions induced significant impairments in performance, however, in the form of a higher proportion of leftward choices (**Figure 2B-C**).

We wanted to determine whether these impairments resulted predominantly from a sensory deficit or an impairment in the rat's ability to accumulate evidence over time. As a model-free approach to this end, we conducted psychophysical reverse correlation (PRC) to assess how rats used evidence over time. Because the stimulus is Poisson, the exact number of clicks on each side can vary from trial to trial even though they are generated with a programmed mean. Rats may thus be more likely to choose a side when there is an excess of clicks on that side relative to the generative rate, so calculating the excess click rate associated with certain trials can inform us of which periods of stimulus had greatest leverage on the rats' decisions. For example, if a rat disregards the early stimulus period, the PRC should be shallower at that period, as an excess click count during that period is less likely to drive the associated choice. Therefore, a contraction in PRC in specific areas indicates a change in how the rat is evaluating information over time, potentially an accumulation deficit, while a contraction

in PRC across the stimulus period is more consistent with sensory deficit, since all evidence is comparably discounted.

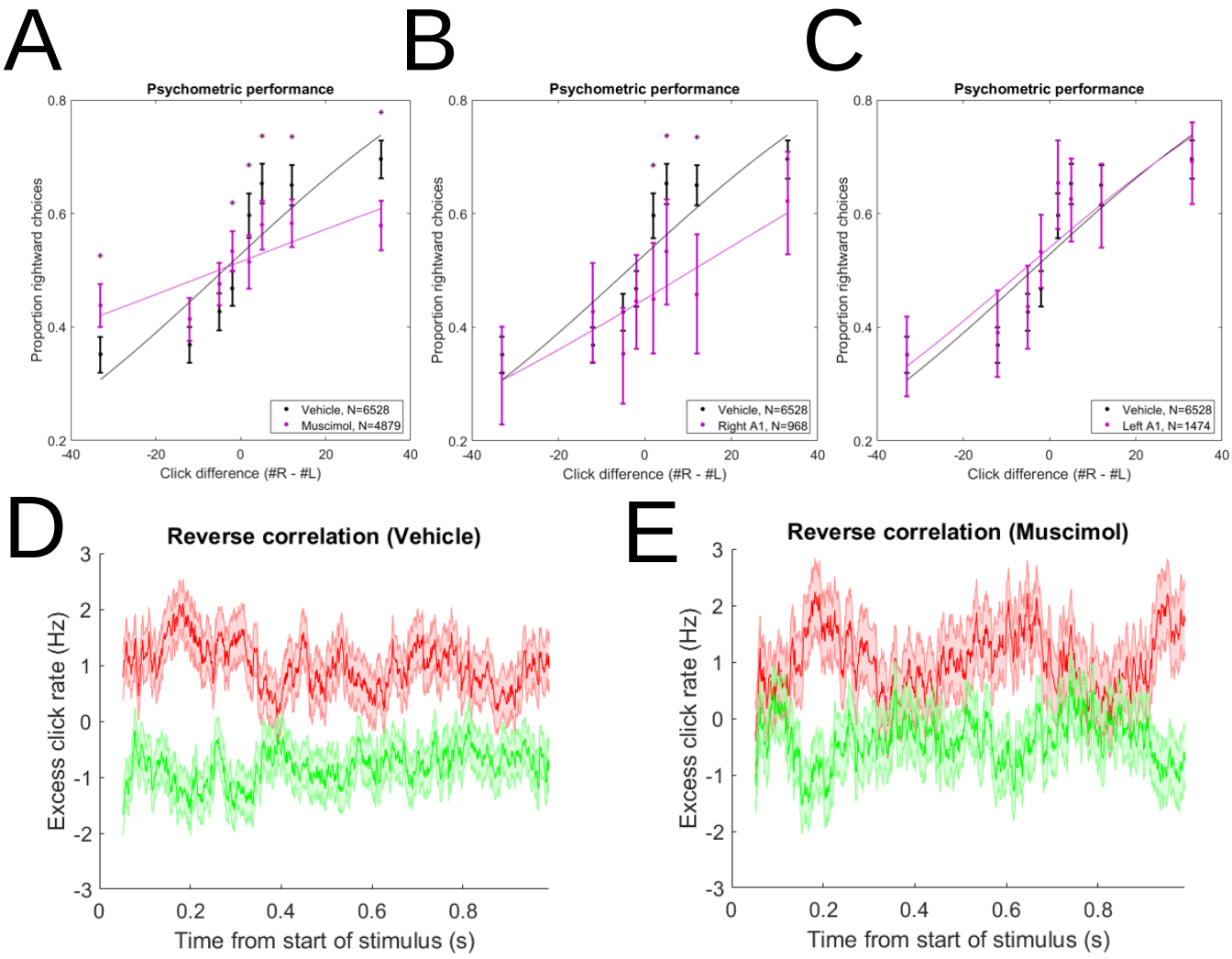

Figure 2: Task performance and effects of muscimol inactivation of A1. A) Performance following bilateral inactivation of A1, pooled from eight subjects. Proportion of rightward choices as a function of the different of right and left clicks. Error bars show SEM and asterisks show significant difference ($p<0.05$) via two-proportion Z-test. Curves are sigmoidal functions fit to the data points for visualization. **B)** Same as A for rightward inactivation of A1. **C)** Same as A for leftward inactivation of A1. **D)** Psychophysical reverse correlations for vehicle sessions. Red trace shows the excess click rate (i.e. the difference between the actual click rate and click rate expected based on the generative rate) for rightward choices. Green trace shows the same for leftward choices. Shading shows SEM. **E)** Same as D for bilateral muscimol sessions.

Figure 2D shows the pooled PRCs across all subjects for the vehicle condition. We found that, in line with the demands of the task, rats used information throughout the trial, with a separation of PRC traces throughout the stimulus period. However, with bilateral muscimol inactivation, the PRC contracted, with overlap between the stimulus at multiple epochs throughout the stimulus period (**Figure 2E**). The PRCs thus suggest a deficit that occurs at least primarily through sensory impairment.

Finally, we wanted to see if these deficits persisted in a task in which linear accumulation of evidence over time is not optimal for task success. We inactivated A1 on a separate auditory change detection task, previously described in Chapters 2 and 3 (**Figure 3A**). Here, rats again engaged a center port, which triggered a single train of clicks with a generative rate of 20 Hz. At a random point in time, the click rate increased by a variable magnitude, at which point the rat had 0.8 s to withdraw from the port. Rats achieved higher hit rates (**Figure 3B**) and lower reaction times (**Figure 3C**) with greater change magnitudes. Unlike in the discrimination task, performance on the change detection task was not significantly impaired with A1 inactivation, including the incidence of false alarms, responses in the absence of a change (**Figure 3D**). For these trials, we computed PRCs using the clicks leading up to the false alarm, which indicated the pattern of evidence that tended to trigger false alarms. We found that PRCs did not differ significantly between vehicle and muscimol conditions in terms of timescale (i.e. the period the PRC exceeded the baseline) but muscimol PRCs did have a slightly lower amplitude than the vehicle PRCs (**Figure 3E**). This difference in PRC pattern did

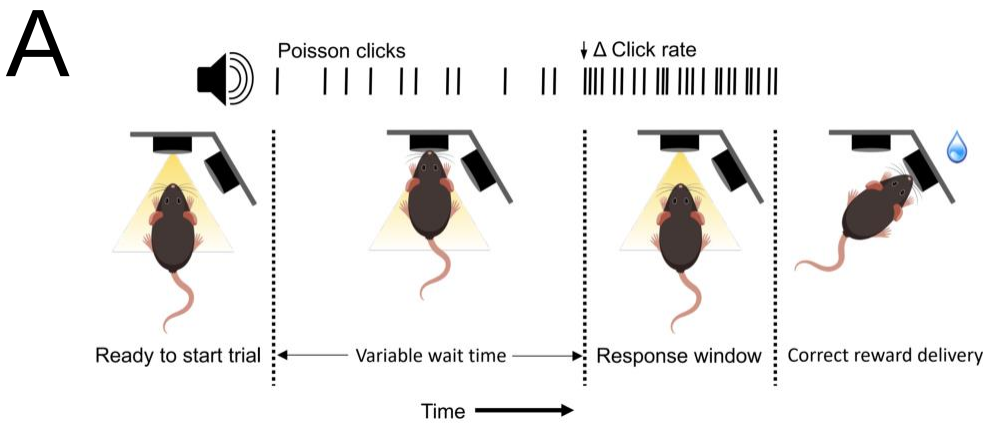
A
Poisson clicks
Δ Click rate
Ready to start trial
Variable wait time
Response window
Correct reward delivery
Time

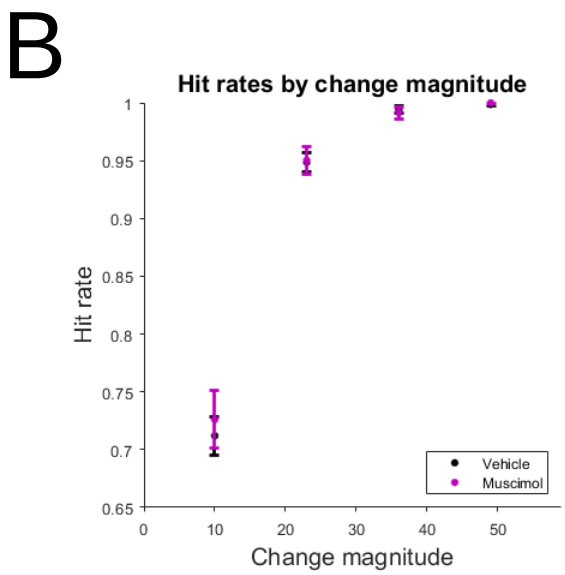
B
Hit rates by change magnitude
Hit rate
Change magnitude
Vehicle
Muscimol

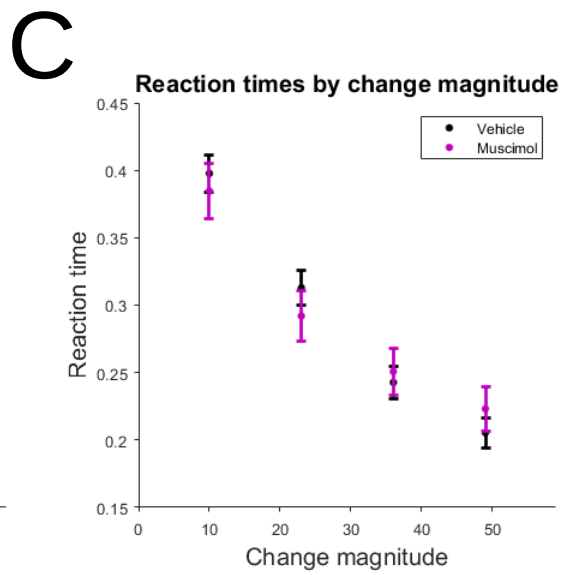
C
Reaction times by change magnitude
Reaction time
Change magnitude
Vehicle
Muscimol

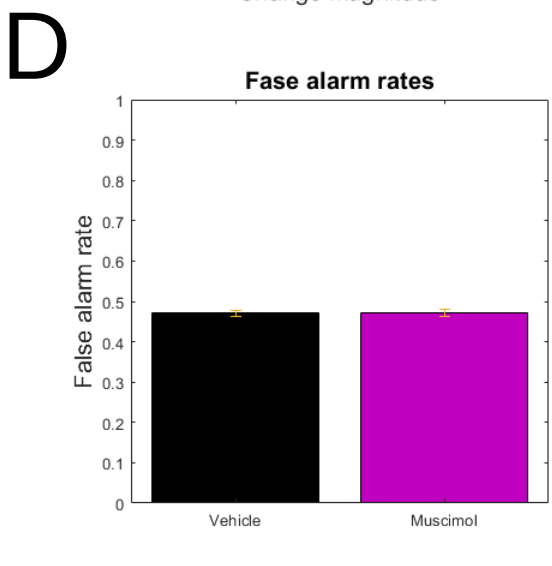
D
Fase alarm rates
False alarm rate
Vehicle
Muscimol

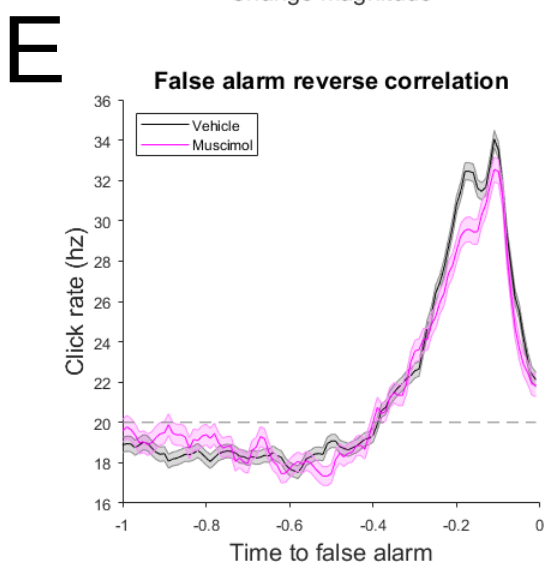
E
False alarm reverse correlation
Vehicle
Muscimol
Click rate (hz)
Time to false alarm

Figure 3: Change detection task performance and effects of muscimol inactivation of A1. A) Task schematic for change detection task. A rat engages a central port which triggers a single train of auditory clicks. At a random point in time, the click rate increases by a variable magnitude, and the rat must remove its nose within 0.8 s. Nose removal during this period results in a "hit." Failure to respond results in a "miss." Response during the pre-change baseline period results in a "false alarm." Correct responses are rewarded with water via a side port. **B)** Hit rate by change magnitude, separated by vehicle (black) and muscimol (purple). Error bars show 95% CI. **C)** Reaction time by change magnitude. Same conventions as B. **D)** False alarm rates. Same conventions as B. **D)** Reverse correlations for false alarm trials. Click rates are aligned to false alarm times, such that the traces show the patterns of evidence that tended to trigger false alarms. Shading shows SEM.

not seem to be sufficient to drive a disparity in performance, though, suggesting that A1 has minimal causal role in auditory change detection over short timescales compared to auditory discrimination over long timescales.

Discussion

In this study, we tested the necessity of primary auditory cortex (A1) in accumulation of evidence over time in auditory decision making. We found that, in an auditory discrimination task performed by rats, bilateral inactivation of A1 impairs performance. Psychophysical reverse correlation revealed this impairment to be driven by a sensory deficit rather than a deficit in the rat's ability to accumulate auditory evidence over time. This is in line with previous findings demonstrating A1's role in sound localization (Heffner, 1978; Malhotra and Lomber, 2007); the discrimination task does not bear on the spectral properties of the stimuli but rather the quantity of stimuli with respect to the directional source. Therefore, it is reasonable to suggest the observed deficit may source partly from a loss of this localization function.

Interestingly, unilateral inactivation only resulted in significant impairment with right A1 inactivation, possibly suggesting a lateralized role in this type of evidence

processing. Indeed, lateralized function in A1 has been identified in processing of language (Springer et al., 1999), stimulus timing (Rybalko et al., 2010), and estimation of stimulus change hazards (Celsis et al., 1999). Left A1 inactivation resulted in a slight but non-significant bias toward the right, so it is possible both sides of A1 contribute to auditory decisions, but rats are better able to compensate for a particular side. Rats exhibited a slight rightward bias, so it also may be that right A1 inactivation reduced bias in general, while left A1 inactivation had minimal effect because leftward choices were already relatively unfavored.

In contrast with inactivation effects on discrimination performance, A1 inactivation on an auditory change detection task did not result in significant impairment to performance. In this task, rats evaluated evidence over short timescales, and the decision depended only on properties of a single stream of evidence. Assessment of reverse correlations on change detection performance did not indicate any change in the timescale over which rats evaluated evidence over time following A1 inactivation. Therefore, it is likely the lack of A1 inactivation effect on change detection performance highlights a different feature of A1's function related to differences between this task and the detection task, such as a lack of localization component in the change detection task.

Methods

Subjects

A total of 11 male Long-Evans rats from 1-2 years were used for this study. 8 rats were used for the discrimination task experiment and 3 rats were used for the change

detection task experiment. Rats were water restricted outside of behavioral sessions but were given free access to water thirty minutes following completion of a 80 minute session for one hour.

Apparatus

Tasks were programmed and run in MATLAB (Mathworks) and facilitated by Bpod (Sanworks) to measure real-time behavioral output. Operant chambers used to facilitate behavioral data collection consisted of three ports made of stainless steel. Each port contains an infrared LED beam that detects rat nose insertion upon obstruction of the beam, as well as an LED light that signals to rats when the port is active, and a lick spout protruding from the center of the port. Above each side port is a speaker.

Behavior

We trained 11 male Long-Evans rats on the discrimination task as described previously (Brunton et al., 2013; Erlich et al., 2015; Hanks et al., 2015). Rats insert their nose into an LED-illuminated center port. This triggers two streams of auditory pulses (“clicks”), one emitting from a speaker from the left and one from a speaker to the right. The clicks played for 1.0 s, at the end of which the central LED would turn off and the LEDs on the two side ports would illuminate. Rats reported their choice by poking the side port associated with their choice, left or right. A correct choice resulted in a water reward. Premature withdrawal from the central port before stimulus ended resulted in violation trials, which were excluded from analysis. The clicks played at a mean generative rate of 40 Hz combined between the sides but were generated through a

Poisson process, such that the actual number of clicks could vary about that mean rate from trial to trial. On each trial, the proportion of clicks emitting from each side also varied, which determined the difficulty of the trial. The average generative click differences between the two sides were 2, 5, 12, and 33.

For the change detection experiment, 3 male Long-Evans rats trained on the change detection task described in Chapter 3. Briefly, rats inserted their noise into a center port in the previously described apparatus to trigger a single stream of clicks with a 20 Hz generative rate. At a random point in time, the click rate increased by a variable magnitude that determined the difficulty of the trial. At the point of change, rats had 0.8 s to withdraw their nose from the central port to achieve a “hit.” Failure to respond in time resulted in a “miss.” Premature port withdrawal (i.e. while the stimulus was still at baseline) resulted in a “false alarm.” On 30% of trials, catch trials, rats were required to maintain port fixation until the stimulus ended at a random time, resulting in a “correct rejection.” The average increases in click rate were +10 Hz, +23 Hz, +36 Hz, and +49 Hz.

Reverse correlations

Reverse correlations are calculated as the residual of click numbers actually occurring in trials of a given type (left or right) relative to the expected click numbers given the generative rate (Brunton et al., 2013). To calculate a reverse correlation, an incremental click rate for each trial is calculated for each 0.05 s increment of the stimulus through convolution of clicks with a causal Gaussian kernel. Trials of a given *generative* click rate were grouped, and the expected generative rate for each increment was subtracted from the actual click rate for each trial of that group. These

residuals are then averaged together in a separate group based on the rat's choice. The resulting average represents the periods of the stimulus that tended to influence decisions. Epochs during which the right and left traces overlap do not influence the decision on average, because the rat wat not significantly more likely to choose right when more rightward clicks occurred than expected during that period, and vice versa for a left choice.

References

Brunton, B.W., Botvinick, M.M., and Brody, C.D. (2013). Rats and Humans Can Optimally Accumulate Evidence for Decision-Making. Science *340*, 95–98. https://doi.org/10.1126/science.1233912.

Celsis, P., Boulanouar, K., Doyon, B., Ranjeva, J.P., Berry, I., Nespoulous, J.L., and Chollet, F. (1999). Differential fMRI Responses in the Left Posterior Superior Temporal Gyrus and Left Supramarginal Gyrus to Habituation and Change Detection in Syllables and Tones. NeuroImage *9*, 135–144. https://doi.org/10.1006/nimg.1998.0389.

Chandler, H.C., King, V., Corwin, J.V., and Reep, R.L. (1992). Thalamocortical connections of rat posterior parietal cortex. Neuroscience Letters *143*, 237–242. https://doi.org/10.1016/0304-3940(92)90273-A.

Cheatwood, J.L., Reep, R.L., and Corwin, J.V. (2003). The associative striatum: cortical and thalamic projections to the dorsocentral striatum in rats. Brain Research *968*, 1–14. https://doi.org/10.1016/S0006-8993(02)04212-9.

Erlich, J.C., Brunton, B.W., Duan, C.A., Hanks, T.D., and Brody, C.D. (2015). Distinct effects of prefrontal and parietal cortex inactivations on an accumulation of evidence task in the rat. ELife Sciences *4*, e05457. https://doi.org/10.7554/eLife.05457.

Gimenez, T.L., Lorenc, M., and Jaramillo, S. (2015). Adaptive categorization of sound frequency does not require the auditory cortex in rats. Journal of Neurophysiology *114*, 1137–1145. https://doi.org/10.1152/jn.00124.2015.

Gold, J.I., and Shadlen, M.N. (2007). The Neural Basis of Decision Making. Annual Review of Neuroscience *30*, 535–574. https://doi.org/10.1146/annurev.neuro.29.051605.113038.

Guo, L., Weems, J.T., Walker, W.I., Levichev, A., and Jaramillo, S. (2019). Choice-Selective Neurons in the Auditory Cortex and in Its Striatal Target Encode Reward Expectation. J. Neurosci. *39*, 3687–3697. https://doi.org/10.1523/JNEUROSCI.2585-18.2019.

Hanks, T.D., and Summerfield, C. (2017). Perceptual Decision Making in Rodents, Monkeys, and Humans. Neuron *93*, 15–31. https://doi.org/10.1016/j.neuron.2016.12.003.

Hanks, T.D., Kopec, C.D., Brunton, B.W., Duan, C.A., Erlich, J.C., and Brody, C.D. (2015). Distinct relationships of parietal and prefrontal cortices to evidence accumulation. Nature *520*, 220–223. https://doi.org/10.1038/nature14066.

Heffner, H. (1978). Effect of auditory cortex ablation on localization and discrimination of brief sounds. Journal of Neurophysiology *41*, 963–976. https://doi.org/10.1152/jn.1978.41.4.963.

Jaramillo, S., and Zador, A.M. (2011). The auditory cortex mediates the perceptual effects of acoustic temporal expectation. Nature Neuroscience *14*, 246–251. https://doi.org/10.1038/nn.2688.

Malhotra, S., and Lomber, S.G. (2007). Sound Localization During Homotopic and Heterotopic Bilateral Cooling Deactivation of Primary and Nonprimary Auditory Cortical Areas in the Cat. Journal of Neurophysiology *97*, 26–43. https://doi.org/10.1152/jn.00720.2006.

McGeorge, A.J., and Faull, R.L.M. (1989). The organization of the projection from the cerebral cortex to the striatum in the rat. Neuroscience *29*, 503–537. https://doi.org/10.1016/0306-4522(89)90128-0.

Noppeney, U., Ostwald, D., and Werner, S. (2010). Perceptual Decisions Formed by Accumulation of Audiovisual Evidence in Prefrontal Cortex. J Neurosci *30*, 7434–7446. https://doi.org/10.1523/JNEUROSCI.0455-10.2010.

Ratcliff, R., and McKoon, G. (2008). The Diffusion Decision Model: Theory and Data for Two-Choice Decision Tasks. Neural Comput *20*, 873–922. https://doi.org/10.1162/neco.2008.12-06-420.

Ratcliff, R., and Rouder, J.N. (1998). Modeling Response Times for Two-Choice Decisions. Psychol Sci *9*, 347–356. https://doi.org/10.1111/1467-9280.00067.

Roitman, J.D., and Shadlen, M.N. (2002). Response of Neurons in the Lateral Intraparietal Area during a Combined Visual Discrimination Reaction Time Task. J. Neurosci. *22*, 9475–9489. .

Rybalko, N., Šuta, D., Popelář, J., and Syka, J. (2010). Inactivation of the left auditory cortex impairs temporal discrimination in the rat. Behavioural Brain Research *209*, 123–130. https://doi.org/10.1016/j.bbr.2010.01.028.

Scott, B.H., and Mishkin, M. (2016). Auditory short-term memory in the primate auditory cortex. Brain Research *1640*, 264–277. https://doi.org/10.1016/j.brainres.2015.10.048.

Selemon, L.D., and Goldman-Rakic, P.S. (1985). Longitudinal topography and interdigitation of corticostriatal projections in the rhesus monkey. J. Neurosci. *5*, 776–794. https://doi.org/10.1523/JNEUROSCI.05-03-00776.1985.

Shadlen, M.N., and Newsome, W.T. (1996). Motion perception: seeing and deciding. Proceedings of the National Academy of Sciences *93*, 628–633. https://doi.org/10.1073/pnas.93.2.628.

Siegel, M., Buschman, T.J., and Miller, E.K. (2015). Cortical information flow during flexible sensorimotor decisions. Science *348*, 1352–1355. https://doi.org/10.1126/science.aab0551.

Springer, J.A., Binder, J.R., Hammeke, T.A., Swanson, S.J., Frost, J.A., Bellgowan, P.S.F., Brewer, C.C., Perry, H.M., Morris, G.L., and Mueller, W.M. (1999). Language dominance in neurologically normal and epilepsy subjects: A functional MRI study. Brain *122*, 2033–2046. https://doi.org/10.1093/brain/122.11.2033.

Xiong, Q., Znamenskiy, P., and Zador, A.M. (2015). Selective corticostriatal plasticity during acquisition of an auditory discrimination task. Nature *521*, 348–351. https://doi.org/10.1038/nature14225.

Yartsev, M.M., Hanks, T.D., Yoon, A.M., and Brody, C.D. (2018). Causal contribution and dynamical encoding in the striatum during evidence accumulation. ELife *7*, e34929. https://doi.org/10.7554/eLife.34929.

Yu, L., Hu, J., Shi, C., Zhou, L., Tian, M., Zhang, J., and Xu, J. (2021). The causal role of auditory cortex in auditory working memory. ELife *10*, e64457. https://doi.org/10.7554/eLife.64457.

Zhong, L., Zhang, Y., Duan, C.A., Deng, J., Pan, J., and Xu, N. (2019). Causal contributions of parietal cortex to perceptual decision-making during stimulus categorization. Nat Neurosci *22*, 963–973. https://doi.org/10.1038/s41593-019-0383-6.

Znamenskiy, P., and Zador, A.M. (2013). Corticostriatal neurons in auditory cortex drive decisions during auditory discrimination. Nature *497*, 482–485. https://doi.org/10.1038/nature12077.o

Chapter 5: General Conclusion

Summary of this dissertation

I have examined three properties of perceptual decision making in the brain concerning how the brain uses sensory evidence over time to guide actions. First, I conducted a study testing the extent to which humans evaluate evidence over multiple timescales for perceptual decision making. Specifically, I found that humans maintain multiple temporal representations of the same sensory evidence that are flexibly recruited for different purposes, in our case, change detection decisions and confidence judgments about those decisions. Humans are able to evaluate evidence over a shorter timescale during the initial decision, then access evidence over a longer timescale depending on how the situation evolves. This function emerges when the subject has no ability to predict when stimulus presentation ends, meaning they maintain a representation of evidence that no longer had bearing on the decision during stimulus presentation. These empirical results are supported by a computational model demonstrating a single timescale of evidence evaluation is insufficient to explain subject behavior. As such, the findings rule out models of decision making in which a single timescale of evidence evaluation is maintained for decision making.

To identify neural mechanisms that could support this flexibility in evaluation timescale, I implanted rat posterior parietal cortex (PPC) with Neuropixel probes to measure the responses of PPC neurons leading up to change detection decisions. In contrast with previously observed responses during tasks in which evidence is evaluated over long timescales, PPC neurons showed transient, more ballistic responses to evidence leading up to decisions. Furthermore, the timescale over which rats evaluated evidence at the psychophysical level correlated with the timescale over

which the neurons integrated individual units of evidence. Finally, through reversible pharmacological inactivation, I identified a causal role of PPC in change detection decisions that seemed to originate from an influence of PPC on the timescale over which evidence is evaluated. Together, this study identifies a new function of PPC in driving decisions involving free response choices bearing on evidence evaluated over short timescales and provides a putative neural foundation for the behavioral observations I made in the human study.

The final project included in this dissertation tested the role of primary auditory cortex (A1) in accumulation of auditory evidence over time. It is unclear whether regions like PPC perform integration of raw sensory evidence into decision-related variables or if observed responses are simply inherited from upstream sensory regions. To test the hypothesis that A1 performs this integration function in auditory decision making, I reversibly inactivated A1 on both an auditory discrimination task and a detection task. I found that A1 is necessary for performance over the discrimination task, which involves evaluation of evidence over a long timescale, but not the detection task. In addition, deficits induced in the discrimination task via A1 inactivation are explicable through a primarily sensory impairment rather than an impairment in the rat's ability to accumulate evidence over time toward a decision. As such, it appears that the striking neural responses in association areas like PPC likely emerge locally instead of through sensory inputs.

Outstanding questions

Here, I outline several unanswered questions brought about by the results of the above studies and propose further lines of study that could potentially address these questions.

1) Can humans evaluate evidence over multiple timescales simultaneously? We've shown that humans can retroactively access older information that was initially not used for decisions, suggesting humans track evidence over multiple timescales. The questions that follows naturally is whether the brain can maintain representations of the same evidence over multiple timescales in cases where multiple competing choices require evaluation over different timescales. For example, we could combine a detection task in which subjects must detect transient changes in a stimulus while also tracking a separate statistic of the stimulus that is discriminable over the entire course of the stimulus. This task would reveal whether the brain is restricted to one timescale of evaluation that may be optimal for one purpose or the other but not both.
2) Are confidence judgments in the brain inherently founded on a timescale of evidence evaluation separate from initial decisions? Although it has been shown that several brain circuits computing and driving judgments of confidence in decisions can be isolated from the circuits that drive the decisions themselves (Kepecs et al., 2008; Kiani and Shadlen, 2009; Komura et al., 2013; Lak et al., 2014; Rutishauser et al., 2018), it is unclear whether the dynamics of choice confidence, including the periods of evidence on which these judgments bear, differ from the dynamics of evidence integration leading to decisions. To answer

this question, addition of a confidence component to our change detection task combined with simultaneous recording of neural responses from cell populations implicated in initial decision formation and in confidence judgments could reveal the extent to which decisions and confidence judgments are informed by similar stimulus properties.

3) How is the timescale of evidence integration in PPC cells modulated? PPC cells show propensity to adjust their temporal dynamics to suit task demands, but it is unclear how this is accomplished at the system level. Two broad possibilities are that the timescale is modulated locally or the timescales are inherited from upstream regions. In the former case, PPC interneurons could be tuned to reduce activity of evidence-integrating cells over time through negative feedback (Song et al., 2017, 2020). Alternatively, PPC could inherit these timescales from the various nodes in the greater decision making network in the brain. Recording from other regions implicated in evidence integration (e.g. striatum, prefrontal cortex) during a similar task could be key to understanding the point of processing in the brain at which that evidence processing is tuned to task demands.
4) Can PPC neurons dynamically tune their integration timescales as conditions change? Although we see in the results of Chapter 3 that PPC neurons have flexible dynamics of evidence integration, we do not know if these dynamics can adapt to changing task demands within a task. For example, as the rat adapts its behavior based on environmental feedback for the rat's decisions, do PPC neural dynamics reflect the adaptation? To test this, we can record PPC neural activity

during the change detection task and test whether the dynamics change when task statistics are altered to elicit new behavioral strategies. For example, altering the response window would require a different solution on the part of the rat; a shorter response window requires a shorter evidence evaluation timescale. Therefore, if the rat modifies its behavior accordingly, we can more directly test the hypothesis that PPC dynamics are modified during learning of new decision rules.

5) Is PPC neural activation sufficient to drive decision commitment? Unlike many tasks used to study the role of PPC in perceptual decisions, our task involves a free response component, so the timing of the decision is both a critical aspect of task performance and presumably requires neural functions distinct from tasks in which the environment controls the time of the decision. Chapter 3's results demonstrate PPC is necessary for establishing the timescale of evidence evaluation for these free response decisions, but to directly test whether PPC controls the time of decision commitment, we can conduct experiments in which PPC neurons are stimulated and the change in probability of response following stimulation is measured (Hanks et al., 2006).
6) Are deficits in auditory decision making induced by A1 inactivation also driven by a change in accumulation timescale? Although the results of Chapter 4 suggest a largely sensory role for A1 in evaluation of auditory evidence over time, there may be a latent accumulation role that is simply dominated by the sensory deficit. Models of accumulation to bound involving both sensory and accumulation parameters have been previously applied to behavioral data using the same

discrimination task as in my study (Brunton et al., 2013; Erlich et al., 2015), so application of this model to the data presented in Chapter 4 would better elucidate the contributions of A1 to sensory processing and accumulation of evidence over time specifically to inform decisions.

References

Brunton, B.W., Botvinick, M.M., and Brody, C.D. (2013). Rats and Humans Can Optimally Accumulate Evidence for Decision-Making. Science *340*, 95–98. https://doi.org/10.1126/science.1233912.

Erlich, J.C., Brunton, B.W., Duan, C.A., Hanks, T.D., and Brody, C.D. (2015). Distinct effects of prefrontal and parietal cortex inactivations on an accumulation of evidence task in the rat. ELife Sciences *4*, e05457. https://doi.org/10.7554/eLife.05457.

Hanks, T.D., Ditterich, J., and Shadlen, M.N. (2006). Microstimulation of macaque area LIP affects decision-making in a motion discrimination task. Nat. Neurosci. *9*, 682–689. https://doi.org/10.1038/nn1683.

Kepecs, A., Uchida, N., Zariwala, H.A., and Mainen, Z.F. (2008). Neural correlates, computation and behavioural impact of decision confidence. Nature *455*, 227–231. https://doi.org/10.1038/nature07200.

Kiani, R., and Shadlen, M.N. (2009). Representation of Confidence Associated with a Decision by Neurons in the Parietal Cortex. Science *324*, 759–764. https://doi.org/10.1126/science.1169405.

Komura, Y., Nikkuni, A., Hirashima, N., Uetake, T., and Miyamoto, A. (2013). Responses of pulvinar neurons reflect a subject's confidence in visual categorization. Nature Neuroscience *16*, 749–755. https://doi.org/10.1038/nn.3393.

Lak, A., Costa, G.M., Romberg, E., Koulakov, A.A., Mainen, Z.F., and Kepecs, A. (2014). Orbitofrontal cortex is required for optimal waiting based on decision confidence. Neuron *84*, 190–201. https://doi.org/10.1016/j.neuron.2014.08.039.

Rutishauser, U., Aflalo, T., Rosario, E.R., Pouratian, N., and Andersen, R.A. (2018). Single-Neuron Representation of Memory Strength and Recognition Confidence in Left Human Posterior Parietal Cortex. Neuron *97*, 209-220.e3. https://doi.org/10.1016/j.neuron.2017.11.029.

Song, Y.-H., Kim, J.-H., Jeong, H.-W., Choi, I., Jeong, D., Kim, K., and Lee, S.-H. (2017). A Neural Circuit for Auditory Dominance over Visual Perception. Neuron *93*, 940-954.e6. https://doi.org/10.1016/j.neuron.2017.01.006.

Song, Y.-H., Hwang, Y.-S., Kim, K., Lee, H.-R., Kim, J.-H., Maclachlan, C., Dubois, A., Jung, M.W., Petersen, C.C.H., Knott, G., et al. (2020). Somatostatin enhances visual processing and perception by suppressing excitatory inputs to parvalbumin-positive interneurons in V1. Sci Adv *6*, eaaz0517. https://doi.org/10.1126/sciadv.aaz0517.